2014

Novel regulator genes controlling mesenchymal stromal cell function and adipose tissue remodelling

Isabel de Deus e Sousa

DEPARTAMENTO DE CIÊNCIAS DA VIDA

FACULDADE DE CIÊNCIAS E TECNOLOGIA
UNIVERSIDADE DE COIMBRA

Novel regulator genes controlling mesenchymal stromal cell function and adipose tissue remodelling

Isabel Sofia de Deus e Sousa

2014

DEPARTAMENTO DE CIÊNCIAS DA VIDA

FACULDADE DE CIÊNCIAS E TECNOLOGIA
UNIVERSIDADE DE COIMBRA

Novel regulator genes controlling mesenchymal stem cell function and adipose tissue remodelling

Dissertação apresentada à Universidade de Coimbra para cumprimento dos requisitos necessários à obtenção do grau de Mestre em Biologia Celular e Molecular, realizada sob a orientação científica do Doutor Alexandros Vegiopoulos (German Cancer Research Center, Heidelberg, Germany) e do Professor Doutor Carlos Palmeira (Departamento de Ciências da Vida, Universidade de Coimbra).

Isabel Sofia de Deus e Sousa

2014

This thesis was written at the German Cancer Research Center (DKFZ) in Heidelberg, Germany, in the period of September to June 2014 under the supervision of Dr. Alexandros Vegiopoulos.

Acknowledgements

First of all I would like to thank Dr. Alexandros Vegiopoulos for the opportunity to work in his group on this interesting project, for his support and guidance on every experiment, for all the discussions and advice, and also for taking time to read and comment this thesis, and for answering all my questions in the process.

I would like to thank Prof. Dr. Stephan Herzig for the opportunity to do my master thesis in the A170 division of Metabolism and Metabolic Control.

I would also like to thank Prof. Dr. Carlos Palmeira for accepting to be my supervisor, to Prof. Dr. Emília Duarte for the support and help during my Master, and to all the professors that inspired and helped me during my studies in the University of Coimbra.

Also I would like to thank all the members of the A171 group: Irem, Julia, Irina, Rohollah and Dagmar for their help in many experiments, for answering my questions, for their warm welcome and for making me feel part of the group. A special thanks to Irem for all the progenitor isolations, for taking care of my cells when I was ill, for all the advice in many experiments and protocols, for never getting tired to answer my endless questions and for being a really good friend.

Additionally I would like to thank all the A170 lab members who helped me in anyway during this project, for the advice on protocols and for sharing reagents that often saved my experiments. A special thanks to Asrar, Aishwarya, Jessica Furhmeister and Jessica Chan for all the conversations, breaks and cakes that made work in the lab and my time in Heidelberg much more enjoyable.

To all my 'biochemical' friends that made these past five years memorable and worth every moment. A special thanks to Ricardo for the friendship, the coffees and the crazy moments. Paula, forever my lab partner, thanks for being a great friend, for the tee breaks, all the conversations and discussion over science and much more!

A big thanks to Tânia for the constant support, the tough love when I needed it, for all the help and cheering up, this year would not have been the same without you girl!

Thank you Pedro for all your caring, for your support and patience, for believing in me and for always being able to put a smile on my face.

Last but not least, a great thank you goes to my family and specially my parents for giving me the opportunity to fulfill my dreams, for their unconditional love and support, for believing in me and always being there for me.

Abstract

A high calorie diet and sedentary lifestyle have led to the spiralling increase in obesity rates around the world. Remodelling of white adipose tissue (WAT) in response to chronic energy excess is accomplished by enlargement of existing adipocytes (hypertrophy) and generation of new ones by recruitment of mesenchymal stromal cells (MSC) resident in adipose depot. Increasing energy expenditure can be accomplished by activation of brown adipose tissue (BAT) thermogenesis and formation of beige adipocytes in white depots (browning). The mechanisms regulating these processes are still fairly unknown. Prostaglandins have been shown to promote MSC recruitment and browning, in particular PGI_2, and recently sphingosine kinase 1 (Sphk1) was identified as an important gene in BAT thermogenic activation in response to cold exposure. Sphk1 is an enzyme of the sphingolipid pathway, and has been found upregulated in obesity along with its product sphingosine-1-phosphate and ceramide.

The aim of this study was to determine the role of Sphk1 in MSC recruitment and differentiation, and also the role in mature adipocyte function. siRNA-mediated knock down of Sphk1 in brown adipocytes significantly reduced expression of thermogenic genes and norepinephrine (NE) responsiveness, and also reduced basal lipolysis, indicating a clear impairment of brown adipocyte function in the absence of Sphk1/S1P signalling. In addition, Sphk1 knock down in white and $cPGI_2$-induced beige adipocytes markedly reduced expression of general adipogenic markers and genes regulating lipolysis, which surprisingly translated into an increase in lipolysis in beige adipocytes.

On the other hand, Sphk1 knock down in brown progenitors significantly reduced differentiation, which indicates that Sphk1 is required for normal brown adipocyte differentiation. Moreover, Sphk1 knock down in undifferentiated WAT MSCs significantly reduced expression of adipogenic genes, both in normal conditions and in the presence of $cPGI_2$, indicating that Sphk1 regulates white and beige adipogenesis in a similar way. Genes involved in mitochondrial biogenesis were also significantly reduced, which may compromise the oxidative capacity of adipocytes. Furthermore, knock down of Sphk1 significantly increased apoptosis and cell death of differentiating adipocytes, measured by increased AnnexinV staining detected by flow cytometry. Additionally, EdU labelling allowed detection of cell accumulation in S/G2/M phase and reduction in cell proliferation. Both results could explain the observed reduction in adipogenesis. Finally, in line with its known effects, S1P added to differentiating WAT MSC reduced adipogenesis and promoted cell proliferation.

Overall, these results show that Sphk1/S1P signalling plays an important role in recruitment and differentiation of adipocyte progenitors, with particular relevance for brown adipocyte development. Therefore, it is relevant to further explore the role of sphingolipids in regulation of adipose tissue, with potential for therapeutic application in metabolic diseases.

Keywords: adipose mesenchymal stromal cells, sphingosine kinase-1, adipogenesis

Resumo

Maus hábitos alimentares e um estilo de vida sedentário contribuem para o aumento das taxas de obesidade em todo o mundo. A remodelação do tecido adiposo branco em resposta ao excesso crónico de energia resulta do aumento de tamanho dos adipócitos existentes (hipertrofia) e da formação de novos adipócitos através do recrutamento de células mesenquimais do estroma residentes no tecido adiposo. O aumento dos gastos energéticos pode ser conseguido através da activação da termogénese no tecido adiposo castanho e formação de adipócitos beges dentro de tecido adiposo branco (*browning*). Os mecanismos reguladores destes processos ainda estão muito por explorar. Sabe-se que prostaglandinas como PGI_2 promovem o recrutamento e *browning* de células mesenquimais do estroma, e recentemente a enzima esfingosina cinase-1 (*Sphk1*) foi identificada como um importante regulador da activação termogénica do tecido adiposo castanho em resposta a baixas temperaturas. Sphk1 pertence à via de sinalização de esfingolípidos, e em obesidade os seus níveis encontram-se elevados, assim como o seu produto esfingosina-1-fosfato (*S1P*) e ceramida.

Esta tese teve objectivo determinar o papel da *Sphk1* no recrutamento e diferenciação de células mesenquimais do estroma, e também a sua função em adipócitos maduros. O silenciamento de *Sphk1* através de siRNA em adipócitos castanhos reduziu significativamente a expressão de genes envolvidos na termogénese e resposta a estimulação por norepinefrina (NE), e reduziu também a taxa basal de lipólise, o que indica que a função de adipócitos castanhos é claramente afectada na ausência de *Sphk1/S1P*. Para além disso, o silenciamento de Sphk1 em adipócitos brancos e beges, induzidos por adição de $cPGI_2$, reduziu significativamente a expressão de genes reguladores da adipogénese e lipólise, o que no entanto se traduziu num aumento da taxa de lipolise em adipócitos beges.

Por outro lado, o silenciamento de *Sphk1* em células progenitoras de adipócitos castanhos diminuiu significativamente a sua diferenciação, o que indica que Sphk1 é necessária para o processo de diferenciação de adipócitos castanhos. Mais ainda, o silenciamento de *Sphk1* em células progenitoras do tecido adiposo branco reduziu significativamente a expressão de genes marcadores de adipogénese, em condições normais e na presença de $cPGI_2$, o que indica que Sphk1 tem um papel semelhante na regulação da diferenciação de adipócitos brancos e beges. A expressão de genes mitocondriais também foi reduzida significativamente, o que pode comprometer a capacidade oxidativa dos adipócitos. Para além disso, o silenciamento de *Sphk1* aumentou significativamente apoptose e morte celular de adipócitos durante o processo de diferenciação, medido por marcação das células com AnnexinV e detecção por citometria de fluxo. Esta técnica também permitiu detectar marcação de DNA com EdU, e revelou que há uma acumulação de células na fase S/G2/M e redução da proliferação celular na ausência de *Sphk1*. Ambos os resultados permitem explicar a redução na adipogénese observada nas experiencias anteriores. Por último, a adição de S1P a células progenitoras do tecido adiposo branco reduziu adipogénese e promoveu proliferação celular.

Concluindo, estes resultados mostram que a sinalização de Sphk1/S1P tem um papel importante no recrutamento e diferenciação de células progenitoras de adipócitos, com especial relevância no desenvolvimento de adipócitos castanhos. Por isso é relevante continuar a explorar o papel dos esfingolípidos na regulação do tecido adiposo, dado o seu potencial para aplicações terapêuticas em doenças metabólicas.

Index

Abbreviations

#	Number
%	Percentage
°C	Degree Celcius
µg	Micrograms
µl	Microliter
µM	Micromolar
abd	Abdominal
AC	Adenyl cyclase
Acaca	Acetyl-Coenzyme A carboxylase alpha
ACC	Acetyl-coenzyme A carboxylase
ACL	Adenosine triphosphate citrate lyase
ADSCs	Adipose-derived stem cells
aP2	Adipocyte-type fatty acid-binding protein
ARs	Adrenergic receptor
ATGL	Adipose triglyceride lipase
ATP	Adenosine triphosphate
BAT	Brown adipose tissue
bFGF	Basic fibroblast growth factor
BMP	Bone morphogenetic protein
BSA	Bovine serum albumin
C/EBP (Cebp)	CCAAT/enhancer-binding protein
$CaCl_2$	Calcium chloride
cAMP	Cyclic adenosine monophosphate
CD	Cluster of differentiation
cGMP	Cyclic guanosine monophosphate
Cidea	Cell death-inducing DNA fragmentation factor alpha-like effector A
CL	Cl316243
cm	Centimeter
CO_2	Carbon dioxide
CoA	Coenzyme A
COX-2	Cyclooxygenase-2
Cox7a1	Cytochrome c oxidase, subunit VII a 1
Cox8b	Cytochrome c oxidase, subunit VIII b
$cPGI_2$	Carbaprostacyclin
CPT1B	Carnitine palmitoyltransferase 1B
CREB	Cyclic AMP response element-binding protein
DAPI	4',6-diamidino-2-phenylindole
Dio2	Deiodinase
DMEM	Dulbecco's modified eagle medium
DMSO	Dimethyl sulfoxide
DNA	Deoxyribonucleic acid
DNaseI	Desoxirribonuclease I
D-PBS	Dulbecco's phosphate buffered saline

EDTA	Ethylenediaminetetraacetic acid
EdU	5-ethynyl-2´-deoxyuridine
Elovl 6	Elongation of very long-chain fatty acid protein 6
ERK	Extracellular signal-regulated kinase
EtOH	Ethanol
Fabp4	Fatty acid-binding protein 4
FACS	Fluorescence-activated cell sorting
FAS	Fatty acid synthase
Fasn	Fatty acid synthase (gene)
FCS	Fetal calf serum
FDG	[^{18}F]-2-fluoro-D-2-deoxy-D-glucose
FFA	Free fatty acids
g	Grams
g	Gravitational acceleration
GCs	Glucocorticoids
GLP-1	Glucagon-like peptide 1
GLUT4	Glucose transporter 4
GPCR	G protein coupled receptor
h	Hour
H_2O	Water
HEPES	4-(2-hydroxyethyl)-1-piperazineethanesulfonic acid
HSL	Hormone-sensitive lipase
iBAT	Interscapular brown adipose tissue
IBMX	3-isobutyl-1-methylxanthine
IGF-1	Insulin-like growth factor-1
IgG	Immunoglobulin G
ing	Inguinal
IRS	Insulin-receptor substrates
JNK	Jun amino-terminal kinase
KCl	Potassium chloride
KOH	Potassium hydroxide
Lin	Lineage
Lipe	Hormone-sensitive lipase (gene)
M	Molar
mg	Miligrams
$MgCl_2$	Magnesium chloride
MGL	Monoacylglycerol lipase
ml	Mililiter
mM	Milimolar
MSC	Mesenchymal stromal cell
Myf5	Myogenic factor 5
MyoD	Myogenic differentiation
Na_2CO_3	Sodium carbonate
Na_2SO_4	Sodium sulfate
NaCl	Sodium chloride

NaH_2PO_4	Sodium dihydrogen phosphate
NE	Norepinephrine
NF-κB	Nuclear factor κb
ng	Nanogram
nM	Nanomolar
NPRs	Natriuretic peptide receptors
NPs	Natriuretic peptides
OXPHOS	Oxidative phosphorilation
P/S	Penicillin / streptomycin
PBS	Phosphate buffered saline
PDGFRα	Platelet-derived growth factor receptor alpha
PET	Positron emission tomography
PFA	Paraformaldehyde
PG	Prostaglandin
PGC1α	Peroxisome proliferator-activated receptor gamma coactivator 1 alpha
PGI_2	Prostacyclin
PGIS	Prostacyclin synthase
PI	Propidium iodide
PKA	Protein kinase A
PKB	Protein kinase B
PKG	Protein kinase G
Plin1	Perilipin 1
pmol	Picomole
Pnpla2	Patatin-like phospholipase domain containing 2
PPAR	Peroxisome proliferator-activated receptor
PRDM16	Positive regulatory domain containing 16
Pref-1	Preadipocyte factor 1
PS	Phosphatidylserine
Retn	Resistin
RNA	Ribonucleic acid
RT	Room temperature
RT-qPCR	Reverse transcription-quantitative polymerase chain reaction
S1P	Sphingosine-1-phosphate
S1PR	Sphingosine-1-phosphate receptor
Sca-1	Stem cell antigen-1
SCD	Stearoyl-coenzyme A desaturase
Scd1	Stearoyl-Coenzyme A desaturase 1
SEM	Standard error of the mean
siRNA	Small interfering ribonucleic acid
SNS	Sympathetic nervous system
Sphk1	Sphingosine kinase-1
Sphk2	Sphingosine kinase-2
SREBP1c	Sterol regulatory element binding transcription factor 1
SVF	Stromal vascular fraction
T3	Triiodothyronine
T4	Thyroxine

Tbp	TATA box binding protein
TG	Triglycerides
TGF-β	Transforming growth factor-beta
TLRs	Toll-like receptors
TNF-α	Tumor necrosis factor-alpha
UCP1	Uncoupling protein 1
VLDL	Very low density lipoproteins
WAT	White adipose tissue
Wnt	Wingless-type MMTV integration site

1. Introduction

Obesity and the metabolic syndrome are becoming a worldwide epidemic, affecting more than 30% of the world's adult population and with increasing prevalence also in children (World Health Organization 2013). Some major health consequences of obesity and metabolic syndrome are increasing risk of developing type 2 diabetes mellitus, dyslipidemias, non-alcoholic fatty liver and cardiovascular disease, with recent studies also indicating a correlation with Alzheimer's disease and cancer (Tseng et al. 2010; Hursting et al. 2012). Therefore it is highly relevant to improve the knowledge on adipose tissue biology and regulation of metabolism.

1.1. Adipose tissue biology

Considered for a long time to have the sole function of storing energy, adipose tissue is also the body's largest endocrine organ, secreting hormones, cytokines, and proteins that influence cells and tissues throughout the body, regulating metabolism, reproduction and lifespan, as well as conferring thermal and traumatic protection (Zeve et al. 2009). In mammals, adipocytes have previously been classified as white and brown according to their function: white adipose tissue (WAT) is primarily responsible for storing energy, and brown adipose tissue (BAT) promotes energy expenditure. White adipocytes typically contain a single large lipid droplet (unilocular) surrounded by a thin layer of cytoplasm, with a small flattened nucleus located in the periphery and poor organelle content. Brown adipocytes are characterized by multiple small lipid droplets (multilocular), a centrally located spherical nucleus and an abundant cytoplasm. The brown colour of BAT derives from a rich vascular network and abundant mitochondrial content.

Recent data suggest that there are two distinct types of brown fat: classical brown fat derived from a Myf-5 cellular lineage and UCP1- positive cells that emerge in white fat from a non-Myf-5 lineage (Seale et al. 2008). These novel brown-like cells that reside within WAT, especially inguinal WAT, were termed beige/brite adipocytes. Beige cells resemble white fat cells in having extremely low basal expression of UCP1, but, like classical brown fat, they respond to cyclic AMP (cAMP) stimulation with high UCP1 expression and respiration rates (Wu et al. 2012).

In humans, WAT is dispersed throughout the body with major intra-abdominal/visceral depots around the omentum, intestines, and perirenal areas, as well as subcutaneous depots in the buttocks, thighs, and abdomen. Importantly, visceral depots are strongly associated with metabolic complications, such as significantly increasing the risk of hyperlipidemia, diabetes and cardiovascular disease, while subcutaneous depots appear protective against metabolic deregulations (Lafontan & Berlan 2003). Some adipose tissue is responsive to sex hormones (breasts and thighs), accounting for the differences in body shape between sexes. Fat distribution changes with age, decreasing in subcutaneous fat and increasing in intra-abdominal fat.

In contrast, BAT is found in axillary, cervical, perirenal, and periadrenal regions in human fetuses and newborns, but decreases shortly after birth. In adults, [^{18}F]-2-fluoro-D-2-deoxy-D-glucose (FDG) positron emission tomography (PET) has allowed detection of areas of metabolically active BAT in the cervical, supraclavicular, axillary and paravertebral regions. In rodents, BAT is also most abundant in the neonatal period and is concentrated in the interscapular region (Gesta et al. 2007).

Depot-specific differences may be related not only to the metabolism of fat cells but also to their capacity to form new adipocytes. Additionally, regional differences may result from variations in hormone receptor distribution as well as from specific local environmental characteristics as a consequence of differences in innervation and vascularization.

WAT is the primary site for energy storage in the form of triglycerides (TG) (lipogenesis) during times of caloric abundance and release of fatty acids and glycerol (lipolysis) in times of energy demand. In order to perform its storage function, WAT expresses the machinery required for triglyceride synthesis from circulating lipoprotein-derived fatty acids as well as from hormone-stimulated glucose uptake. The liver and small intestine are the major sources of lipoprotein-derived fatty acids, and those freshly absorbed in the intestine are transported in chylomicrons and esterified with glycerol phosphate in the liver to TG, and further transported in very low density lipoproteins (VLDL). In humans, glucose is the most important precursor of fatty acids, and WAT possesses glucose transporter 4 (GLUT4) which controls its uptake in a hormone-dependent manner: *de novo* lipogenesis from glucose is stimulated by insulin, ghrelin, glucagon-like peptide 1 (GLP-1) and gastric inhibitory peptide (Frühbeck & Gómez-Ambrosi 2013).

De novo lipogenesis is the metabolic pathway that synthesizes fatty acids from excess carbohydrates, which can then be incorporated into triglycerides for energy storage and also contribute to an increase in the synthesis and secretion of VLDL particles (Strable & Ntambi 2010). In adipose tissue, fatty acids can be synthesized from several precursors, such as glucose, lactate, and certain amino acids, with glucose being quantitatively the most important in humans (Frühbeck & Gómez-Ambrosi 2013). Inside the adipocyte, glucose is metabolized both in the cytosol and in the mitochondria, to produce cytosolic acetyl-CoA catalyzed by ATP-citrate lyase (ACL) (Figure 1). Acetyl-CoA is a requisite carbon donor in the *de novo* synthesis of fatty acids, as it supplies the first acyl group in a growing fatty acid chain, and it is the substrate used by acetyl-CoA carboxylase (ACC) to catalyze the synthesis of malonyl-CoA. Fatty acid synthase (FAS) synthesizes the saturated fatty acid palmitate from malonyl-CoA. Fatty acid elongation is catalyzed by Elovl 6 (elongation of very long-chain fatty acid protein 6), and stearoyl-CoA desaturase (SCD) catalyzes the conversion of saturated fatty acids, like palmitate and stearate, to their monounsaturated fatty acid counterparts.

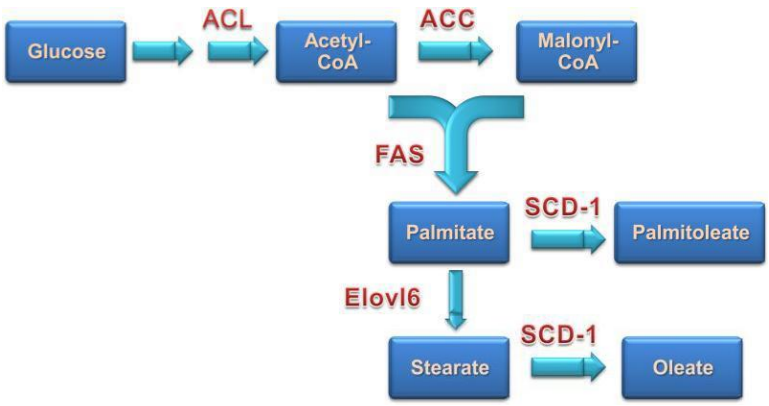

Figure 1: Schematic of pathways involved in *de novo* lipogenesis. ACL, ATP citrate lyase; ACC, acetyl-CoA carboxylase; FAS, fatty acid synthase; SCD-1, stearyl-CoA desaturase; Elovl6, elongation of very long-chain fatty acids protein 6. From Lodhi et al. 2011**.**

The mobilization of fat stores in response to fasting, exercise and cold exposure is under tight hormonal regulation, mainly by plasma insulin and catecholamines released by the sympathetic nervous system (SNS). Release of norepinephrine (NE) stimulates β-adrenergic receptors (ARs), including β1- and β2-ARs in white adipocytes and β3-ARs in brown and also white adipocytes, promoting lipolysis and thermogenesis (Lafontan & Langin 2009). The β-ARs are coupled to the G-alpha subunit of stimulatory G proteins, activating adenylyl cyclase (AC) and promoting the increase in intracellular cAMP levels, which activates protein kinase A (PKA) (Figure 2). Alternatively, natriuretic peptides (NPs), released mainly from the heart, induce BAT thermogenic activation through interaction with NP receptors (NPRs), stimulating cGMP production and activation of protein kinase G (PKG) (Villarroya & Vidal-Puig 2013). Both PKA and PKG phosphorylate the lipolytic enzyme HSL (hormone-sensitive lipase) and the structural protein perilipin, whose phosphorylation induces an important physical alteration of the lipid droplet surface that facilitates initiation of lipolysis and the action of HSL. The sequential hydrolysis of intracellular TG into free fatty acids (FFA) and glycerol is performed by ATGL (adipose triglyceride lipase), HSL, and MGL (monoacylglycerol lipase), which have hydrolytic activity towards TG, diacylglycerols, and monoacylglycerols, respectively (Lafontan & Langin 2009). MGL is constitutively expressed in adipose tissue, leaving HSL and ATGL as the rate-limiting enzymes responsible for regulating TG mobilization. The resulting FFA and glycerol can be released in the blood stream and transported to other organs, mainly liver, skeletal muscle, heart, and brown fat.

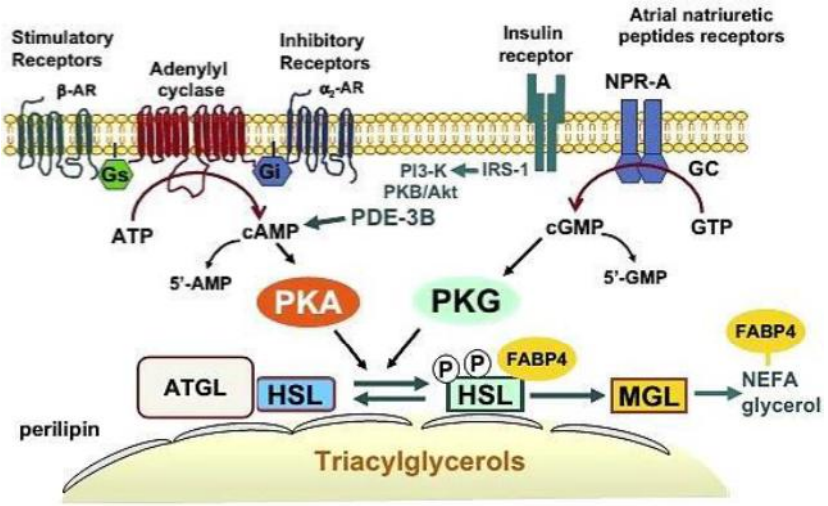

Figure 2: Major pathways involved in the stimulation of lipolysis. ATGL, adipose triglyceride lipase; FABP4, adipocyte fatty acid binding protein 4; GC, guanylyl cyclase; Gi, inhibitory GTP-binding protein; Gs, stimulatory GTP-binding protein; HSL, hormone-sensitive lipase; MGL, monoacylglycerol lipase; NEFA, nonesterified fatty acid; NPR-A, type A natriuretic peptide receptor. Adapted from Lafontan & Langin 2009.

BAT is important in both basal metabolic rate and increased energy expenditure in response to stimuli, e.g. cold, playing an important role in the regulation of body temperature. Thermogenesis is accomplished through the expression of uncoupling protein 1 (UCP1), a 32 kDa protein found in the inner mitochondrial membrane, which uncouples the proton electrochemical gradient generated by the electron transport chain from oxidative phosphorylation (generation of ATP), allowing dissipation of the electrochemical energy as heat. The strong innervation by the SNS regulates BAT activity, which is stimulated by cold exposure (Bartness et al. 2010). It is also an

extremely well vascularized tissue, enabling the supply of oxygen and substrates, as well as the transfer/distribution of heat (Nnodim & Lever 1988).

Intracellularly, FFA undergo β-oxidation to fuel thermogenesis in brown adipocytes, and also act as ligands to the nuclear receptors peroxisome proliferator-activated receptor (PPAR) α/δ, promoting expression of *Ucp1* and OXPHOS genes in order to enhance mitochondrial function (Zechner et al. 2012). Notably, lipolysis is crucial for activation of thermogenesis in brown adipocytes. Long-chain fatty acids resulting from lipolysis are required to activate UCP1, serving as permanently attached UCP1 substrates that help to carry protons through UCP1 (Fedorenko et al. 2012).

In case of chronic calorie excess, adipocytes expand to store triglycerides and prevent lipotoxicity. However, when adipose tissue reaches maximal storage capacity, hyperlipidemia can cause lipotoxicity and ectopic fat accumulation in organs such as the liver, muscle, and heart, leading to the development of insulin resistance and metabolic syndrome (Virtue & Vidal-Puig 2008).

In addition to regulate lipid metabolism, adipose tissue also functions as an endocrine organ, secreting adipocytokines such as leptin, resistin, and adiponectin that modulate systemic metabolism. At the same time it expresses receptors for most of these factors, which warrants an extensive crosstalk at a local and systemic level in response to specific external stimuli or metabolic changes. Leptin signals to the central nervous system (hypothalamus) to promote satiety, glucose homeostasis and energy expenditure, improving insulin sensitivity in liver and muscle (Minokoshi et al. 2002). Adiponectin promotes glucose uptake and FFA oxidation, also contributing to improve insulin sensitivity (Yamauchi et al. 2001), and resistin is an inflammatory molecule with hyperglycemic action (Steppan et al. 2001). Moreover, adipocytes also secrete pro-inflammatory cytokines such as tumor necrosis factor-α (TNF-α), which inhibits insulin signaling and promotes insulin resistance (Galic et al. 2010).

1.2. Adipose tissue remodeling

Adipose tissue is characterized by a marked cellular heterogeneity, comprising adipocytes, pre-adipocytes, fibroblasts, endothelial cells, resident leucocytes and multipotent stem cells able to differentiate into several cell types. Pre-adipocytes have the ability to proliferate and differentiate into mature adipocytes, conferring adipose tissue a constant functional plasticity, which determines its ability to expand throughout life (Moreno-navarrete & Fernández-real 2012). Adipocyte progenitor/stem cells have been located interspersed in the adipose tissue and often contacting with blood vessels (Tang et al. 2008). Within the stromal vascular fraction (SVF) are adipose-derived stem cells (ADSCs), and also strikingly similar mesenchymal stromal cells (MSC), that can differentiate in vitro to adipogenic, chondrogenic and osteogenic lineage (Zeve et al. 2009). Adipocyte progenitors have been identified and isolated using cell surface-markers and lineage tracing. Using fluorescence-activated cell sorting (FACS), adipose progenitor cells were identified as $Lin^-CD29^+CD34^+Sca1^+CD24^+$ cells, losing CD24 expression as they become further committed to the adipocyte lineage ($CD24^-$ adipocyte precursors). Both populations express PDGFRα and are adipogenic in vitro, but only $CD24^+$ cells are capable of generating functional white adipose tissue after transplantation (Berry & Rodeheffer 2013). In vivo, the $CD24^+$ adipocyte progenitors generate the $CD24^-$ adipogenic cell population (pre-adipocytes) that further differentiates into mature adipocytes, expressing the late adipogenic markers PPARγ2 and

CCAAT/enhancer-binding protein (C/EBP) α (Berry & Rodeheffer 2013). PDGFRα$^+$ cells are bipotential adipocyte progenitors because they differentiate into beige adipocytes in adult WAT in response to β-adrenergic stimulation, and differentiate into white adipocytes in adult WAT in response to high-fat feeding (Lee et al. 2012), contributing to adult WAT remodeling. Brown adipocytes in the classical brown fat depots, unlike white adipocytes, are related to the myogenic lineage, characterized by Myf5 expression (Seale et al. 2008). Myf5-expressing precursors give rise to skeletal muscle and brown adipose tissue, providing a potential connection with the energy-burning function of BAT.

1.3. Regulation of white and brown adipocyte differentiation

When appropriately stimulated, immature progenitor/stem cells undergo a multistep process of commitment to the adipocyte lineage. Recruitment to this lineage gives rise to pre-adipocytes, which then undergo multiple rounds of mitosis (mitotic clonal expansion) and differentiate into adipocytes (Tang & Lane 2012). Adipogenesis is a sequential pathway of differentiation involving a cascade of transcription factors and cell-cycle proteins regulating the commitment and differentiation phases of adipocyte development. Members of the family of bone morphogenetic proteins (BMP), specifically BMP2, BMP4 and BMP7, as well as the transcription factors peroxisome proliferator-activated receptor gamma PPARγ and C/EBPs are pivotal to drive these different phases (Figure 2).

BMPs are members of the transforming growth factor-β (TGF-β) superfamily and play a critical role in the commitment of MSCs into the adipocyte lineage. BMP2 and BMP4 promote white adipogenesis, whereas BMP7 activates a full program of brown adipogenesis, suppressing early adipogenic inhibitors, such as Pref-1, and Wnts, and at the same time inducing the key molecular determinant positive regulatory domain containing 16 (PRDM16) that activates the complete brown adipogenesis program and blocks the induction of myotube-specific genes such as Myf5, MyoD and myogenin. PRDM16 binds and coactivates PPARγ with subsequent induction of specific brown fat features, including increased mitochondrial biogenesis and expression of UCP1 (Frühbeck & Gómez-Ambrosi 2013).

Multiple positive and negative regulators of the differentiation program converge upon PPARγ to influence the conversion of immature cells to mature adipocytes. PPARγ is the master regulator of adipogenesis and is both necessary and sufficient for adipocyte differentiation, and is also required for maintenance of the terminal differentiated state of adipocytes. of the three isoforms (PPARγ1, PPARγ2 and PPARγ3), PPARγ2 is the predominant one in primary adipocytes and is more efficient at promoting adipogenesis (Rosen & MacDougald 2006).

Several members of the C/EBP family also play a critical role in adipocyte differentiation, with C/EBPβ and C/EBPδ driving PPARγ expression in the early stages of differentiation, and C/EBPα maintaining PPARγ expression later on in the process. After induction of differentiation, cyclic AMP response element-binding protein (CREB) becomes phosphorylated and activates the expression of C/EBPβ (Zhang et al. 2004). Once expressed PPARγ and C/EBPα positively feedback on each other through their respective C/EBP regulatory elements, this action is presumed to perpetuate the adipocyte phenotype in mature adipocytes (Algire et al. 2013). Although C/EBPα is required for white adipogenesis, PPARγ is the central regulator of adipose differentiation. Sterol regulatory element binding transcription factor 1 (SREBP1c) is expressed in the later stages of

differentiation and promotes transcription of genes encoding lipogenic enzymes, contributing to the adipocyte phenotype (Tang & Lane 2012).

BMP7 triggers the commitment of mesenchymal progenitor cells to brown adipocyte lineage, including induction of early regulators of brown fat program (PGC1α and PRDM16), and also plays a crucial role in embryonic brown fat development (Tseng et al. 2010). Induction of PRDM16 expression in $Myf5^+$ cells directs them to differentiate into brown adipocytes. PRDM16 also coactivates PGC1α, PGC1β, and C/EBPβ, acting as a transcriptional coregulator of the brown fat program. In the absence of PRDM16, these precursor cells will develop into muscle cells (Wu et al. 2013).

Peroxisome proliferator-activated receptor gamma coactivator 1α (PGC1α) is a dominant regulator of mitochondrial biogenesis and oxidative metabolism, and is highly expressed in tissues with high oxidative metabolism, such as the skeletal muscle and BAT. PGC1α is required for basal and cAMP-induced mitochondrial biogenesis and thermogenesis, inducing the expression of UCP1 and key enzymes of the mitochondrial respiratory chain. PGC1α increases the transcriptional activity of a series of nuclear ligand-binding receptors, including PPARα, PPARγ and thyroid hormone receptor (Cannon & Nedergaard 2004). PGC1α-independent mechanisms involved in the controls of UCP1 expression and/or mitochondrial biogenesis include the cell death-inducing DNA fragmentation factor α-like effector A (CIDEA), which is expressed at high levels in BAT and directly interacts with UCP1 suppressing its activity (Gesta et al. 2007).

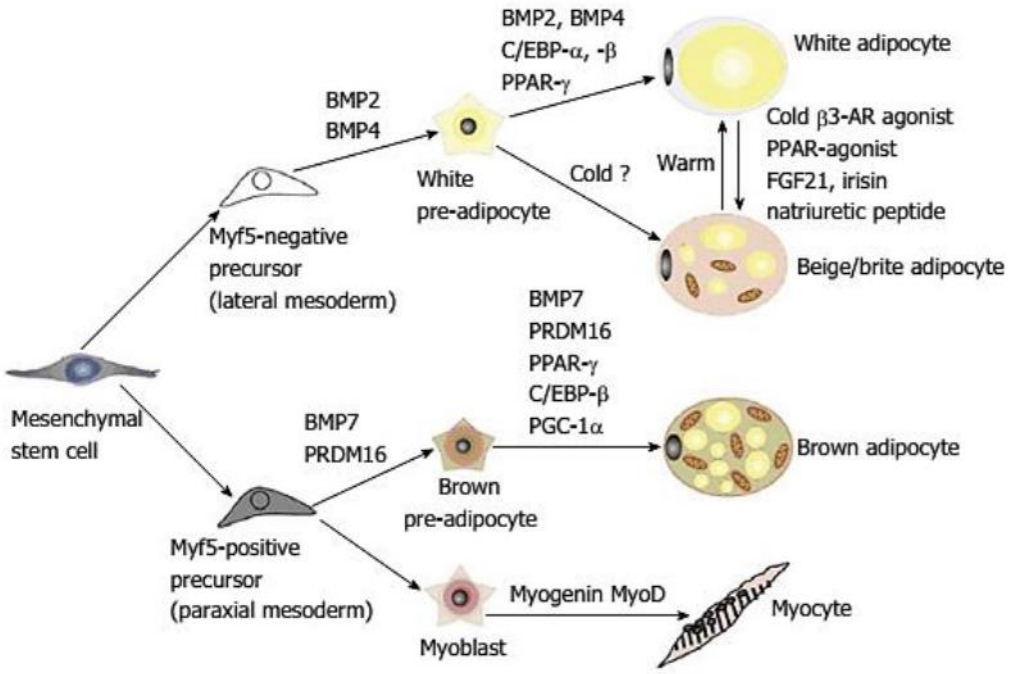

Figure 3: Schematic representation of differentiation of white, beige and brown adipocytes. White and beige adipocytes derive from Myf^- precursors, whereas Myf^+ precursors originate brown adipocytes and myocytes, depending on the expression of PRDM16. From Park et al. 2014.

General markers of adipogenesis include GLUT4, fatty acid-binding protein 4 (FABP4, also known as aP2), lipogenic enzymes, and leptin, and brown adipocytes are characterized by the presence of UCP1, PGC1α, CIDEA and carnitine palmitoyltransferase 1B (CPT1B) (Beranger et al. 2013).

Recruitment of MSC to the adipocyte lineage *in vivo* is stimulated by excessive energy intake over an extended time period. This metabolic state generates signals that induce MSCs to enter the commitment pathway leading to hyperplasia and the preadipocyte phenotype. Several factors have been identified that commit or inhibit the conversion of pluripotent MSCs to the adipocyte lineage, including hormones, cytokines, growth factors and some pharmacological compounds (Moreno-navarrete & Fernández-real 2012).

Insulin, insulin-like growth factor-1 (IGF-1), thyroid hormones, glucocorticoids (GCs) and PPARγ agonists promote differentiation of MSC into adipocytes. Insulin/IGF-1 signalling is crucial for adipogenesis, with loss of insulin-receptor substrates (IRS) inhibiting adipocyte development (Moreno-navarrete & Fernández-real 2012). Thyroid hormone triiodothyronine (T3) plays a central role in normal development, differentiation and metabolic homeostasis, stimulating basal metabolic rate and adaptive thermogenesis, and inducing adipogenic gene expression (Mullur et al. 2014). GCs are potent inducers of adipogenesis in vitro, stimulating nuclear hormone receptors that activate expression of PPARγ and C/EBPδ. Dexamethasone, a synthetic GC, is believed to operate through activation of the GC receptor, and its adipogenic activity results partly from induction of C/EBPα and PPARγ (Zilberfarb et al. 2001).

1.4. Adaptive thermogenesis and adipose tissue 'browning'

Adaptive thermogenesis is a physiological response to cold exposure and diet consisting of regulated heat production mostly by the mitochondria in skeletal muscle and BAT. Cold exposure induces shivering thermogenesis in skeletal muscle and non-shivering thermogenesis in brown fat to maintain body temperature (Tseng et al. 2010). This process is essential for homeothermic animals, ensuring normal cellular and physiological function under environmental challenge.

Thermogenesis is tightly regulated by the SNS and the endocrine system. Increased sympathetic signalling in response to cold exposure promotes NE release which stimulates β-ARs in BAT, promoting lipolysis and thermogenesis by activation of UCP1. In addition, prolonged cold exposure or treatment with β-adrenergic agonists and PPARγ agonists also stimulates the formation of brown-like adipocytes within white adipose depots (beige/brite adipocytes)(Chechi et al. 2013). These beige adipocytes resemble white fat cells in having extremely low basal expression of UCP1, but, like classical brown fat, they respond to cAMP stimulation with high UCP1 expression and respiration rates (Wu et al. 2013). The formation of beige adipocytes is referred to as browning.

In contrast to the classic brown adipocytes, beige cells have been shown to originate from $Myf5^-$ progenitor cells, much like white adipocytes (Chechi et al. 2013), but their development still requires PRDM16 like in BAT. Several molecules have been implicated in the recruitment and development of beige adipocytes. Cyclooxygenase-2 (COX-2) is a rate-limiting enzyme in prostaglandin (PG) synthesis and has been shown to play a role in regulating the recruitment and activation of beige fat in WAT (Vegiopoulos et al. 2010). Prostacyclin (PGI_2) is one of the major prostaglandins and is synthesized from arachidonic acid by COX coupled to PGI_2 synthase (PGIS). PGI_2 signals through a G protein coupled receptor (IP), increasing intracellular cAMP levels and activating PKA or promoting calcium mobilization via phospholipase C activation, and also acts as a PPARγ ligand (Lim & Dey 2002). NE-induced COX-2 activity in WAT promotes MSC differentiation into beige adipocytes, contributing to thermogenesis and systemic energy expenditure.

Adaptive thermogenesis in BAT also depends on local conversion of T4 (thyroxine) to T3 (triiodothyronine) by deiodinase (DIO2) in brown adipocytes (Mena et al. 2013). Agonism of thyroid receptors by the active thyroid hormone (T3) increases *Ucp1* gene expression through direct DNA binding and also potentiates β-adrenergic signalling in brown adipocytes.

1.5. Novel regulator genes of adipose MSC: Sphingosine kinase-1

Subsequent experiments were performed by the research group of Vegiopoulos to gain more insight into the signaling process of MSC activation and browning by $cPGI_2$ and adrenergic stimulation. RNA expression profiling by microarray was used to allow identification of novel intercellular mediators and signaling pathways controlling tissue remodeling in white fat, in particular targets and pathways downstream of $cPGI_2$ in adipose tissue MSCs.

The MSC model used in these experiments consists of $Lin^-CD29^+CD34^+Sca1^+$ adipocyte progenitors isolated from the SVF of white and brown adipose tissue that are differentiated for 8 days using an adipogenic cocktail containing dexamethasone, for the first 2 days, and insulin. The latter was removed 2 days before NE stimulation at day 8 because insulin reduces NE responsiveness. Carbaprostacyclin ($cPGI_2$), a stable analog of PGI_2, is used *in vitro* to promote browning of WAT progenitors. This is a suitable model for white and induced-brown differentiation, as shown by the expression of adipogenic and brown markers (Figure 4).

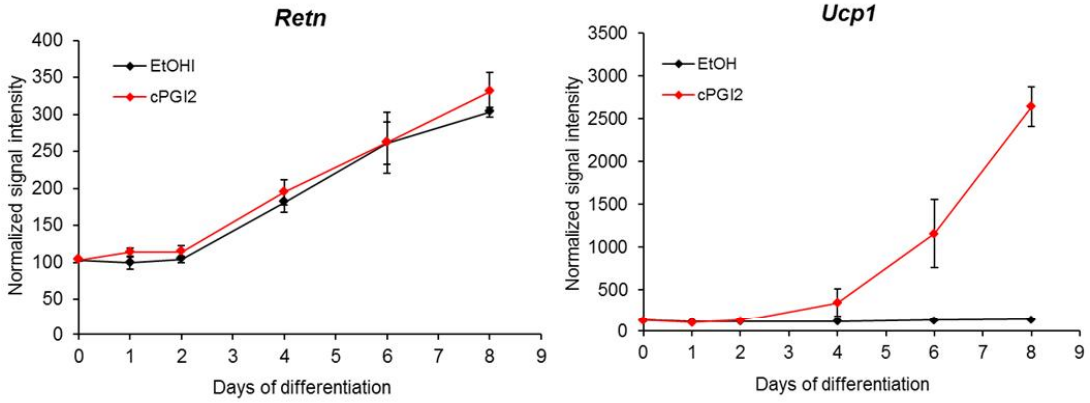

Figure 4: Time course expression of adipogenic marker *Retn* and brown marker *Ucp1* in WAT MSCs. IngWAT MSCs were differentiated with $cPGI_2$ to induce browning, or vehicle (EtOH) as control. Gene expression was analyzed by microarray before induction of differentiation (Day 0) and at different time points during differentiation (Day 1, 2, 4, 6 and 8) (Vegiopoulos, unpublished data).

MSCs were isolated from the SVF of adipose tissue, and differentiated in vitro with and without $cPGI_2$, followed by NE stimulation at day 8 of differentiation. Analysis of differential gene expression identified sphingosine kinase-1 (*Sphk1*) as a gene upregulated by NE stimulation, both in inguinal WAT (Ing) and BAT adipocytes (Figure 3A). Array data from published in vivo experiments using prolonged cold exposure and injection of mice with β3-AR agonist CL316243 (CL) showed that *Sphk1* is induced in WAT by both acute and prolonged stimulation (Li et al. 2005; Xue et al. 2009) (Figure 3B,C). It appears to be quickly induced after stimulation and still maintain high levels of expression after a long time.

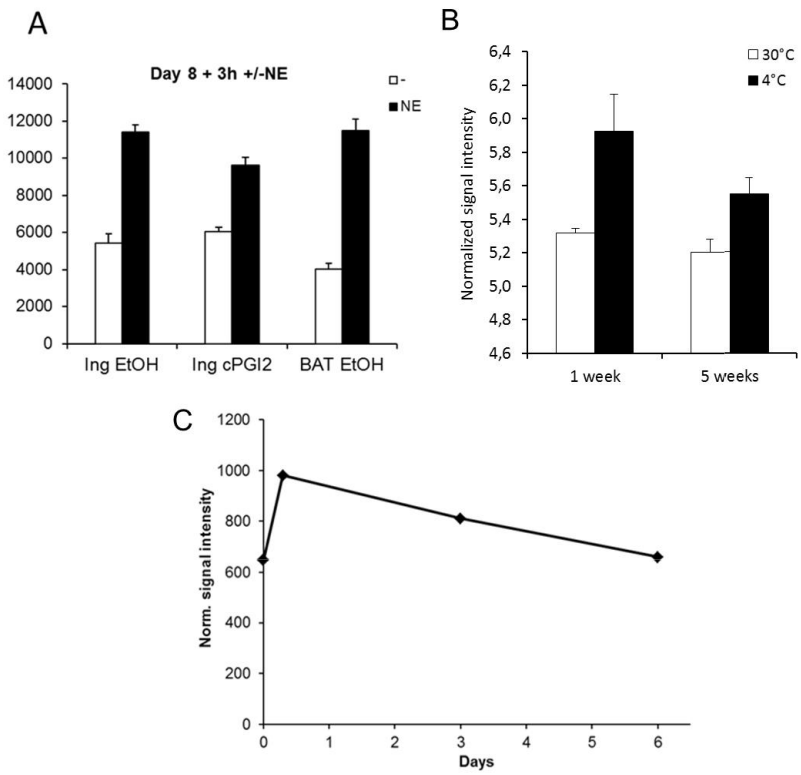

Figure 5: Expression profile of Sphk1 in response to adrenergic stimulation and cold exposure. (A) WAT and BAT MSCs were differentiated with $cPGI_2$ or vehicle (EtOH), and stimulated with NE for 3h at day 8 of differentiation (Vegiopoulos, unpublished data). (B) Male C57/Bl6 mice were exposed to cold (4°C) for 1 week or 5 weeks; controls were kept at 30°C. Microarray data from Xue et al. 2009. (C) CL was administered to male 129S1Sv1mJ mice for 8 hours, 3 or 6 days to mimic cold exposure. Epidydimal fat was used for RNA expression profiling. Microarray data from Li et al. 2005.

The expression profile performed by Vegiopoulos *et al.* also showed that Sphk1 is upregulated by induction of adipogenic differentiation, with and without $cPGI_2$ to induce browning, and the expression levels remain elevated until the final stages of the process (Figure 5), which supports a relevant role for Sphk1 in white adipocyte differentiation and browning.

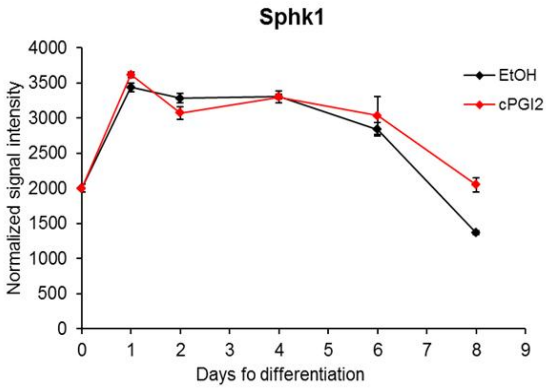

Figure 6: Time course expression profile of Sphk1 in adipogenic differentiation. IngWAT MSCs were differentiated with $cPGI_2$ to induce browning, or vehicle (EtOH) as control. Gene expression was analyzed by microarray before induction of differentiation (Day 0) and at different time points during differentiation (Day 1, 2, 4, 6 and 8) (Vegiopoulos, unpublished data).

1.6. Sphk1 in sphingolipid metabolism

Sphingosine kinase-1 is a key enzyme in the sphingolipid metabolic pathway (Figure 7), and its product, sphingosine-1-phosphate (S1P), is an important lipid mediator that plays a role in many biological processes. Sphingolipids are more than structural membrane components, they are also the source of an important family of bioactive signaling molecules, the sphingolipid metabolites, which regulates numerous physiological and pathological processes. Sphk forms an essential checkpoint that regulates the relative levels of S1P, sphingosine, and ceramide (Hla & Dannenberg 2012). S1P promotes cellular proliferation, stimulates survival and protects against apoptosis (Cuvillier et al. 1996). By contrast, its precursors, ceramide and sphingosine are associated with cell-growth arrest and are important regulatory components of stress responses and apoptosis. As these metabolites are interconvertible and have opposing effects on cell fate, it has been proposed that the balance between levels of S1P versus sphingosine and ceramide acts as a 'cellular rheostat' that determines cell survival or death (Alvarez et al. 2007a).

Two isozymes have been cloned and characterized in mammals, Sphk1 and Sphk2, and both have a broad and overlapping tissue distribution, with SphK1 predominating in lung and spleen and SphK2 predominating in the heart, brain and liver (Liu et al. 2000). In vivo, SphK1 and SphK2 are at least partially redundant, because the double Sphk1/Sphk2 knockout is lethal, in contrast to the respective single knockout mice, which are viable (Olivera et al. 2013). Numerous agonists activate SphK1, including growth factors, hormones, pro-inflammatory cytokines, lipopolysaccharide, and many GPCR ligands, and this activation is crucial for their full actions (Pitson 2011). Most agonists induce extracellular signal-regulated kinase (ERK)-dependent phosphorylation of SphK1, leading to its translocation from the cytosol to the plasma membrane where its substrate sphingosine resides. In contrast to SphK1, which is localized mainly in the cytosol, SphK2 is present in several intracellular compartments, depending on cell type, and much less is known about its activation (Maceyka et al. 2012).

Intracellular S1P levels are regulated tightly by the equilibrium between its formation, catalyzed by sphingosine kinases, and its degradation, catalyzed by S1P lyase and S1P phosphatases (Alvarez et al. 2007a). S1P produced in response to agonists has the ability to function intracellularly as a second messenger or after secretion in an autocrine/paracrine fashion to activate S1P receptors present on the surface of the same cell or on nearby cells. There are five specific cell surface G-protein-coupled receptors for S1P, termed S1PR1–5, all with low nanomolar dissociation constants (Pham et al. 2008). Concentrations of S1P in blood and lymph plasmas are high, in the high nanomolar to low micromolar ranges, whereas S1P concentrations in tissues are kept low, creating an S1P gradient important to regulate its biological functions. Differential signaling induced by binding of S1P to these receptors is due to distinct, though sometimes overlapping, coupling to diverse heterotrimeric G proteins. Cellular and temporal expression of S1PRs determines their specific role in various organ systems, but they are particularly critical for regulation of the cardiovascular, immune, and nervous systems, with the most well-known contributions of S1PR signaling being modulation of vascular barrier function, vascular tone, and regulation of lymphocyte trafficking. Expression patterns of the five S1PRs vary in tissues and also during development and ageing. S1P1, S1P2, and S1P3 are essentially ubiquitously expressed, whereas expression of S1P4 and S1P5 are highly restricted to distinct cell types (Blaho & Hla 2014).

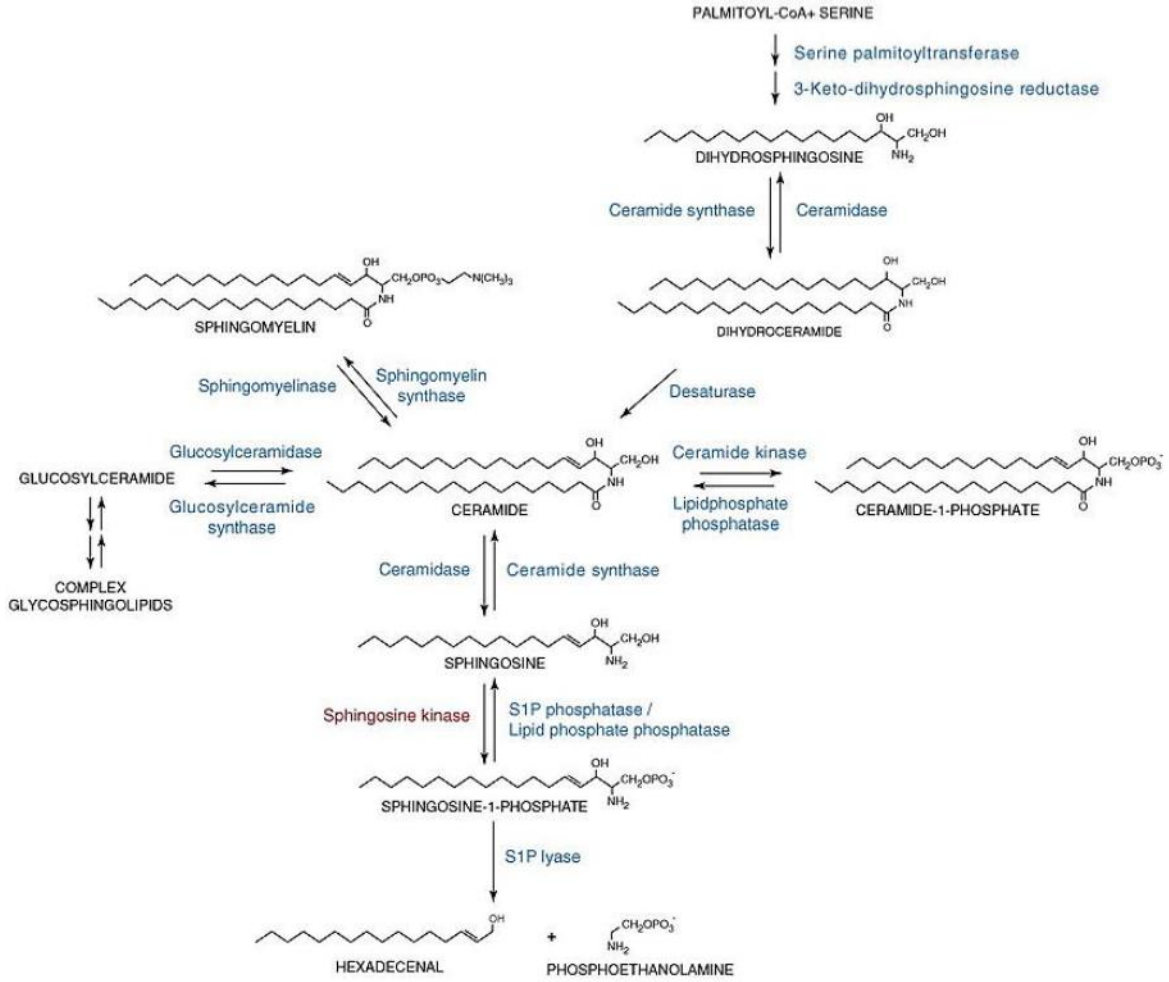

Figure 7: Sphingolipid biosynthetic and degradation pathways. Sphingolipid structures are shown, along with the key metabolic enzymes involved in their formation and degradation. Sphingosine kinase is highlighted in red. From Pitson 2011.

In order to maintain elevated extracellular concentrations for the formation of a gradient, S1P is secreted via specific transporters. Plasma S1P is bound to HDL (~65%) and albumin (~30%), and studies suggest that the beneficial property of HDL to reduce the risk of cardiovascular disease may in part depend on S1P (Argraves & Argraves 2007). In contrast to S1P, ceramide in plasma is associated mostly with VLDL and LDL.

The most well characterized effects of S1P are on vascular and immune systems. In the vascular system, S1P activation of its receptors regulates vascular tone, vascular permeability, angiogenesis, atherosclerosis, and heart function (Hla & Dannenberg 2012). In the immune system, the S1P gradient is critical for migration of immune cells from secondary lymphoid organs into the circulatory system, also playing a relevant role in inflammatory response.

SphK1 and increased S1P levels enhance proliferation, expedite the G1–S transition of the cell cycle and increase DNA synthesis (Olivera et al. 1999). In addition, SphK1 protects against apoptosis by inhibiting the mitochondrial or intrinsic death pathway, blocking the stress-activated protein kinase, Jun amino-terminal kinase (JNK), and by activating nuclear factor κB (NF-κB) (Spiegel & Milstien 2003).

1.7. Ceramide in obesity

Formation of S1P by Sphk1 is part of the ceramide degradation pathway, contributing to clearance of excessive ceramide. Extracellular stimuli such as cytokines, hormones, and cell stress induce sphingolipid synthesis, lead to the accumulation of ceramides and ceramide metabolites. Ceramides are increased in serum, skeletal muscle and liver of obese rodents and humans, and correlate negatively with insulin sensitivity and positively with circulating IL6, thereby playing an important role in the development of insulin resistance and low-grade chronic inflammation present in obesity (Kolak et al. 2012). Several reports using both in vitro and in vivo model systems have implicated ceramide accumulation in the pathogenesis of multiple diseases associated with obesity, including diabetes, cardiomyopathy, and atherosclerosis (Chavez & Summers 2012).

The mechanism by which ceramide induces insulin resistance results mostly by blocking Akt/PKB signaling necessary for translocation of GLUT4 to the plasma membrane, thus preventing insulin-stimulated glucose uptake (Summers et al. 1998). In addition to mediating nutrient handling, Akt activates anabolic pathways (e.g., glycogen and protein synthesis) while inhibiting catabolism, leading to a marked upregulation in nutrient storage. Akt also activates prosurvival and inhibits autophagic enzymes, leading to a net increase in cellular growth and stability (Bikman & Summers 2011).

Obesity-induced accumulation of saturated fats leads to activation of toll-like receptors (TLRs), which induce the transcription of inflammatory cytokines such as TNFα, and also increase ceramide synthesis, contributing to insulin resistance (Holland, Bikman, et al. 2011).

Impaired mitochondrial function has also been associated with insulin resistance. Mitochondria possess the enzymes for ceramide synthesis, and ceramide accumulation in mitochondria has been shown to alter membrane permeability, inhibit electron transport chain intermediates, and promote oxidative stress, leading to induction of apoptosis (Siskind 2005). Adiponectin has opposing actions to ceramide, promoting improvement of metabolic syndrome and insulin resistance, and many of its effects are primarily mediated by activation of ceramidase activity and reduction of ceramide levels, which is converted to the pro-survival sphingolipid S1P (Holland, Miller, et al. 2011).

1.8. Objective of the study

Sphingolipid metabolism and signaling have been explored in the context of obesity and associated pathological states, such as diabetes, cardiovascular disease, chronic inflammation, and cancer. Little is still known about the molecules and pathways regulating adipose MSC and tissue remodeling. Given the relevance of sphingosine kinase and S1P in many physiological processes related to adipose tissue and metabolic syndrome, it is of interest to investigate their role in adipose tissue development and remodeling. This work aimed to answer the following questions:

i. What is the function of Sphk1 in the regulation of MSC activation, proliferation, and induced brown differentiation?

ii. What is the role of Sphk1 in the regulation of mature adipocyte function?

As experimental strategy, loss-of-function experiments using siRNAs against Sphk1 were performed in MSCs isolated from brown and white adipose tissue. The knockdown was performed before induction of differentiation to investigate the role of Sphk1 in MSC activation, proliferation and differentiation. To assess the role of Sphk1 in mature adipocyte function independently of differentiation effects, the knockdown was performed at a late stage of the differentiation process. WAT MSCs were stimulated with $cPGI_2$ throughout the differentiation process to induce a brown phenotype, and differentiated MSCs were stimulated with NE to assess responsiveness to adrenergic stimulation. Read outs included quantification of expression of brown and adipogenic marker genes (i, ii), analysis of NE-stimulated lipolysis (ii), and analysis of cell cycle and apoptosis (i).

2. Materials and Methods

2.1. Materials

Solutions and buffers

Krebs-Ringer Buffer (KRB):
115 mM NaCl
5.9 mM KCl
1.2 mM $MgCl_2$
1.2 mM NaH_2PO_4
1.2 mM Na_2SO_4
2.5 mM $CaCl_2$
25 mM Na_2CO_3
Diluted in H_2O
Adjust pH to 7.4

KRB supplemented:
5% BSA
5 mM glucose
25 mM HEPES/KOH pH 7.4

PBS 1% BSA 50ml:
0.5 g BSA
50 ml PBS (1x)

Click-it reaction cocktail (1x):
219 µl PBS (1x)
5 µl copper protectant
1,25 µl fluorescent dye Alexa 647
25 µl reaction buffer additive (1x)

10x binding buffer:
0.1 M Hepes (pH 7.4)
1.4 M NaCl
25 mM $CaCl_2$

Collagenase solution 5ml:
83,2 µl BSA 30%
75 µl HEPES (1M)
500 µl FCS
25 µl DNaseI (10mg/ml)
4,3 ml DMEM
16 ml $CaCl_2$ (1M)
7,5 mg Collagenase

BSA buffer 50ml:
49,1 ml PBS (1x)
835 µl 30% BSA
100 µl 0,5M EDTA

Cell culture additives

Cell culture aditives	Stock
Recombinant murine bFGF	100 µg/ml in D-PBS, 0.1% BSA
Dexamethasone	250 µM in H_2O, 50% ethanol
Recombinant human insulin (from yeast)	1 mg/ml in H_2O, 16.67 mM HCl
Triiodo-L-Thyronine (T3)	30 µM (-20°C) in H_2O, 20 mM NaOH
Carbaprostacyclin ($cPGI_2$)	10 mM in ethanol
L-(-)-norepinephrine bitartrate (NE)	10 mM in H_2O
DNase I	10 mg/ml in water

siRNAs

Stealth siRNA duplexes	Catalog #	Company
Sphk1 MSS247715(3_RNAI)	MSS247715	Invitrogen, Karlsruhe, Germany
Sphk1 MSS247716(3_RNAI)	MSS247716	Invitrogen, Karlsruhe, Germany
Sphk1 MSS247717(3_RNAI)	MSS247717	Invitrogen, Karlsruhe, Germany
Stealth RNAi™ siRNA Negative Control, Med GC	12935-300	Ambion

RT-qPCR probes

Taqman gene expression assays from Applied Biosystems

Gene	Assay ID	Gene name
Acaca	Mm01304279_m1	Acetyl-Coenzyme A carboxylase alpha
Cidea	Mm00432554_m1	Cell death-inducing DNA fragmentation factor α subunit-like effector A
Cox7a1	Mm00438297_g1	Cytochrome c oxidase, subunit viia 1
Cox8b	Mm00432648_m1	Cytochrome c oxidase, subunit viiib
Dio2	Mm00515664_m1	Deiodinase, iodothyronine, type II
Fabp4	Mm00445880_m1	Fatty acid binding protein 4, adipocyte
Fasn	Mm00662319_m1	Fatty acid synthase
Lipe	Mm00495359_m1	Hormone-sensitive lipase
Plin1	Mm00558672_m1	Perilipin 1
Pnpla2	Mm00503040_m1	Patatin-like phospholipase domain containing 2
Pparg	Mm00440945_m1	Peroxisome proliferator activated receptor gamma
Prdm16	Mm00712556_m1	PR domain containing 16
Retn	Mm00445641_m1	Resistin
Scd1	Mm00772290_m1	Stearoyl-Coenzyme A desaturase 1
Sphk1	Mm00448841_g1	Sphingosine kinase 1

Self-made probes	Sequence (5' → 3')	
Tbp - TATA box binding protein	primer for	TTGACCTAAAGACCATTGCACTT
	primer rev	TTCTCATGATGACTGCAGCAAA
	probe	TGCAAGAATGCTGAATATAATCCCAAGCG
Pgc1α - PPAR γ co-activator 1	primer for	GATGGCACGCAGCCCTAT
	primer rev	CTCGACACGGAGAGTTAAAGGAA
	probe	CATTGTTCGATGTGTCGCCTTCTTGCT
Cebpα - CCAAT/enhancer binding protein α	primer for	AAAGCCAAGCCGTCGGTGGAC
	primer rev	CTTTATCTCGGCTCTTGCGC
	probe	CGAGTACCGGGTACGGCGGGAAC
Cebpβ - CCAAT/enhancer binding protein β	primer for	AAGCTGAGCGACGAGTACAAGA
	primer rev	GTCAGCTCCAGCACCTTGTG
	probe	CGAGCGCAACAACATCGCGG
Ucp1 – uncoupling protein 1	primer for	CCTTCCCGCTGGACACTG
	primer rev	CCTAGGACACCTTTATACCTAATGGT
	probe	CAAAGTCCGCCTTCAGATCCAAGGTG

Antibodies

Antibodies	Isotype	Company, catalogue number
CD16/32 (FcBlock)	Rat	ebioscience/Natutec, 14-0161-82
Ter119-biotin	Rat	ebioscience/Natutec, 13-5921-81
CD31-biotin	Rat	ebioscience/Natutec, 13-0311-81

CD45-biotin	Rat	ebioscience/Natutec, 13-0451-81
UCP1	Rabbit	Abcam, ab10983
Anti-rabbit IgG Alexa Fluor 488	Goat	Invitrogen, A11070
Annexin V-FITC		BD Pharmingen, 556420

Kits

Kit	Distributor
Click-iT Plus EdU Alexa Fluor 647 Flow Cytometry Assay Kit	Life Technologies, Darmstadt, Germany
NEFA-HR(2) kit	Wako, Neuss
QuantiTect Reverse Transcription Kit	Qiagen, Hilden, Germany
QuantiTect SYBR Green PCR kit	Qiagen, Hilden, Germany
RNeasy Micro Kit	Qiagen, Hilden, Germany

Chemical and reagents

Chemical	Distributor
4',6-Diamidino-2-phenyindole (DAPI), dilactate	Sigma, Munich, Germany
Bovine serum albumin (BSA)	Sigma, Munich, Germany
Calcium chloride ≥98% dried power	Roth, Karlsruhe, Germany
Carbaprostacyclin ($cPGI_2$)	Cayman/BIOZOL
Chloroform	DKFZ, Germany
Collagenase Type ll	Sigma, Munich, Germany
D-(+)-Glucose anhydrous	Applichem, Darmstadt, Germany
Dexamethasone	Sigma, Munich, Germany
DMSO (Dimethyl sulfoxide)	Sigma, Munich, Germany
DNase I	Roche, Mannheim, Germany
Dulbecco's modified Eagle's medium (DMEM) high glucose	Invitrogen, Karlsruhe, Germany
Dulbecco's Phosphate Buffered Saline (D-PBS) (1X)	Invitrogen, Karlsruhe, Germany
EDTA (Ethylenediaminetetraacetic acid)	Sigma, Munich, Germany
Ethanol (99%)	DKFZ, Germany
Fetal calf serum (FCS)	Invitrogen, Karlsruhe, Germany
FxCycle™PI/RNase Staining Solution	Life Technologies, Darmstadt, Germany
HCS LipidTOX™ Red Neutral Lipid Stain	Life Technologies, Darmstadt, Germany
HEPES	Invitrogen, Karlsruhe, Germany
IBMX (3-isobutyl-1-methylxanthine)	Sigma, Munich, Germany
Insulin human (recombinant yeast)	Sigma, Munich, Germany
Isopropanol	Sigma, Munich, Germany
Laminin	Santa Cruz, Dallas, USA
Lipofectamine RNAiMax Reagent	Invitrogen, Karlsruhe, Germany

Magnesium chloride ($MgCl_2$)	Sigma, Munich, Germany
Norepinephrine	Sigma, Munich, Germany
optiMEM	Invitrogen, Karlsruhe, Germany
Paraformaldehyde	Sigma, Munich, Germany
Penicillin / Streptomycin (P/S)	Invitrogen, Karlsruhe, Germany
Potassium chloride (KCl)	Sigma, Munich, Germany
Qiazol Lysis Reagent	Qiagen, Hilden, Germany
Rec. murine bFGF	R&D systems, Wiesbaden, Germany
Sodium carbonate decahydrate ($Na_2CO_3 \cdot 10H_2O$)	Merck, Darmstadt, Germany
Sodium chloride (NaCl)	Sigma, Munich, Germany
Sodium dihydrogen phosphate monohydrate ($NaH_2PO_4 \cdot H_2O$)	Applichem, Darmstadt, Germany
Sodium hydroxide (NaOH)	Sigma, Munich, Germany
Sodium sulfate anhydrous (Na_2SO_4)	Applichem, Darmstadt, Germany
Sphingosine-1-phosphate (S1P)	Biomol, Hamburg, Germany
TaqMan Gene Expression Mastermix	Life Technologies, Darmstadt, Germany
Triiodo-L-Thyronine (T3)	Sigma, Munich, Germany
Trypsin-EDTA solution	Invitrogen, Karlsruhe, Germany
UltraPure DNaseRNase-Free Distilled Water	Invitrogen, Karlsruhe, Germany

Consumables

Consumable	**Distributor**
10 cm petri dishes	Greiner, Kremsmünster, AU
24-well cell culture plates	Neolab
48-well cell culture plates	Neolab
6-well cell culture plates	Neolab
Anti-Sca1 MicroBeads	Miltenyi Biotec
BIOCOAT Laminin-coated 24-well plates	BD Falcon
Filters (0.22 µm)	Millipore, Eschborn
Filters (0.45 µm)	Millipore, Eschborn
Gloves (Gentle Skin)	Meditrade, Kiefersfelden
Gloves (Safe Skin Purple Nitrile)	Kimberly Clark, BE
Micro test tubes (1.5 ml, 2 ml)	Steinbrenner, Wiesenbach
MicroAmp Fast Optical 96 well	Applied Biosystems, Darmstadt
MicroAmp Optical Adhesive Film	Applied Biosystems, Darmstadt
MS Columns	Miltenyi Biotec
Octo MACS Separator Starter Kit	Miltenyi Biotec
Pasteur pipettes	Brand, Wertheim
PCR tubes (200 µl)	Eppendorf, Hamburg
Petri dishes	Greiner, Kremsmünster, AU
Pipette tips (0.1 – 1000 µl)	Starlab, Helsinki, FI
Pipette tips (0.1 – 1000 µl) (Tip One Filter Tips)	Starlab, Helsinki, FI

Pre-Separation Filters	Miltenyi Biotec
Safelock micro test tubes (1.5 ml and 2 ml)	Eppendorf, Hamburg
Serological pipettes (5 ml, 10 ml, 25 ml, 50 ml)	BD Biosciences, San Jose, USA
Streptavidin MicroBeads	Miltenyi Biotec
Syringes (5ml, 10 ml, 50ml Luer Lock)	Terumo, Leuven
Test tubes (15 ml and 50 ml)	Falcon, Gräfeling-Lochham
Tissue culture dish (10 cm)	Falcon, Gräfeling-Lochham

2.2. Methods

2.2.1. Cell Biology

All experiments with cells were performed under sterile conditions. Cells were cultivated at 37°C, 5% CO_2 and 95% humidity. All media and additives were warmed to 37°C prior to use.

General culture medium: DMEM high glucose with 10% FCS, 1% P/S and freshly added 10 ng/ml bFGF.

Thawing of BATkl2 cell line

Cells were stored in liquid nitrogen tanks in 1 ml aliquots containing $5x10^5$ cells in freeze medium. Following thawing at 37°C in waterbath, cells were added dropwise to 5 ml warm culture medium, spin down at 300 *g* for 2 minutes at RT and resuspended in 1 ml culture medium. Cells were seeded in 6-well tissue culture plates previously coated with 0.2% gelatin, in 2 ml culture medium. Gelatin coating was done by incubating cell culture plates with a 0.2% gelatin solution for 15 minutes at 37°C. Medium was changed 24 hours after seeding to remove remaining DMSO.

Cultivation of BATkl2 cell line

BATkl2 cells were cultivated on 10 cm tissue culture dishes in 10 ml culture medium or 6-well tissue culture plates in 2 ml culture medium for expansion. A confluency of 80% as well as a passage of 14 was not exceeded to avoid diminished differentiation capacity.
For passaging, cells were first washed with 1x PBS and trypsinized, and the detached cells were resuspended in 10 ml fresh culture medium without bFGF. Cell suspension was centrifuged at 300 *g* for 2 minutes and the pellet was resuspended in 1 ml fresh culture medium with bFGF for counting. Viable cell count was performed using a Neubauer counting chamber and a 1:1 dilution with Trypan blue. According to experimental design cells were seeded in 24-well cell culture plates previously coated with 0.2% gelatin at a density of 2.5×10^4 cells per well. Culture medium was changed every 2 days and cells were passed every 3-4 days.

Adipogenic differentiation of BATkl2 cell line

BATkl2 cells were differentiated into adipocytes by the addition of dexamethasone, insulin, T3 and 3-isobutyl-1-methylxanthine (IBMX). Cells were cultivated on 0.2% gelatin-coated 24-well cell culture plates in culture medium until reaching 90-100% confluency, and then induced to undergo differentiation by replacing culture medium with differentiation medium as shown in Table 1.

Table 1: Differentiation media for BATkl2 cell line.

Differentiation day	Medium	Composition
0 and 1	Differentiation induction medium	DMEM 10% FCS 1% P/S 500nM Dexamethasone 1 µg/ml Insulin 3 nM T3 500 µM IBMX
2 to 5	Maturation medium (replaced every 2 days)	DMEM 5% FCS 1% P/S 1 µg/ml Insulin 3 nM T3
6 and 7	Final medium	DMEM 5% FCS 1% P/S

Experiments were performed at day 8 of differentiation. Cells were stimulated with 0.5 µM NE for 3 hours before harvesting for RNA isolation.

Isolation of Lin^-Sca^+ adipocyte progenitors (MSC) from adipose tissue

Lin(Ter119, CD31, CD45)-negative/Sca-1-positive progenitors were isolated from inguinal white adipose tissue or from interscapular brown adipose tissue depots of female NMRI mice aged 7-8 weeks old. Mice were sacrificed by cervical dislocation, sterilized with 80% ethanol and adipose tissue depots were dissected. The fat pads were rinsed in 1x D-PBS, minced until no pieces could be observed and subsequently digested in 8-12 ml collagenase solution (DMEM containing 1.5 mg/ml type II collagenase, 3.2 mM HEPES, 0.05 mg/ml $CaCl_2$, 1.5 mg/ml DNase I, 10% FCS and 0.5% BSA), first incubated in 37°C waterbath for 10 minutes and then transferred to 37°C shaker at 140 rpm for 30-40 minutes until a good digestion could be observed. The digestion solution was strained through 300 µm nylon mesh (autoclaved), centrifuged at 145 *g* for 10 minutes at 20°C. The pellet was resuspended in 12 ml BSA buffer (1x D-PBS, 0.5% BSA and 1 mM EDTA) and centrifuged at 300 *g* for 5 minutes at 20°C. The resulting pellet was resuspended in BSA buffer (1 ml for WAT and 0.5 ml for BAT), incubated with CD16/32 antibody (2 µl/100 µl) for 5-10 minutes on ice, followed by incubation with 1 µl/100 µl Ter119-biotin, CD31-biotin, and CD45-biotin antibodies for 30 minutes on ice. After centrifugation at 300 *g* for 5 minutes at 4°C, the pellet was washed with 9x volume BSA buffer and centrifuged again with the same settings. MS Columns (Miltenyi Biotec) were prepared according to pellet size, with an average of 2-4 (WAT) or 4-6 (BAT) mice /column. The pellet was resuspended in 180 µl BSA buffer per column, and incubated with 20 µl Streptavidin MicroBeads (Miltenyi Biotec) per column for 15 minutes on ice. The cell-bead suspension was washed with 4 ml BSA buffer, centrifuged at 300 *g* for 5 minutes at 4°C, and resuspended in 1 ml BSA buffer/column. The columns were prepared with 1 ml BSA buffer, and 1 ml suspension was applied per column while passing through Pre-Separation Filters (Miltenyi Biotec), followed by elution with 3x 0.5 ml BSA buffer and collection of the flow-through. After centrifugation at 300 *g* for 5 minutes at 4°C, the cell pellet was resuspended in 80

µl BSA buffer per 4 mice (WAT) or per 12 mice (BAT), and incubated with 20 µl Anti-Sca1 Microbeads (Miltenyi Biotec) per 80 µl suspension for 15 minutes on ice. Following a washing step with 10x volume BSA buffer and centrifugation at 300 *g* for 10 minutes at 4°C, the cell-bead pellet was resuspended in 500 µl BSA buffer per 4 (WAT) or 12 (BAT) mice before applying to the second column, previously prepared with 500 µl BSA buffer. The columns were washed 3x with 500 µl BSA buffer, removed from the magnet and 1 ml BSA buffer was applied and plunged through to collect the cells. The cell suspension was centrifuged at 300 *g* for 5 minutes at 4°C, and the cells were resuspended in 1 ml culture medium for counting and plated according to experimental design. Cells were washed every 2 days with warm culture medium until the desired confluency was reached.

Adipogenic differentiation of MSCs

Adipose tissue MSCs were differentiated into adipocytes by the addition of dexamethasone, insulin and T3. Cells were cultivated on laminin-coated 24-well culture plates in culture medium until reaching 90-100% confluency, and then induced to undergo differentiation by replacing culture medium with differentiation medium as shown in Table 2. After 2 days the induction medium was replaced by maturation medium, changed every 2 days, until the final medium was added to the cells. To induce browning, media was changed daily with freshly added 1 µM $cPGI_2$ and the same volume of ethanol (vehicle) was added to controls.

Table 2: Differentiation media for adipocyte progenitors.

Differentiation day	Medium	Composition
0 and 1	Differentiation induction medium	DMEM 10% FCS 1% P/S 500nM Dexamethasone 1 µg/ml Insulin 3 nM T3
2 to 5	Maturation medium	DMEM 5% FCS 1% P/S 1 µg/ml Insulin 3 nM T3
6 and 7	Final medium	DMEM 5% FCS 1% P/S

Experiments were performed at day 8 of differentiation. Cells were stimulated with 0.5 µM NE for 3 hours before harvesting for RNA isolation.

siRNA transfection

BATkl2 cells and adipocytes progenitors were transfected with Lipofectamine RNAiMAX transfection reagent (Life Technologies). Cells were plated at a density of 2-2.5x10^4 cells/well and transfected at 60-70% confluency. Per well, 2 µl of the reagent was added to 16 µl of serum free OptiMEM medium, and 10 pmol of siRNA were dissolved in 16 µl of serum free OptiMEM medium. Both mixtures were combined in a 1:1 ratio and incubated for 5 minutes at RT to allow complex formation. The siRNA/Lipofectamine mixture was diluted in culture medium without P/S, in case the transfection was done before differentiation induction, or maturation medium without P/S, in case of transfection post-differentiation induction, and added to the cells. Medium change

was performed after 24 hours, according to experimental design. Target siRNAs, positive and negative controls were added at a final concentration of 20 nM per well.

Lipolysis Assay

Lipolysis assay was performed at day 8 of differentiation. After pre-incubation in Krebs Ringer buffer for 2 hours, cells were stimulated with 0.5 µM NE for 3 hours in Krebs Ringer buffer supplemented with 5% BSA, 5 mM glucose, 25 mM HEPES/KOH pH 7.4. Supernatants were harvested for NEFA measurement.

Apoptosis assay with FITC-AnnexinV staining

Assessment of cell death by apoptosis was performed by staining the cells with FITC-AnnexinV and analysis by flow cytometry. In apoptotic cells, the membrane phospholipid phosphatidylserine (PS) is translocated from the inner to the outer leaflet of the plasma membrane, thereby exposing PS to the external cellular environment. Annexin V is a phospholipid-binding protein with high affinity for PS, and binds to cells with exposed PS. When conjugated to a fluorochrome like FITC, AnnexinV serves as a sensitive probe for flow cytometry analysis of cells that are undergoing apoptosis. FITC Annexin V staining precedes the loss of membrane integrity which accompanies the latest stages of cell death resulting from either apoptotic or necrotic processes. Therefore, this staining is typically used in conjunction with a vital dye, such as propidium iodide (PI), to distinguish between viable and non-viable cells. Viable cells with intact membranes exclude PI, whereas the membranes of dead and damaged cells are permeable to PI. Viable cells are both Annexin V and PI negative, while cells that are in early apoptosis are Annexin V positive and PI negative, and cells that are in late apoptosis or already dead are both Annexin V and PI positive.

To determine the effects of Sphk1 KD in MSC viability and differentiation, cells were transfected and analyzed 24h after transfection (before differentiation induction) and at day 4 of differentiation. Both old medium and wash PBS were collected and centrifuged together with trypsinized cells at 300 *g* for 4 minutes. Pelleted cells were washed with cold PBS, centrifuged again and resuspended in 100 µl 1x binding buffer (10x binding buffer: 0.1M HEPES pH 7.4, 1.4 M NaCl, 25 mM $CaCl_2$). 5 µl of FITC-Annexin V and 10 µl of PI stock solution 50 µg/ml were added to each sample, followed by gentle vortex and incubation for 15 minutes at RT in the dark. Afterwards, 150 µl of binding buffer was added to the cells, which were put on ice until analyzed by flow cytometry. Cells were gated for size, and single stainings were used to gate PI positive/negative populations and Annexin V positive/negative populations.

Cell cycle analysis by EdU labeling

Cell proliferation can be assessed by direct measure of DNA synthesis. EdU (5-ethynyl-2´-deoxyuridine) is a nucleoside analog to thymidine and is incorporated into DNA during active DNA synthesis. Detection is based on a click reaction between EdU and a picolyl azide coupled to a dye,

which can then be detected by flow cytometry. Click-iT® Plus EdU Flow Cytometry Assay Kit (Life Technologies) was used for this assay, with the dye Alexa 647.

Cells were incubated with 10 µM EdU for 3 hours. After EdU pulse the cells were trypsinized, pelleted by centrifugation at 300 *g* for 4 minutes, washed with 3 ml PBS 1% BSA and centrifuged again. Cells were resuspended in 100 µl of fixative (4% PFA), vortexed gently to prevent clumping and incubated for 15 minutes at RT in the dark. After wash with 3 ml PBS 1% BSA, cells were centrifuged and resuspended in 100 µl saponin-based permeabilization and wash reagent. The Click-it reaction cocktail was prepared according to the table provided by the manufacturer, and 250 µl was added per sample, followed by gentle vortex and incubation for 30 minutes at RT in the dark. Cells were then washed in 3 ml saponin-based permeabilization and wash reagent, centrifuged and resuspended in 150 µl FxCycle™PI/RNase Staining Solution (Life Technologies), gently vortexed and incubate for 15-30 minutes at RT in the dark. The tubes were placed on ice until analyzed by flow cytometry.

Cells were gated for size and doublet exclusion, followed by compensation of PI and Alexa 647 in the respective channels. Cells were also gated as G1 and S/G2/M depending on the amount of EdU incorporated.

Immunocytochemistry

Cell nuclei were stained with DAPI to obtain an estimate of cell proliferation in response to S1P treatment. At day 8 of differentiation with S1P, cells were washed twice with PBS and fixed in 4% PFA at RT for 10 minutes. After being washed 3 times with PBS, cells were incubated in PBS with DAPI in 1:10 000 dilution at RT for 30 minutes, protected from light. After incubation, cells were washed twice with PBS and imaged using a Zeiss Cell Observer fluorescence microscope (Carl Zeiss, Jena, Germany). The images were analyzed using AxioVision Software (Carl Zeiss, Jena, Germany), and mean total intensity was determined using Fiji Software (open source).

2.2.2. Molecular Biology

RNA isolation from BATkl2 cell line

Cells were harvested in 1 ml QIAzol (Qiagen), transferred to RNase free 1.5 ml safe-lock Eppendorf tubes and stored at -80°C until processing. After thawing at 4°C, 200 µl of chloroform was added to the lysates. Mixtures were shaken vigorously for 15 sec and allowed to stand on ice for 5-10 minutes for phase separation. After centrifugation at 13000 rpm for 15 minutes at 4°C, the upper aqueous phase containing RNA was transferred to fresh RNase-free 1.5 ml tubes and 1 volume of isopropanol was added, mixed thoroughly and stored at -80°C for at least 20 minutes. Thawed samples were centrifuged at 13000 rpm for 30 minutes at 4°C and the supernatant was removed. RNA pellet was washed twice with 75% ethanol (900 µl for the first wash and 600 µl for the second) and centrifuged at 13000 rpm for 10 minutes at 4°C. The supernatant was aspirated and the remaining ethanol was evaporated at 60°C. The pellets were dissolved in 20 µl RNase-free water and incubated at 60°C for 10 minutes with shaker at maximum speed to increase solubilisation. Samples were stored at -80°C until further use.

RNA isolation from adipocyte progenitors

Cells were harvested in 1 ml QIAzol (Qiagen), transferred to RNase free 1.5 ml safe-lock Eppendorf tubes and stored at -80°C until processing. Phase separation was performed as described for BATkl2 cells. The upper aqueous phase was transferred to fresh RNase-free 1.5 ml tubes and 1 volume of 75% EtOH was added. RNA was purified using the RNeasy micro kit (Qiagen) according to the manufacturer's instructions. RNA was eluted in 16 µl RNase-free water and stored at -80°C until further use.

Measurement of RNA concentration

The RNA concentration was determined spectrophotometrically at 260 nm using the NanoDrop ND-1000 spectrophotometer. The ratios 260 nm/280 nm and 260 nm/230 nm were also determined to assess the purity of RNA samples and the presence of contaminants.

cDNA synthesis

The synthesis of complementary DNA was performed using the QuantiTect Reverse Transcription Kit (QIAGEN) according to the manufacturer's instructions. Between 100 to 1000 ng of template RNA were used, depending on sample RNA concentration, and the final cDNA samples were diluted 1:10 in RNase free water and stored at -20°C.

Quantitative real time – PCR (RT-qPCR)

5 µl of the diluted cDNA samples obtained from reverse transcription were used for quantitative RT-PCR. For TaqMan assay, a master mix was prepared containing 10 µl TaqMan Gene Expression Mastermix, 4 µl DNase/RNase-free water and 1 µl TaqMan Gene Expression Assay per individual reaction. Technical duplicates were performed for all samples. For QuantiTect SYBR Green assay, a master mix was prepared containing 10 µl QuantiTect SYBR Green PCR Master Mix, 3 µl DNase/RNase-free water and 2 µl QuantiTect Primer Assay per individual reaction. Water was used as negative control and samples containing no reverse transcriptase served as controls for genomic DNA contamination. 20 µl PCR reactions were transferred per well onto a MicroAmp Optical 96 well reaction plate and quantitative PCR was performed using the StepOnePlus Real Time PCR System (Applied Biosystems, Foster City, CA). The TaqMan Gene Expression Assays used were obtained from Applied Biosystems or MWG, Quantitect Primer Assays were obtained from QIAGEN, and are listed in the materials section. For the custom-made probe reaction setup (MWG), water and primer volumes were adjusted to obtain the corresponding final concentration. For the Taqman assay the following cycling parameters were used: 50°C for 2 minutes, 95°C for 10 minutes, 40x 95°C for 15 seconds and 60°C for 1 minute (data acquisition); and for the SYBR assay: 95°C for 15 minutes; 40x 95°C for 20 seconds, 57°C for 30 seconds, 72°C for 30 seconds (data acquisition); melting curve in the end. Data was analyzed using the StepOne™ Software (Applied Biosystems, Foster City, CA).

2.2.3. Biochemistry

Quantification of free fatty acids

Free Fatty Acids were determined in cell supernatants using a colorimetric assay from WAKO (NEFA kit) following the manufacturer's instructions. 5 µl and 25 µl of cell supernatants were measured in duplicates. A standard curve was determined using a standard solution provided with the kit, and OD-values were determined at 550 nm.

2.2.4. Animals for isolation of adipose tissue MSCs

Female NMRI mice purchased from Charles River (Brussels) at the age of 7 weeks were used for isolation of adipose tissue MSC. The animals were housed according to international standard conditions with a 12 h dark - 12 h light cycle and had unrestricted access to standard diet and water. Animal handling and experimentation was performed in accordance with NIH guidelines and approved by local authorities (Regierungspräsidium Karlsruhe, Germany).

2.2.5. Statistical analysis

Statistical analysis was performed using SigmaPlot Software (SYSTAT Software) a one- or two-way analysis of variance (ANOVA) with Holm-Sidak post-tests, or t-test in one-factorial experiments. $P<0.05$ was considered statistically significant: *$P<0.05$, **$P<0.01$, ***$P<0.001$.

3. Results

3.1. Analysis of *Sphk1* expression in white and brown adipocyte models

Elevated levels of Sphk1/S1P have been associated with metabolic disease but also with physiological response to various stimuli. Microarray expression profiling data produced in the group have shown that *Sphk1* is up-regulated by adrenergic stimulation and cold exposure, both in inguinal WAT (ingWAT) and interscapular BAT (iBAT) (see Figure 5 in Introduction). The response to cold exposure was confirmed by measuring mRNA levels from iBAT and abdominal WAT (abdWAT) of mice exposed to cold (4°C) for 1 hour, 3 hours, 8 hours and 24 hours (Figure 8).

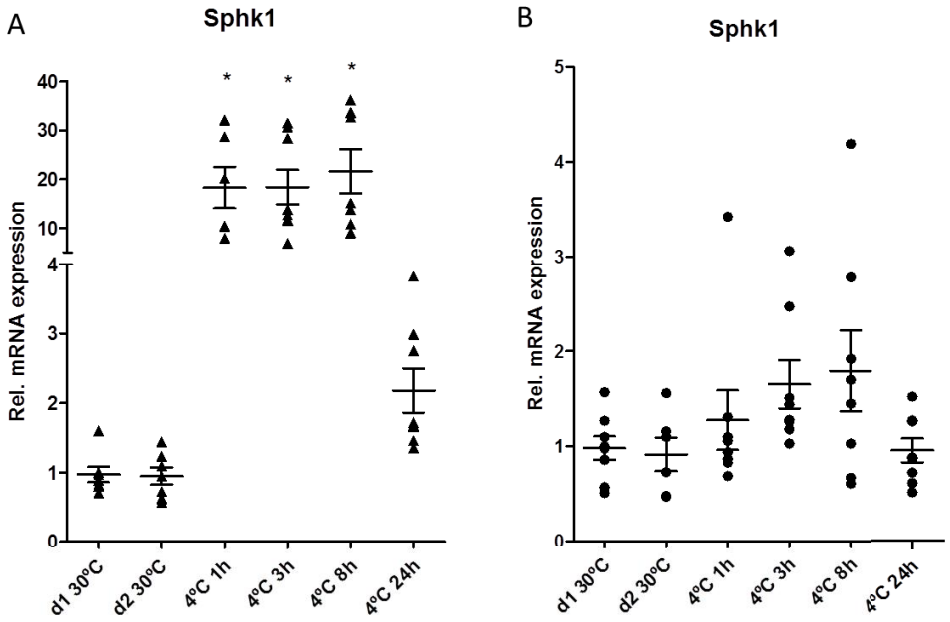

Figure 8: Expression of *Sphk1* in (A) iBAT and (B) abdWAT of mice exposed to cold (4°C) for 1h, 3h, 8h and 24h. Expression levels were determined by RT-qPCR. Values were normalized to the housekeeping gene TATA box binding protein (*Tbp*), and fold change was determined in relation to d1 30°C. d1 and d2 represent control groups sacrificed on different days (day 1 and day 2). n=7-8, mean ± SEM, ANOVA on ranks, Dunn post-hoc test compared to d1 30°C, *P<0.05.

In iBAT, *Sphk1* expression increased 6 fold from 1 hour to 8 hours in cold compared to control temperature (30°C), and decreased after 24 hours, indicating a transient upregulation. In abdWAT there was a tendency for increased *Sphk1* expression with cold, but was not significant. *Sphk1* upregulation in response to cold exposure is greater in iBAT than in abdWAT, but both seem transient, as the expression decreases to control levels after 24h. The strong increase in Sphk1 expression in iBAT clearly indicates an important role for Sphk1/S1P signaling in the thermogenic activation of BAT in response to cold exposure.

Expression of *Sphk1* was also measured in *in vitro* models, namely MSCs isolated from ingWAT and iBAT, and also a BAT cell line named BATkl2 (Figure 9). The BATkl2 is a growth factor-dependent clonal line obtained by applying the 3T3 immortalization protocol on murine interscapular fat MSCs (Lin-Sca1+) in the presence of bFGF as a growth factor. Adipocyte progenitors were isolated by magnetic-activated cell sorting (MACS®) based on the surface

expression of stem cell antigen-1 (Sca-1), after hematopoietic lineage depletion for Ter119 (erithroid cells), CD31 (endothelial cells)and CD45 (leukocytes) positive cells, which results in a population of approximately 75% identity with Lin-CD29+CD34+Sca1+ population enriched in adipocyte progenitors (Rodeheffer et al. 2008). *Sphk1* expression was measured in differentiated white and brown MSCs, and in BATkl2 adipocytes to determine if these *in vitro* models express the enzyme and would be suitable to study its function. Also, white MSCs were stimulated with $cPGI_2$ to induce browning and stimulated with NE to determine Sphk1 responsiveness to adrenergic stimulation. In line with the expression profiling data of MSC differentiated with $cPGI_2$ presented in Figure 6 (see Introduction), expression of *Sphk1* was not regulated by $cPGI_2$ in ingWAT, and induction by NE stimulation was much stronger in brown adipocytes (Figure 9 B,C) compared to white adipocytes (Figure 9 A).

Considering these results, *Sphk1* function was first analyzed in BATkl2 adipocytes, a cell line that serves as a model for brown MSCs and adipocytes.

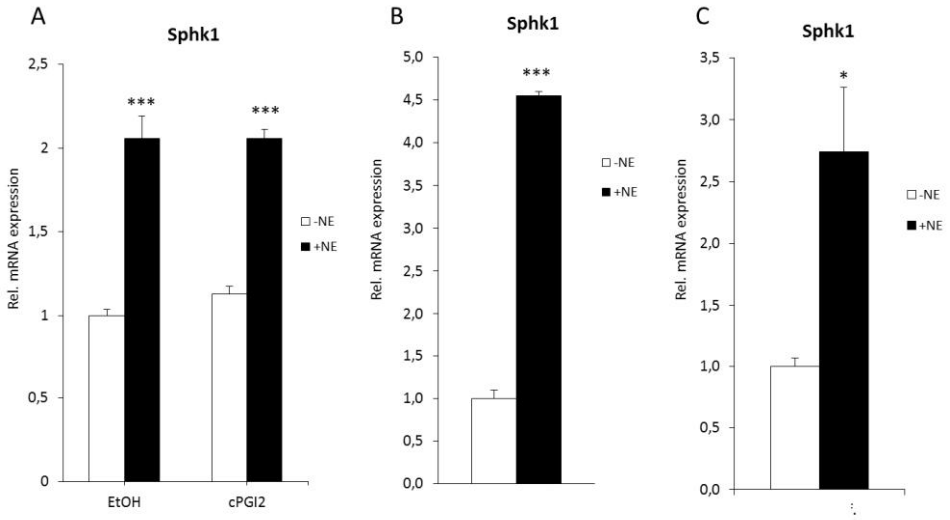

Figure 9: Expression of *Sphk1* in *in vitro* differentiated adipocytes from (A) ingWAT, (B) iBAT and (C) BATkl2 cell line stimulated with NE. MSCs were isolated from ingWAT and BAT by selection of Lin^-Sca^+ cells. Cells were induced to differentiate *in vitro* for 8 days and stimulated with 0.5 µM NE for 3h before harvest. ingWAT MSCs were stimulated with 1 µM $cPGI_2$ (vehicle ethanol) during differentiation to induce a brown phenotype. After RNA isolation and cDNA synthesis, expression levels of *Sphk1* were determined by RT-qPCR. Expression was normalized to the housekeeping *Tbp*, and fold change was determined in relation to unstimulated groups (-NE/EtOH). n=3, mean ± SEM, two-way ANOVA and Holm-Sidak post-hoc test compared to EtOH-NE (A) and t-test compared to –NE (B, C). NE effect *P<0.05, ***P<0.001.

3.2. Analysis of *Sphk1* function in the brown adipocyte cell line BATkl2

3.2.1. Late knock down of *Sphk1* affects mature function of BATkl2 adipocytes

Sphk1 expression varies during differentiation (see Figure 6 in Introduction), with an initial increase in the first day after induction followed by a reduction that is substantially stable until around day 6, when it strongly decreases. *Sphk1* was inhibited in the BATkl2 cell line using small interfering RNAs (siRNAs) to achieve *Sphk1* knock down at a later stage in the differentiation process in order to investigate its role in adipocyte maturation and function independently of its effects on differentiation.

BATkl2 cells were induced to differentiate and transfected at day 5 of differentiation with siRNAs Sphk1_2 and Sphk1_3 against *Sphk1*, and also unspecific siRNA as negative control (NC). At day 8 of differentiation adipocytes were stimulated with 0.5 µM NE for 3 hours and cells were harvested for RNA isolation. After cDNA synthesis, expression levels of *Sphk1* were measured by RT-qPCR to determine knock down efficiency. The transfection of maturing adipocytes was very efficient (Sphk1_2 84% KD; Sphk1_3 87% KD), with a strong reduction in *Sphk1* inducibility upon NE stimulation (Sphk1_2 -83%; Sphk1_3 -71%). To assess the effects of *Sphk1* late knock down, the expression of brown and adipogenic markers was determined by RT-qPCR (Figure 10). *Ucp1*, *Pgc1α* and *Prdm16* were used as brown markers, and *Pparγ*, *Cebpβ* and *Fabp4* were used as markers of general adipogenic differentiation. The effects on basal *Ucp1* expression were not consistent between siRNAs (3 fold increase with Sphk1_2, no change with Sphk1_3), but inducibility in response to NE stimulation was significantly reduced (Sphk1_2 -60%, Sphk1_3 -30%). *Pgc1α*, a transcriptional coactivator that regulates *Ucp1* expression and mitochondrial biogenesis (Huang et al. 2011), was significantly reduced at basal level with Sphk1_2 (-34%), and NE responsiveness was significantly reduced with both siRNAs (-23%). *Prdm16*, a transcription co-regulator fundamental for brown adipocyte differentiation (Schulz & Tseng 2013), was significantly downregulated at both basal and stimulated levels (Sphk1_2 -81%, Sphk1_3 -90%), and NE responsiveness was blunted. *Pparγ*, the transcription factor master regulator of adipogenesis (Seale 2010), was significantly reduced by *Sphk1* knock down (-21% with both siRNAs) at the basal level. The basal levels of *Cebpβ*, a transcription factor that regulates brown differentiation (Seale 2010), were not affected but NE inducibility was significantly reduced (Sphk1_2 -62%, Sphk1_3 -77%). The effects on *Fabp4*, a cytosolic lipid-binding protein highly expressed in adipocytes involved in fatty acid transport (Lafontan & Langin 2009), were small and not consistent, with Sphk1_2 causing a reduction and Sphk1_3 causing an increase in both basal and stimulated levels.

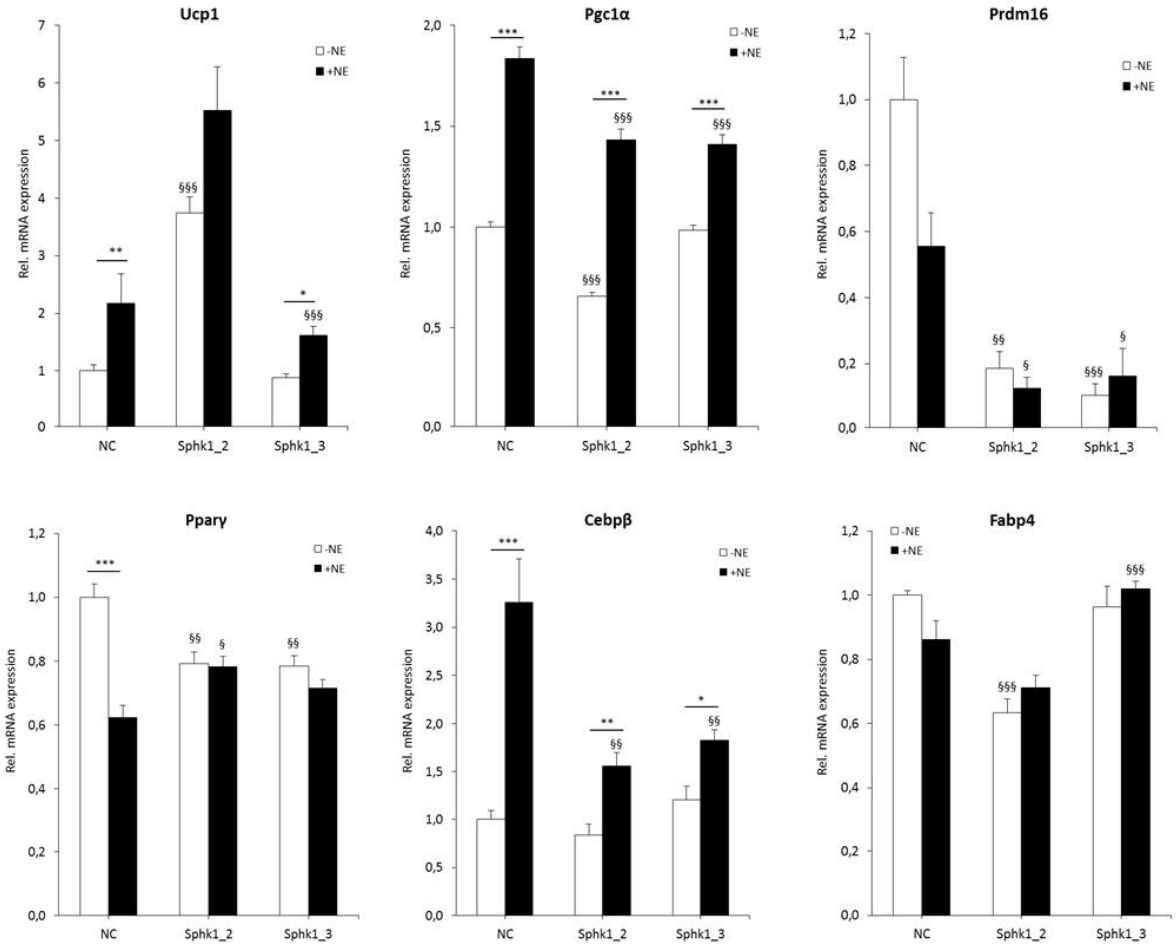

Figure 10: Effect of *Sphk1* late knock down on expression of brown (top) and adipogenic (bottom) marker genes in differentiated BATkl2 adipocytes. Cells were transfected at day 5 of differentiation with siRNAs Sphk1_2 and Sphk1_3 at 20nM final concentration using RNAiMax reagent, including unspecific siRNA as negative control (NC). At day 8 cells were stimulated with 0.5 µM NE for 3 h. After RNA isolation and cDNA synthesis, expression of brown and adipogenic markers was determined by RT-qPCR. Expression levels were normalized to the housekeeping *Tbp*, and fold change was determined in relation to NC. n=3, mean ± SEM, two-way ANOVA and Holm-Sidak post-hoc test compared to NC, NE effect *P<0.05, **P<0.01, ***P<0.001 (§ for KD effect).

To further determine the effects of *Sphk1* late knock down on mature adipocyte function, the expression of mitochondrial genes *Cox7a1* and *Cox8b*, was assessed by RT-qPCR. Cytochrome c oxidase subunit VIIa polypeptide 1 (*Cox7a1*) and cytochrome c oxidase subunit VIIIb (*Cox8b*) are subunits of cytochrome c oxidase, the terminal oxidase in the mitochondrial respiratory chain, also known as complex IV. These subunits are encoded by nuclear genes, are highly expressed in brown fat and are important for its thermogenic function (Wu et al. 2012).

Sphk1 knock down at a late stage of the differentiation process caused an increase in *Cox8b* expression, greater with siRNA Sphk1_2 than Sphk1_3, at the basal level (1.6 fold) and more significantly upon NE stimulation (2.3 fold) (Figure 11). NE responsiveness was also reduced with both siRNAs. *Cox7a1* expression was reduced by *Sphk1* knock down at a basal level with both siRNAs (-21%, -42%), and NE responsiveness was blunted.

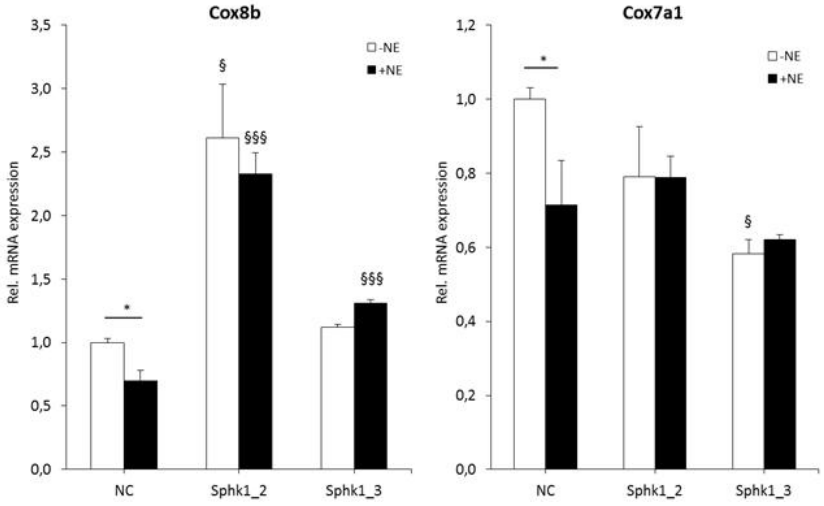

Figure 11: Effect of *Sphk1* late knock down on the expression levels of mitochondrial genes *Cox8b*, *Cox7a1*. Cells were transfected at day 5 of differentiation with siRNAs Sphk1_2 and Sphk1_3 at 20nM final concentration using RNAiMax reagent, including unspecific siRNA as negative control (NC). At day 8 cells were stimulated with 0.5 µM NE for 3 h. After RNA isolation and cDNA synthesis, expression of *Cox8b* and *Cox7a1* was determined by RT-qPCR. n=3, mean ± SEM, two-way ANOVA and Holm-Sidak post-hoc test compared to NC, KD effect §P<0.05, §§§P<0.001 (* for NE effect).

Taken together, these results indicate that knocking down *Sphk1* at a later stage of the differentiation process may significantly affect mature adipocyte function, in a way that reducing expression of brown marker and mitochondrial genes might compromise their thermogenic function.

3.2.2. Sphk1 knock down reduces differentiation of BATkl2 cells

In order to investigate the role of Sphk1 in brown adipocyte differentiation, the expression of *Sphk1* was inhibited before induction of differentiation. siRNAs targeting *Sphk1* were tested in undifferentiated BATkl2 cells to determine their efficiency. An unspecific siRNA was used as negative control and a previously tested siRNA targeting Prkaca was used as positive control to help determine transfection efficiency. 48 hours after transfection the cells were harvested and expression of *Sphk1* was assessed by RT-qPCR (Table 1). Both transfection and knock down efficiency of siRNAs Sphk1_2 and Sphk1_3 were very good.

Table 2: Knockdonwn efficiency of siRNAs targeting *Sphk1*.

siRNA	Prkaca	Sphk1_2	Sphk1_3
Efficiency	94% KD ***	81% KD ***	59% KD ***

Undifferentiated BATkl2 cells were transfected using RNAiMax reagent with each siRNA at 20nM final concentration per well. Cells were harvested 48 hours after transfection for RNA isolation, cDNA synthesis and analysis of *Sphk1* expression by RT-qPCR. *Prkaca* was used as a positive control for transfection efficiency. Values represent mean expression compared to the negative control (n=3). T-test compared to negative control ***P<0.001; ns, non-significant.

In order to explore whether Sphk1 plays a role in brown adipocyte differentiation, undifferentiated BATkl2 cells were transfected with siRNAs Sphk1_2 and Sphk1_3, as well as unspecific siRNA as negative control, and induced to differentiate 24 hours after transfection. At day 8 of differentiation the cells were stimulated for 3 hours with 0.5 µM NE to assess NE responsiveness, a key property of brown adipocytes. After RNA isolation and cDNA synthesis, the expression of Sphk1 was assessed by RT-qPCR to determine knock down efficiency (Figure 12).

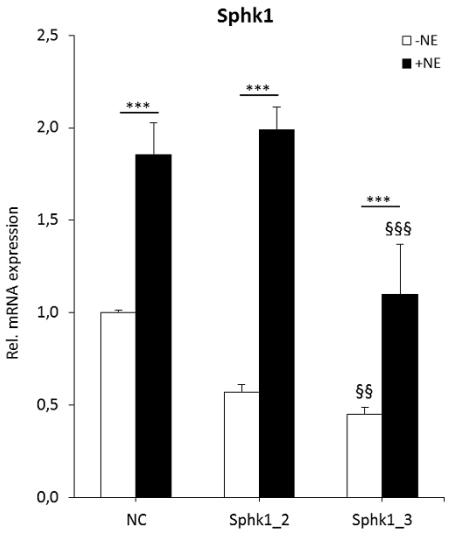

Figure 12: Sphk1 knock down in BATkl2 cells. BATkl2 cells were transfected with siRNAs Sphk1_2 and Sphk1_3 at 20nM final concentration using RNAiMax reagent, including unspecific siRNA as negative control (NC). 24h after transfection cells were induced to differentiate, and at day 8 cells were stimulated with 0.5 µM NE for 3 h. After RNA isolation and cDNA synthesis, *Sphk1* expression was detected by RT-qPCR. Expression levels were normalized to the housekeeping *Tbp*, and fold change was determined in relation to NC. n=3, mean ± SEM, two-way ANOVA and Holm-Sidak post-hoc test compared to NC, NE effect ***P<0.001; KD effect §§P<0.01, §§§P<0.001; interaction P = 0,008.

After 8 days of differentiation, Sphk1 knock down was still present and was stronger with siRNA Sphk1_3 (55% KD). NE responsiveness was not affected by Sphk1_2 but was reduced by Sphk1_3. The expression of brown genes and markers of adipogenic differentiation was determined to evaluate the effect of Sphk1 knock down in brown adipocyte differentiation (Figure 13). Knock down of Sphk1 significantly reduced *Ucp1* expression at a basal level (Sphk1_2 -55%; Sphk1_3 -96%), and inducibility by NE stimulation was also strongly reduced (Sphk1_2 -67%; Sphk1_3 -29%) compared to the negative control. *Pgc1α* was also down-regulated by *Sphk1* knock down, with basal levels declining around 26% with both siRNAs. Inducibility by NE was markedly reduced by Sphk1_2 (-50%) and completely blunted by Sphk1_3. *Prdm16* was significantly reduced by *Sphk1* knock down (Sphk1_2 -57%; Sphk1_3 -91%).

The dowregulation of adipogenic markers was not so significant, and the effect was stronger with siRNA Sphk1_3. The transcription factor gene *Pparγ* was significantly downregulated, both at the basal level (Sphk1_3 -55%) and upon NE stimulation (Sphk1_2 -30%, Sphk1_3 -57%). *Cebpβ*, a transcription factor that drives *Pparγ* as well as brown fat gene expression early in the differentiation process, was significantly downregulated by Sphk1_3 (-51%), and NE induction was also blunted (-54%). *Fabp4*, an important protein in fatty acid

metabolism, was significantly reduced at basal level (Sphk1_3 -65%) and also upon NE stimulation (Sphk1_3 -63%).

Taken together, these results indicate that *Sphk1* function is required for normal differentiation of brown adipocytes.

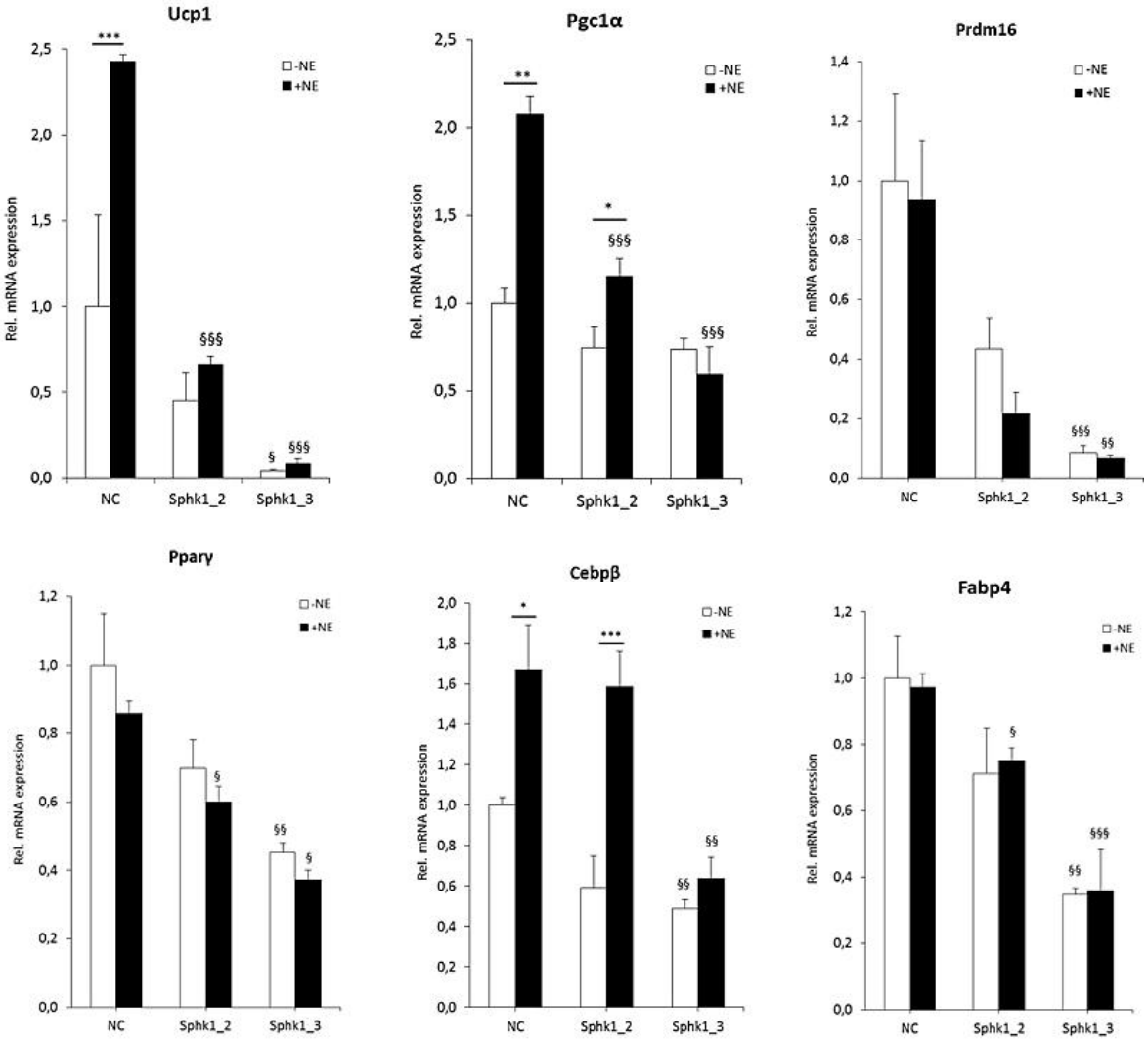

Figure 13: Effect of Sphk1 knock down on expression of brown marker genes (top) and markers of adipogenic differentiation (bottom) in differentiated BATkl2 adipocytes. Cells were transfected with siRNAs Sphk1_2 and Sphk1_3 at 20nM final concentration using RNAiMax reagent, including unspecific siRNA as negative control (NC). 24h after transfection cells were induced to differentiate, and at day 8 cells were stimulated with 0.5 µM NE for 3 h. After RNA isolation and cDNA synthesis, expression of brown and adipogenic markers was determined by RT-qPCR. Expression levels were normalized to the housekeeping *Tbp*, and fold change was determined in relation to NC. n=3, mean ± SEM, two-way ANOVA and Holm-Sidak post-hoc test compared to NC, *P<0.05, **P<0.01, ***P<0.001 (*NE effect, § KD effect); interaction *Pgc1α* P = 0,012.

3.2.3. *Sphk1* knock down reduces basal lipolysis in BATkl2 adipocytes

Any disturbances occurring during adipocyte differentiation will consequently affect adipocyte function, including lipolysis and lipogenesis. To further characterize the effects of *Sphk1* knock down in brown adipocyte differentiation, expression levels of marker genes for lipolysis were also measured by RT-qPCR (Figure 14). *Pnpla2* and *Lipe* encode the rate-limiting enzymes ATGL and HSL, respectively, and *Plin1* encodes the structural protein perilipin that coats the surface of lipid droplets. *Plin1* expression was significantly reduced by Sphk1_3 upon NE stimulation (-64%), and Sphk1_2 caused a similar tendency (-41%). Also, *Sphk1* knock down blunted *Plin1* induction upon NE stimulation. *Pnpla2* and *Lipe* showed a similar effect, with a general tendency for reduced basal expression with Sphk1 knock down, and a significant reduction in expression upon NE stimulation by Sphk1_3 (-68% and -58%, respectively).

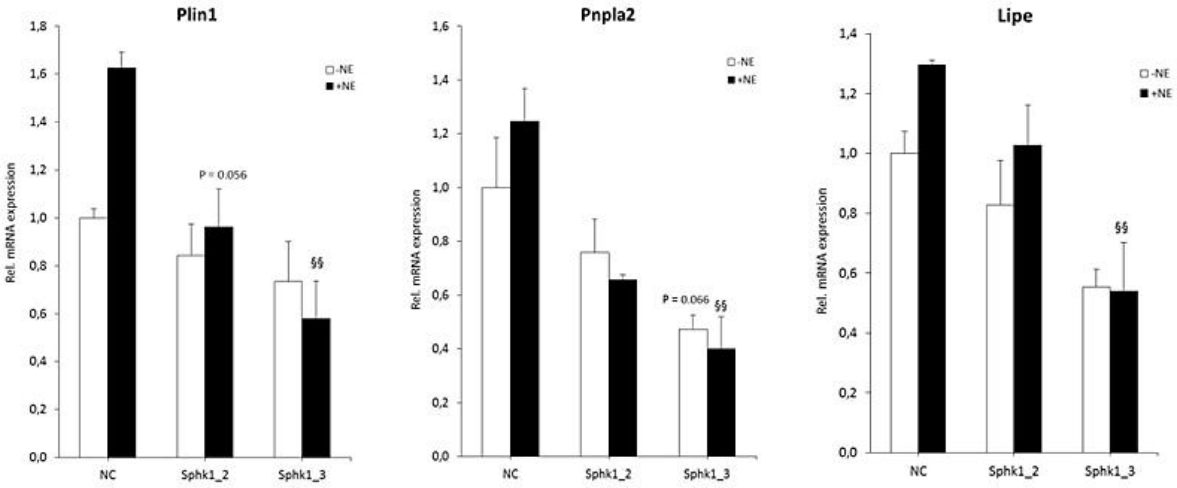

Figure 14: Effect of Sphk1 knock down on expression of lipolysis genes in differentiated BATkl2 adipocytes. Cells were transfected with siRNAs Sphk1_2 and Sphk1_3 at 20nM final concentration using RNAiMax reagent, including unspecific siRNA as negative control (NC). 24h after transfection cells were induced to differentiate, and at day 8 cells were stimulated with 0.5 µM NE for 3 h. After RNA isolation and cDNA synthesis, expression of lipolysis genes was determined by RT-qPCR. Expression levels were normalized to the housekeeping *Tbp*, and fold change was determined in relation to NC. n=3, mean ± SEM, two-way ANOVA and Holm-Sidak post-hoc test compared to NC, KD effect §§P<0.01.

Expression of *de novo* lipogenesis genes was also determined, but there were no significant changes (data not shown).

Furthermore, NE-mediated lipolysis was assessed in order to determine if the effects of Sphk1 knock down on expression of lipolysis genes correlated with alterations in adipocyte triglyceride breakdown. Upon adrenergic stimulation, adipocytes hydrolyze triglycerides into glycerol and non-esterified fatty acids (NEFA), which are partly released to the cell medium. To perform the assay, BATkl2 cells were transfected with Sphk1 siRNAs and induced to differentiate after 24 hours. At day 8 of differentiation adipocytes were serum-starved for 2 hours and then stimulated with 0.5 µM NE for 3 hours. The NEFA concentration in cell supernatants was measured to estimate lipolysis rate (Figure 15). Upon NE stimulation, a similar level of NEFA release was observed in all conditions, but there was a significant reduction in basal lipolysis with

Sphk1 knock down compared to NC (Sphk1_2 -76%; Sphk1_3 -51%). Overall, this indicates that while Sphk1 knock down reduces basal lipolysis rate, the adipocytes are still able increase lipolysis rate in response to adrenergic stimulation.

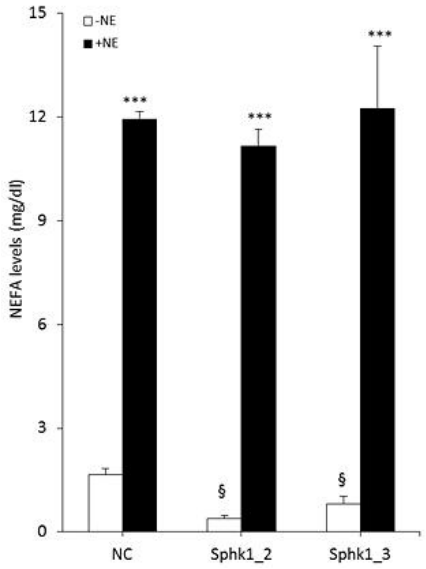

Figure 15: NEFA release from NE-stimulated lipolysis in BATkl2 cells. Cells were transfected with siRNAs Sphk1_2 and Sphk1_3 at 20nM final concentration using RNAiMax reagent, including unspecific siRNA as negative control (NC). 24h after transfection cells were induced to differentiate, and at day 8 cells were serum-starved for 2h and then lipolysis was stimulated with 0.5µM NE for 3h. Rate of lipolysis was estimated by NEFA measurement in cell medium (mg NEFA/dl supernatant). n=3, mean ± SEM, two-way ANOVA and Holm-Sidak post-hoc test compared to NC, NE effect ***P<0.001, KD effect §P<0.05.

To sum up, Sphk1 is necessary for normal brown adipocyte differentiation, and the knock down consequently leads to detrimental effects in adipocyte function, which was measured here by reduced basal lipolysis.

Overall, the effects of *Sphk1* late knock down on expression of brown and adipogenic markers were smaller compared to the early knock down (Table 2), and brown markers were more affected than adipogenic ones, which may indicate that the late knock down has a more prominent effect on brown adipocyte mature function than differentiation. The ability to respond to adrenergic stimulation is pivotal in brown adipocytes, and both early and late Sphk1 knock down significantly reduced NE responsiveness.

Table 3: Comparison between early and late Sphk1 knock down on expression of brown and adipogenic markers.

Genes	Sphk1 early knock down		Sphk1 late knock down	
	Basal	NE resp.	Basal	NE resp.
Ucp1	↓96%	↓67%	-	↓45%
Pgc1α	↓26%	↓85%	↓34%	↓23%
Prdm16	↓90%	↓5 fold	↓85%	↓74%
Cebpβ	↓46%	↓54%	-	↓70%
Pparγ	↓55%	-	↓21%	-
Fabp4	↓65%	-	-	-

Summary of changes in basal expression levels (Basal) and NE responsiveness (NE resp.) of brown and adipogenic genes in cells with Sphk1 knock down before (early knock down) and after (late knock down) differentiation induction. Changes compared to NC and values are average of both siRNAs. 1 fold=100%

3.3. Analysis of *Sphk1* knock down in primary adipose tissue MSCs

3.3.1. *Sphk1* late knock down affects mature function of differentiated iBAT MSC

The results in BATkl2 cells point to a role of Sphk1 in brown adipocytes, and to further explore this in a model with more physiological relevance, the effects of *Sphk1* knock down were investigated in primary mesenchymal stromal cells (MSCs) isolated from the interscapular brown fat of female NMRI mice.

To explore the relevance of *Sphk1* in mature function of differentiated iBAT MSC, cells were isolated and induced to differentiate after reaching the appropriate confluence. At day 5 of differentiation cells were transfected with siRNAs Sphk1_2, Sphk1_3 and negative control, and at day 8 were stimulated with 0.5 µM NE to assess responsiveness. After RNA isolation and cDNA synthesis, the expression of *Sphk1* and several brown and adipogenic markers was determined by RT-qPCR (Figure 16). *Sphk1* knock down was very efficient with both siRNAs (Sphk1_2 78% KD, Sphk1_3 81%KD).

Regarding brown makers, changes in *Ucp1* expression were not consistent between siRNAs, and there was no induction upon NE stimulation in the negative control, which could be attributed to poor differentiation caused by toxic transfection effects. While Sphk1_2 caused a 5 fold increase in basal expression, Sphk1_3 reduced it 80%. Upon NE stimulation, Sphk1_2 increased *Ucp1* expression 3 fold, and with Sphk1_3 the levels were only 50% of NC, which corresponded to 7 fold induction by NE.

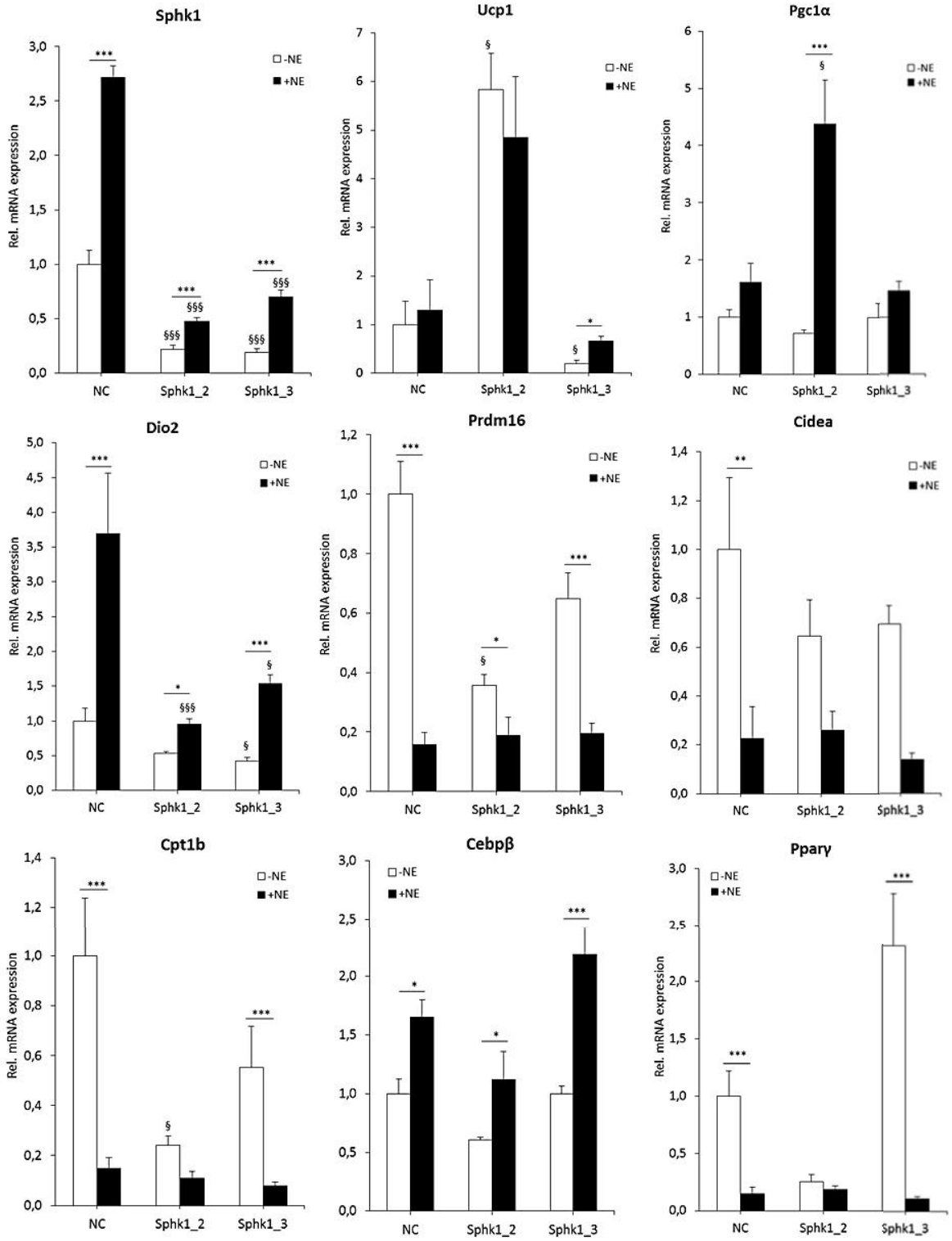

Figure 16: Effect of Sphk1 late knock down on expression of brown and adipogenic marker genes in differentiated iBAT MSCs. Cells were transfected at day 5 of differentiation with siRNAs Sphk1_2 and Sphk1_3 at 20nM final concentration using RNAiMax reagent, including unspecific siRNA as negative control (NC). At day 8 cells were stimulated with 0.5 µM NE for 3 h. After RNA isolation and cDNA synthesis, expression of brown and adipogenic markers was detected by RT-qPCR. Expression levels were normalized to the housekeeping *Tbp*, and fold change was determined in relation to NC. n=3, mean ± SEM, two-way ANOVA and Holm-Sidak post-hoc test compared to NC, NE effect *P<0.05, **P<0.01, ***P<0.001 (§ for KD effect).

Pgc1α basal expression was reduced by Sphk1_2, and upon NE stimulation there was a significant 3 fold induction with Sphk1_2 that was absent both in NC and Sphk1_3. *Dio2* is an important enzyme for brown fat activation, converting T4 into active T3 upon sympathetic stimulation (Schulz & Tseng 2013). *Dio2* basal expression was reduced by Sphk1 knock down (Sphk1_2 -47%, Sphk1_3 -58%), and NE inducibility was also significantly reduced (Sphk1_2 -2.7 fold, Sphk1_3 -2.2 fold). *Prdm16* and *Cpt1b* basal expression was significantly reduced by Sphk1_2 (-64% and -76%, respectively), with Sphk1_3 causing a smaller non-significant reduction (-35% and -45%, respectively). *Cidea*, a mitochondrial protein that regulates Ucp1 activity (Hansen & Kristiansen 2006), had a similar expression pattern, but the reduction caused by Sphk1 knock down was not significant.

Regarding adipogenic markers, *Cebpβ* basal expression was not significantly affected by Sphk1 knock down (Sphk1_2 -40%, P=0.051), but NE inducibility was increased (Sphk1_2 28%, Sphk1_3 82%). *Pparγ* basal expression decreased with Sphk1_2 (-75%) but increased with Sphk1_3 (1.3 fold). *Prdm16*, *Cidea*, *Pparg* and *Cpt1b* expression upon NE stimulation was overall reduced, and the physiological relevance of this is not well understood. On the other hand, *Pgc1α* and *Cebpβ* are known to be upregulated by NE stimulation (Cannon & Nedergaard 2004).

Overall, *Sphk1* late knock down in differentiated iBAT MSCs caused a significant reduction mostly in brown marker genes, indicating a relevant effect in mature adipocyte function. The observed inconsistencies between phenotypes of both siRNAs may be related to off-target effects.

3.3.2. Analysis of *Sphk1* late knock down in mature function of differentiated ingWAT MSCs

Sphk1 is upregulated during differentiation of ingWAT MSC (see Figure 6 in Introduction), and expression *in vivo* shows a tendency to increase in response to cold exposure (see Figure 3 in Introduction). In order to investigate the role of *Sphk1* in white adipocytes, MSCs isolated from ingWAT of NMRI mice were induced to differentiate and transfected at day 5 with siRNA Sphk1_2 and Sphk1_3 to knock down *Sphk1*.

Sphk1 is also induced during differentiation of ingWAT MSC stimulated with $cPGI_2$ (see Figure 6 in Introduction), therefore it was also relevant to determine its role in beige adipocyte differentiation. Throughout the differentiation process, cells were stimulated with 1µM $cPGI_2$ to induce a brown-like (beige) phenotype, and control cells were treated with vehicle (EtOH). $cPGI_2$ signals through the IP receptor and Ppar nuclear receptors to promote expression of brown genes like *Ucp1* (Lim & Dey 2002). At day 8 of differentiation adipocytes were stimulated with 0.5 µM NE to assess responsiveness. After RNA isolation and cDNA synthesis, expression levels of *Sphk1*, brown and adipogenic markers were determined by RT-qPCR (Figure 17). Both siRNAs were very efficient (Sphk1_2 76% KD, Sphk1_3 81% KD) and blunted both $cPGI_2$ and NE induction of *Sphk1*.

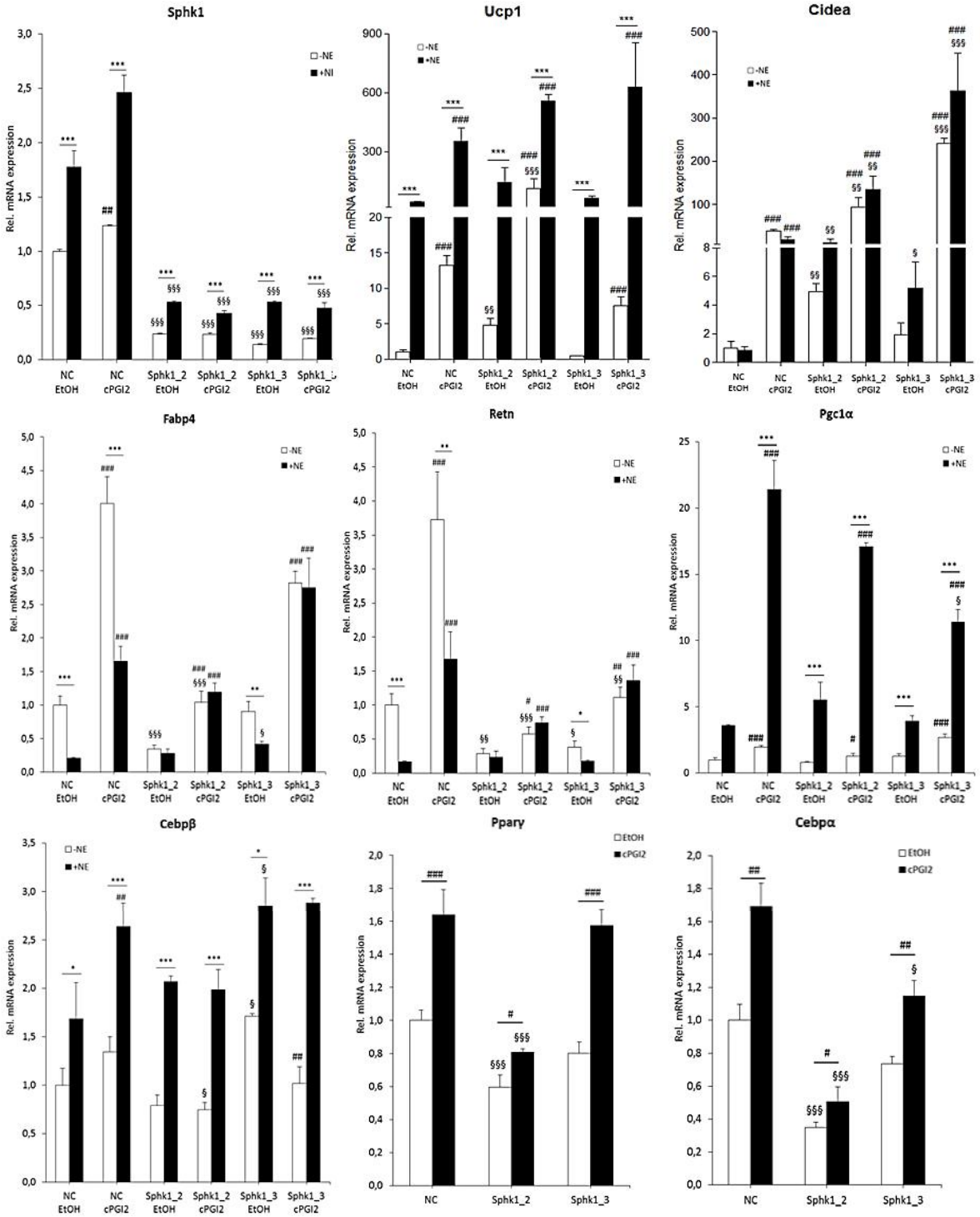

Figure 17: Effect of Sphk1 late knock down on expression of brown and adipogenic marker genes in differentiated ingWAT MSCs. Cells were differentiated with 1µM $cPGI_2$ and transfected at day 5 of differentiation with siRNAs Sphk1_2 and Sphk1_3 at 20nM final concentration using RNAiMax reagent, including unspecific siRNA as negative control (NC). At day 8 cells were stimulated with 0.5 µM NE for 3 h. After RNA isolation and cDNA synthesis, expression of brown markers and of adipogenic markers was detected by RT-qPCR. Expression levels were normalized to the housekeeping *Tbp*, and fold change was determined in relation to NC. n=3, mean ± SEM, two-way ANOVA and Holm-Sidak post-hoc test compared to NC, NE effect *P<0.05, **P<0.01, ***P<0.001 (§ for KD effect, # for $cPGI_2$ effect).

Ucp1 was highly induced by NE and $cPGI_2$ in the negative control, indicating a good differentiation. *Ucp1* basal expression was significantly upregulated by Sphk1_2 (3-4 fold), but Sphk1_3 produced opposite results both in white and beige cells. *Cidea* was overall significantly upregulated with Sphk1 knock down, and the effect was stronger with $cPGI_2$ and NE stimulation (20 fold). *Fabp4* and *Retn* expression patterns were similar, with basal levels being significantly reduced by Sphk1_2 in white (-66% and -71%, respectively) and in beige adipocytes (-74% and -85%, respectively), and NE responsiveness was blunted. Sphk1_3 significantly reduced basal levels of *Retn* in white (-62%) and beige adipocyte (-70%), and blunted NE responsiveness of both genes only in beige adipocytes. *Pgc1α* induction upon NE stimulation was significantly reduced in beige adipocytes (Sphk1_3 -47%). *Cebpβ* induction by $cPGI_2$ was reduced by *Spk1* knock down (Sphk1_2 -44%, Sphk1_3 -24%), and basal and NE induced expression was significantly increased by siRNA Sphk1_3 in white adipocytes (72% and 69%, respectively).

The genes mentioned above respond to NE stimulation, but *Cebpα* and *Pparγ* were determined only in basal conditions. *Pparγ* levels were only significantly reduced by siRNA Sphk1_2 (EtOH -40%, $cPGI_2$ -51%), and *Cebpα* expression was significantly reduced by siRNA Sphk1_2 (EtOH -65%, $cPGI_2$ -70%) and to a lesser extent also by Sphk1_3 (EtOH -27%, $cPGI_2$ -32%).

Overall, late Sphk1 knock down in ingWAT MSCs caused a reduction in adipogenic markers *Fabp4*, *Retn* and *Cebpα*, but the effect on brown markers was not very consistent, except for *Cidea*, which was clearly upregulated both in white and beige adipocytes.

To further explore the effects of late *Sphk1* knock down on mature white and beige adipocyte function, the expression of *de novo* lipogenesis genes and mitochondrial genes was assessed by RT-qPCR (Figure 18). *Acaca* encodes acetyl-CoA carboxylase alpha, *Fasn* encodes fatty acid synthase, and *Scd1* encodes stearoyl CoA desaturase-1. *Sphk1* knock down reduced *Acaca* expression significantly in $cPGI_2$ treated adipocytes (Sphk1_2 -62%, Sphk1_3 -44%) and less in EtOH treated ones (-32% with both). Fasn expression was significantly reduced with siRNA Sphk1_2 under $cPGI_2$ treatment (-63%, and. *Scd1* expression showed a tendency to increase in EtOH groups with *Sphk1* knock down (Sphk1_2 13%, Sphk1_3 75%), but induction by $cPGI_2$ was reduced (Sphk1_2 -50%, Sphk1_3 -41%). Given that the expression of these enzymes was affected variably by Sphk1 late knock down, and no significant alterations in lipid droplet size were observed under the microscope, *Sphk1* late knock down does not appear to significantly alter the capacity of adipocytes to store lipids.

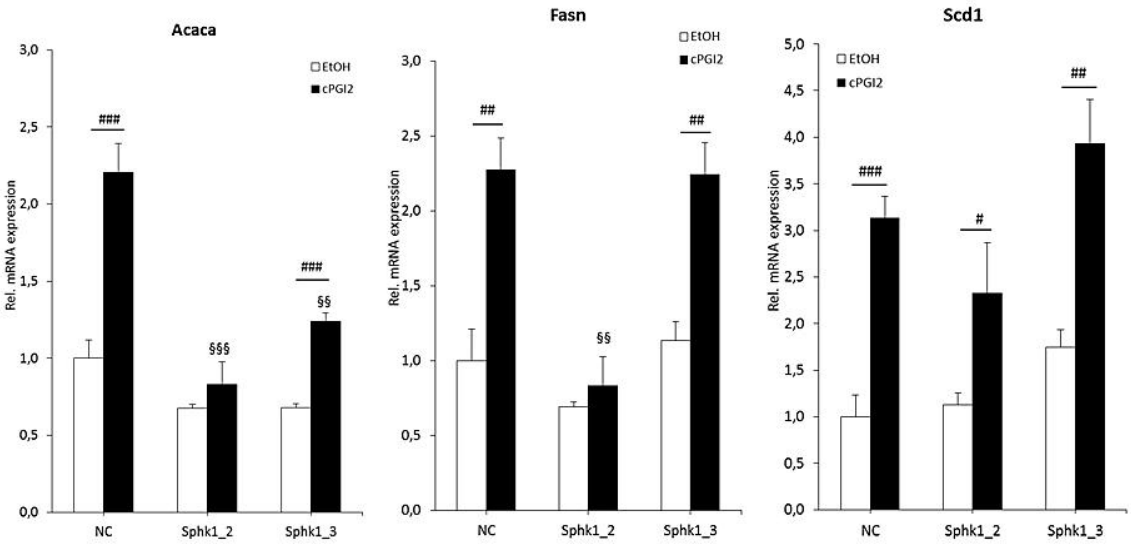

Figure 18: Effect of Sphk1 late knock down on expression of de novo lipogenesis marker genes in differentiated ingWAT MSCs. Cells were differentiated with 1µM $cPGI_2$ and transfected at day 5 of differentiation with siRNAs Sphk1_2 and Sphk1_3 at 20nM final concentration using RNAiMax reagent, including unspecific siRNA as negative control (NC). At day 8 cells were stimulated with 0.5 µM NE for 3 h. After RNA isolation and cDNA synthesis, expression of de novo lipogenesis genes was detected by RT-qPCR. Expression levels were normalized to the housekeeping *Tbp*, and fold change was determined in relation to NC. n=3, mean ± SEM, two-way ANOVA and Holm-Sidak post-hoc test compared to NC, KD effect §P<0.05, §§P<0.01, §§§P<0.001 (# for $cPGI_2$ effect).

Regarding mitochondrial genes (Figure 19), *Cox7a1* expression showed a tendency to decrease with Sphk1 knock down in $cPGI_2$ treated groups (Sphk1_2 -34%, Sphk1_3 -28%). On the other hand, *Cox8b* expression increased with *Sphk1* knock down, both in EtOH (Sphk1_2 124%, Sphk1_3 83%) and $cPGI_2$ treated groups (Sphk1_2 0.5 fold, Sphk1_3 2.45 fold), and Sphk1_3 caused a 3.6 fold increase in induction by $cPGI_2$. These genes did not show similar patterns, indicating that *Sphk1* knock down may affect mitochondrial genes in different ways.

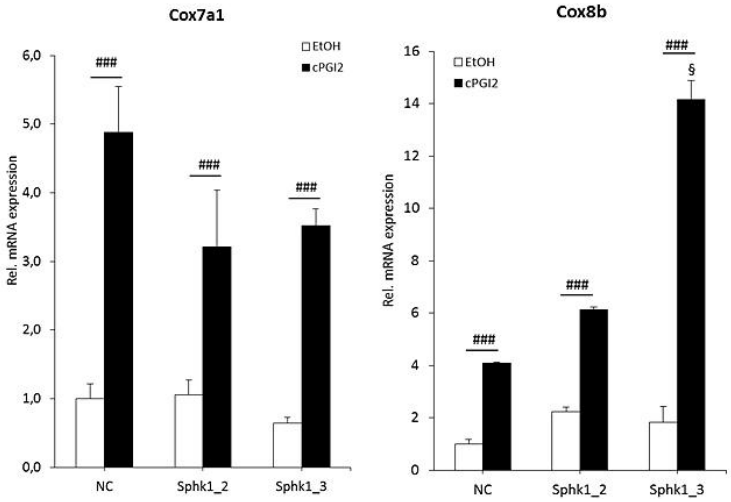

Figure 19: Effect of Sphk1 late knock down on expression of mitochondrial marker genes in differentiated ingWAT MSCs. Cells were differentiated with 1µM $cPGI_2$ and transfected at day 5 of differentiation with siRNAs Sphk1_2 and Sphk1_3 at 20nM final concentration using RNAiMax reagent, including unspecific siRNA as negative control (NC). At day 8 cells were stimulated with 0.5 µM NE for 3 h. After RNA isolation and cDNA synthesis, expression of mitochondrial genes was detected by RT-qPCR. Expression levels were normalized to the housekeeping *Tbp*, and fold change was determined in relation to NC. n=3, mean ± SEM, two-way ANOVA and Holm-Sidak post-hoc test compared to NC, KD effect §P<0.05, §§P<0.01, §§§P<0.001 (# for $cPGI_2$ effect).

Effects on mature adipocyte function were further explored by determining expression of lipolysis genes and performing a lipolysis assay at day 8 of differentiation, using the same conditions of the previous experiment (Figure 13). Sphk1 knock down reduced the expression of *Pnpla2* in unstimulated conditions, most significantly with siRNA Sphk1_2 (EtOH -52%, $cPGI_2$ -76%) than Sphk1_3 (EtOH -26%, $cPGI_2$ -41%), and NE responsiveness was reduced in all groups. *Plin1* expression was also significantly reduced by Sphk1_2 knock down in unstimulated groups (EtOH -59%, $cPGI_2$ -65%), and NE responsiveness was reduced in general with the knock down.

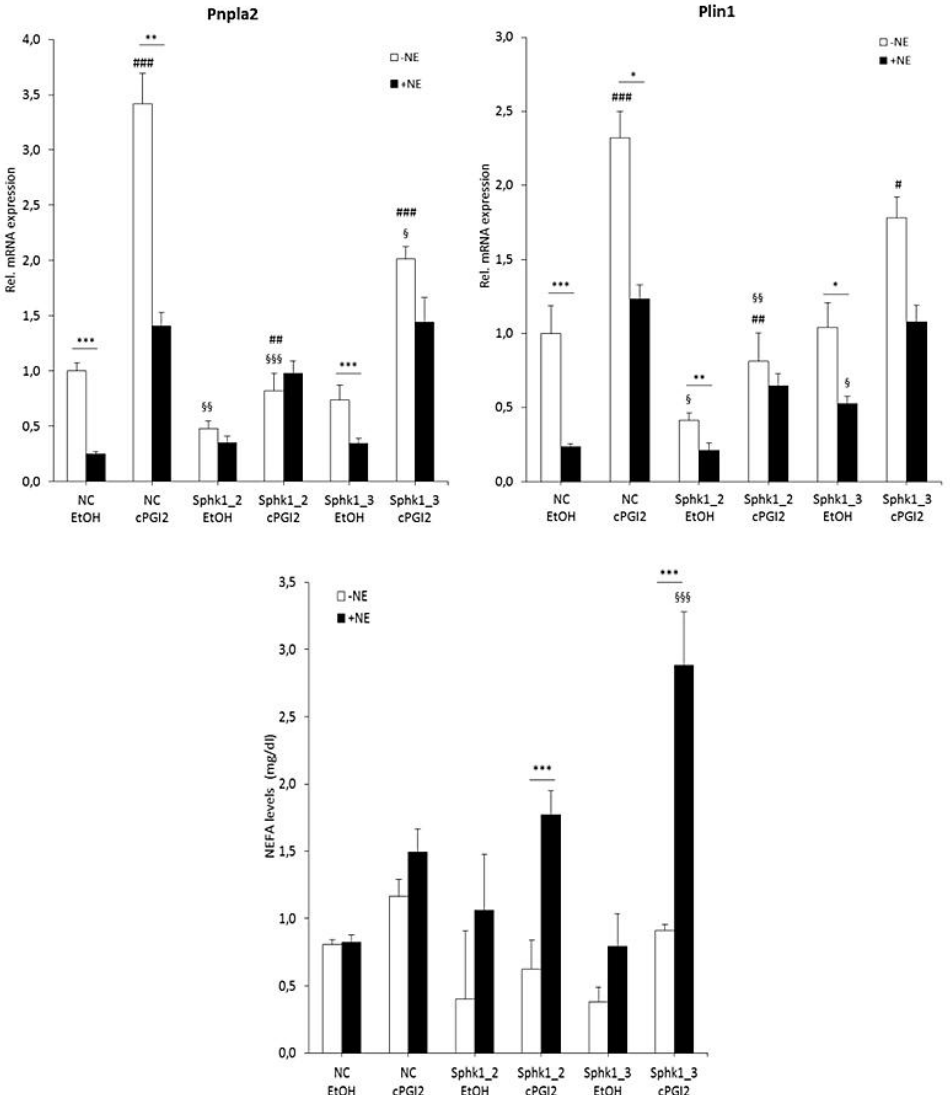

Figure 20: Effect of Sphk1 late knock down on expression of lipolysis genes and lipolysis rate in differentiated ingWAT MSCs. Cells were differentiated with 1µM $cPGI_2$ and transfected at day 5 of differentiation with siRNAs Sphk1_2 and Sphk1_3 at 20nM final concentration using RNAiMax reagent, including unspecific siRNA as negative control (NC). At day 8 cells were stimulated with 0.5 µM NE for 3 h. After RNA isolation and cDNA synthesis, expression of lipolysis markers was detected by RT-qPCR. Expression levels were normalized to the housekeeping *Tbp*, and fold change was determined in relation to NC. For the lipolysis assay, cells were serum-starved for 2h and then lipolysis was stimulated with 0.5µM NE for 3h. Rate of lipolysis was estimated by NEFA measurement in cell medium (mg NEFA/dl supernatant). n=3, mean ± SEM, two-way ANOVA and Holm-Sidak post-hoc test compared to NC, KD effect §P<0.05, §§P<0.01, §§§P<0.001 (# for $cPGI_2$ effect).

For the lipolysis assay, cells were induced to differentiate, transfected at day 5 of differentiation and at day 8 the adipocytes were serum starved for 2 hours before stimulation with 0.5 µM for 3 hours. Lipolysis rate was determined by measuring NEFA released to the supernatant.

Given the reduction in expression of lipolysis genes, it would be expected a reduction in lipolysis. Although the basal rate tended to decrease with *Sphk1* knock down, both in EtOH and $cPGI_2$ groups (-50%), there was an increase in NEFA release upon NE stimulation in cells with *Sphk1* knock down treated with $cPGI_2$ (Sphk1_2 1.84 fold, Sphk1_3 2.15 fold).

Overall, Sphk1 late knock down produced strong effects both in adipogenic genes and markers of adipocyte function. In order to assess the importance of Sphk1 in MSC differentiation, the following experiments were performed with Sphk1 knock down before induction of differentiation.

3.3.3. Analysis of *Sphk1* early knock down in the differentiation process of iBAT MSC

Bearing in mind the strong downregulation of brown and adipogenic genes caused by early knock down of *Sphk1* in BATkl2 cell line, iBAT progenitors were used to assess the physiological relevance of this phenotype. Efficiency of the siRNAs targeting *Sphk1* was tested in iBAT MSCs to ensure similar efficiency as seen in BATkl2 cells. MSCs were transfected with Sphk1_2 and Sphk1_3, including unspecific siRNA as negative control, and 48 hours after transfection cells were harvested for RNA isolation. After cDNA synthesis the levels of *Sphk1* were determined by RT-qPCR (Table 3). Both siRNAs were very efficient in knocking down Sphk1 and were therefore used in subsequent experiments.

Table 4: Efficiency of Sphk1 siRNAs in iBAT MSCs.

siRNA	Sphk1_2	Sphk1_3
Efficiency	61% KD **	85% KD ***

iBAT MSCs were transfected using RNAiMax reagent and 20nM final concentration of each siRNA per well. Cells were harvested 48 hours after transfection for RNA isolation, cDNA synthesis and analysis of *Sphk1* expression by RT-qPCR. The values represent the mean expression compared to the negative control (n=3). One-way ANOVA compared to negative control with Holm-Sidak post hoc test **P<0.01, ***P<0.001.

In order to perform an early knock down, iBAT MSCs were isolated and transfected with siRNAs Sphk1_2 and Sphk1_3, including unspecific siRNA as negative control. 24 hours after transfection cells were induced to differentiate, and at day 8 of differentiation cells were stimulated with 0.5 µM NE for 3 hours. After RNA isolation and cDNA synthesis, expression levels of *Sphk1*, brown and adipogenic markers were determined by RT-qPCR (Figure 21). The knock down was very efficient and was still detected after 8 days of differentiation (Sphk1_2 55%, Sphk1_3 80%). *Ucp1* basal expression was not affected, but NE responsiveness was increased with Sphk1_2 (38%) and reduced with Sphk1_3 (-57%). *Pgc1α* followed a similar pattern, with basal expression unaffected and NE responsiveness significantly increased with Sphk1_2 (91%). *Dio2* basal expression was not significantly affected, but NE induction was significantly increased with

Sphk1_3 (2 fold). *Prdm16* basal expression was slightly reduced with Sphk1 knock down (Sphk1_2 -13%, Sphk1_3 -34%) and NE responsiveness was also reduced (Sphk1_2 -26%, Sphk1_3 -30%). *Cebpβ* basal expression was not significantly affected, but NE responsiveness was reduced with Sphk1_2 (-38%) and increased with Sphk1_3 (1 fold). *Pparγ* levels were increased with Sphk1 knock down at the basal level (Sphk1_2 40%, Sphk1_3 23%) and more significantly upon NE stimulation (Sphk1_2 61%). Expression of *Cidea* and *Cpt1b* was also assessed, but there were no significant alterations (data not shown).

In comparison to the late knock down, the early knock down of Sphk1 caused milder effects on the expression of brown and adipogenic markers. An interesting difference was the upregulation of *Pparγ* and *Dio2* caused by the early knock down. Determining the meaning of this specific difference would require further investigation.

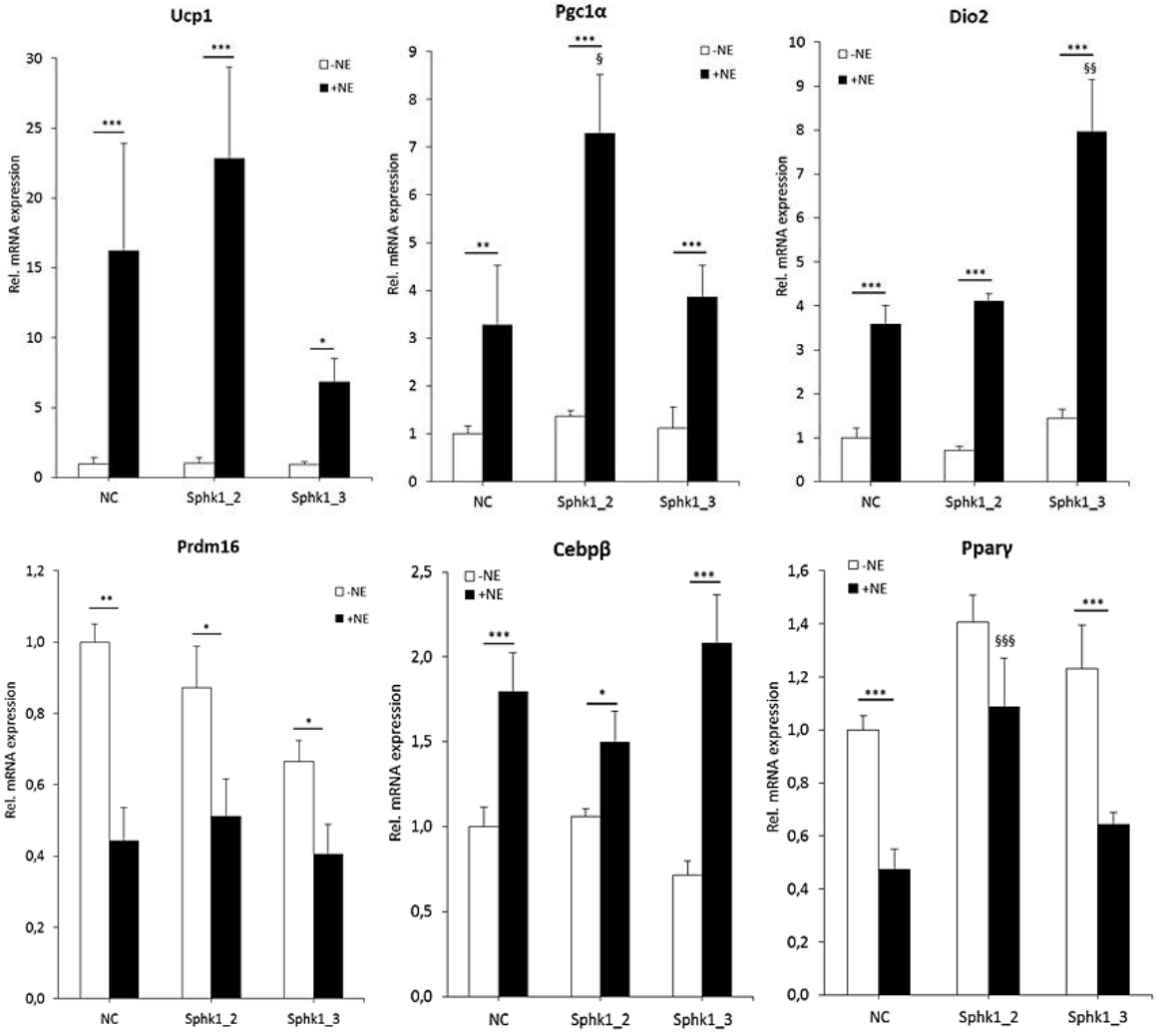

Figure 21: Effect of Sphk1 early knock down on expression of brown and adipogenic marker genes in differentiated iBAT MSCs. Cells were transfected with siRNAs Sphk1_2 and Sphk1_3 at 20nM final concentration using RNAiMax reagent, including unspecific siRNA as negative control (NC). 24h after transfection cells were induced to differentiate, and at day 8 cells were stimulated with 0.5 µM NE for 3 h. After RNA isolation and cDNA synthesis, expression of brown and adipogenic marker genes was detected by RT-qPCR. Expression levels were normalized to the housekeeping *Tbp*, and fold change was determined in relation to NC. n=3, mean ± SEM, two-way ANOVA and Holm-Sidak post-hoc test compared to NC, NE effect *P<0.05, **P<0.01, ***P<0.001 (§ for KD effect).

3.3.4. Analysis of *Sphk1* early knock down in the differentiation process of ingWAT MSCs

Sphk1 early knock down was also performed in ingWAT MSCs to investigate the role of Sphk1 in their activation and differentiation. siRNAs previously used were tested to ensure knock down efficiency (Table 4). Although Sphk1_2 knock down was not significant it was still used to allow comparison to previous experiments.

Table 5 Efficiency of Sphk1 siRNAs in white adipocyte progenitors.

siRNA	Sphk1_2	Sphk1_3
Efficiency	43% KD ns	51% KD *

IngWAT MSCs were transfected using RNAiMax reagent and 20nM final concentration of each siRNA per well. Cells were harvested 48 hours after transfection for RNA isolation, cDNA synthesis and analysis of Sphk1 expression by RT-qPCR. The values represent the mean expression compared to the negative control (n=3). One-way ANOVA compared to negative control with Holm-Sidak post hoc test *P<0.05.

Cells were isolated and transfected with siRNAs Sphk1_2 and Sphk1_3, including unspecific siRNA as negative control. Cells were induced to differentiate 24 hours after transfection and at day 8 of differentiation cells were stimulated with 0.5 µM NE for 3 hours. Throughout the differentiation process, cells were stimulated with 1µM $cPGI_2$ to induce browning, and assess the importance of *Sphk1* in this process. After RNA isolation and cDNA synthesis, expression levels of brown and adipogenic markers were determined by RT-qPCR (Figure 22). Although the knock down was not detectable at day 8 (data not shown), there were significant effects in brown and adipogenic marker genes. The lack of detectable knock down at day 8 could be due to reduced transfection efficiency or increased siRNA degradation.

Ucp1 induction by $cPGI_2$ was significantly reduced by siRNA Sphk1_3 (-83%) in basal conditions, and induction by NE was reduced in white (-51%) and beige cells (-45%). *Cidea* expression changes were not significant but siRNA Sphk1_3 caused a strong reduction at basal level (EtOH undetected, $cPGI_2$ -58%). *Pgc1α* induction by $cPGI_2$was significantly reduced by Sphk1_3, both in basal (-50%) and NE stimulated groups (-40%). In terms of adipogenic markers, *Retn* and *Fabp4* presented a similar expression pattern, with reduced basal expression in beige cells by Sphk1_2 (-61% and -48%, respectively) and by Sphk1_3 (-76% and -52%, respectively), though the changes were only significant for Fabp4. Also, Sphk1_3 significantly reduced NE responsiveness in beige cells (*Retn* -76%, *Fabp4* -51%). *Cebpβ* basal expression was significantly increased in white (Sphk1_2: 2.7 fold; Sphk1_3: 6 fold) and beige adipocytes (Sphk1_3: 3 fold), and NE induction was overall blunted by *Sphk1* knock down. The effects on *Pparγ* expression were not consistent, with only siRNA Sphk1_2 significantly reducing its expression (EtOH -85%, $cPGI_2$ -80%). *Cebpα* basal expression was not significantly affected by *Sphk1* knock down, but $cPGI_2$ induction tended to be reduced (Sphk1_2 -14%, Sphk1_3 -33%).

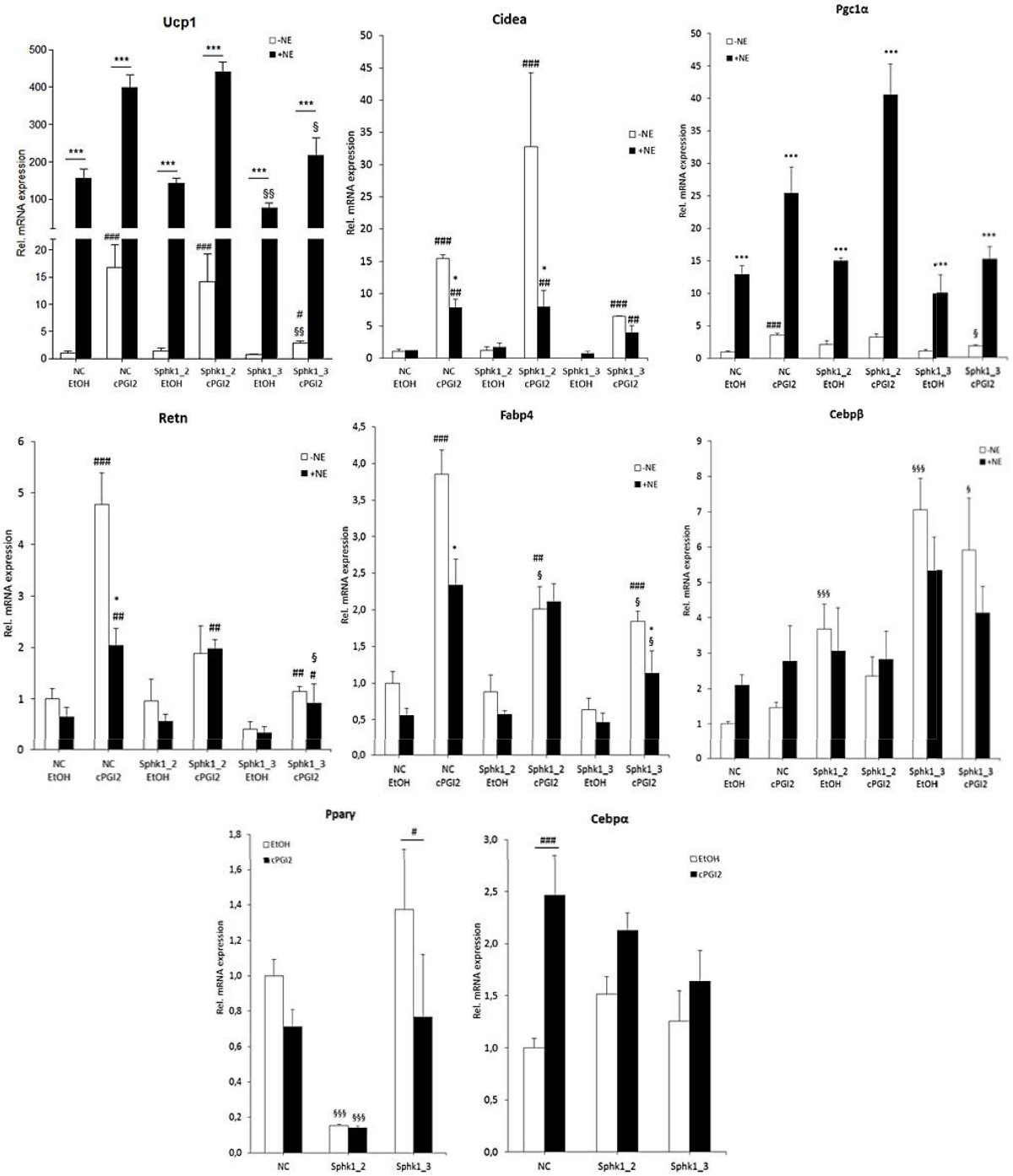

Figure 22: Effect of Sphk1 early knock down on expression of brown and adipogenic marker genes in differentiated ingWAT MSCs. Cells were transfected with siRNAs Sphk1_2 and Sphk1_3 at 20nM final concentration using RNAiMax reagent, including unspecific siRNA as negative control (NC). 24h after transfection cells were induced to differentiate, including 1µM $cPGI_2$, and at day 8 cells were stimulated with 0.5 µM NE for 3 h. After RNA isolation and cDNA synthesis, expression of brown and adipogenic genes was detected by RT-qPCR. Expression levels were normalized to the housekeeping *Tbp*, and fold change was determined in relation to NC. n=3, mean ± SEM, two-way ANOVA and Holm-Sidak post-hoc test compared to NC, NE effect *P<0.05, **P<0.01, ***P<0.001 (§ for KD effect, # for $cPGI_2$ effect).

Pgc1α is the prime regulator of mitochondrial biogenesis, and considering its reduction by *Sphk1* knock down, the expression of mitochondrial genes was also assessed to determine if this could affect mitochondrial biogenesis (Figure 23). Only siRNA Sphk1_3 caused a significant reduction in *Cox7a1* expression (EtOH -61%, $cPGI_2$ -63%), and *Cox8b* tended to be reduced (EtOH -54%, $cPGI_2$ -60%).

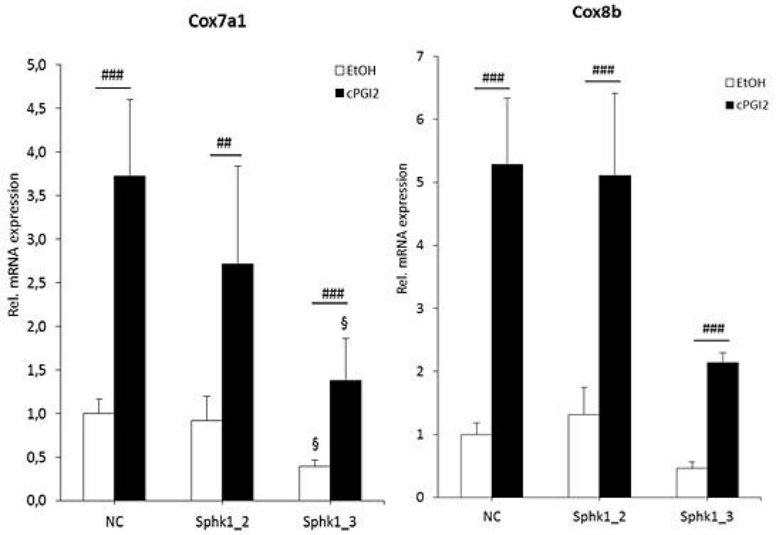

Figure 23: Effect of Sphk1 early knock down on mitochondrial gene expression in differentiated ingWAT MSCs. Cells were transfected with siRNAs Sphk1_2 and Sphk1_3 at 20nM final concentration using RNAiMax reagent, including unspecific siRNA as negative control (NC). 24h after transfection cells were induced to differentiate, including 1µM $cPGI_2$. After RNA isolation and cDNA synthesis, expression of *Cox7a1* and *Cox8b* was detected by RT-qPCR. Expression levels were normalized to the housekeeping *Tbp*, and fold change was determined in relation to NC. n=3, mean ± SEM, two-way ANOVA and Holm-Sidak post-hoc test compared to NC, KD effect §P<0.05, $cPGI_2$ effect ##P<0.01, ###P<0.001.

Compared to the late knock down, the early knock down of Sphk1 in ingWAT MSCs affected more significantly adipogenic genes, with Sphk1_2 causing a strong downregulation of *Pparγ* and a very significant upregulation of *Cebpβ*. Moreover, the early knock down of *Sphk1* produced a more consistent reduction in mitochondrial gene expression in differentiated ingWAT MSCs.

3.3.5. Analysis of *Sphk1* early knock down in cell viability of adipose tissue MSCs

Considering the strong effects on adipocyte differentiation caused by *Sphk1* early knock down, it was also assessed if the knock down of this kinase affects cell viability, given that its product is known to have anti-apoptotic and pro-survival effects. Another reason to assess cell viability was the reduction in adipocyte number observed during the previous differentiation experiments. Viability was analyzed 24 hours after transfection with siRNAs against Sphk1, i.e. before differentiation induction, and at day 4 of differentiation.

In apoptotic cells, the membrane phospholipid phosphatidylserine (PS) is translocated from the inner to the outer leaflet of the plasma membrane, thereby exposing PS to the external cellular environment (Martin et al. 1995). Apoptosis was assessed using AnnexinV staining, which uses AnnexinV, a protein with high affinity for PS, to detect cells undergoing apoptosis. AnnexinV was conjugated to the fluorochrome FITC, which allowed cell analysis by flow cytometry. The

staining was combined with propidium iodide (PI) to allow distinction of cells in different stages of apoptosis: cells that stain only for AnnexinV are in early apoptosis and maintain membrane integrity; cells that also stain for PI are at the end stage of apoptosis or already dead, because loss of membrane integrity is necessary for PI to enter the cell and bind DNA.

Cells were transfected with siRNA Sphk1_2 and Sphk1_3, including unspecific siRNA for negative control and cell-death siRNA for positive control. For the first time point, cells were harvested 24 hours after transfection, stained with AnnexinV and PI, and analyzed by flow cytometry. Cell debri was excluded and single stainings were used to set compensation and gate PI positive and AnnexinV positive cell populations (Figure 24 A). There was an increase in apoptotic cells and dead cells in ingWAT with *Sphk1* knock down (Figure 24 B, D), but in iBAT there was a significant decrease in apoptotic cells with *Sphk1* knock down and a tendency for increase in dead cells (Figure 24 C,E).

On the other hand, at day 4 of differentiation (Figure 25) there was a much more significant increase in apoptosis and cell death with *Sphk1* knock down. This was observed not only in ingWAT MSCs (Figure 25 A), with 4-5% more $AnnexinV^+$ cells in *Sphk1* knock down groups compared to NC, and 3% more PI^+ cells, but also in iBAT MSCs (Figure 25 B), with 6% and 2.5% more $AnnexinV^+$ cells, and 6% and 2% more PI^+ cells. These results indicate that *Sphk1* knock down significantly affects cell viability during differentiation, but this effect is not immediate after knock down. The increase in amount of cells undergoing apoptosis during differentiation could explain the reduction in expression of adipogenic and brown marker genes, indicating that the increase in cell death is specific for differentiating MSCs, and further supporting the conclusion that Sphk1 is necessary for normal adipogenic differentiation. Moreover, the strong increase in apoptosis in iBAT MSC further supports the importance of Sphk1 for brown adipocyte differentiation.

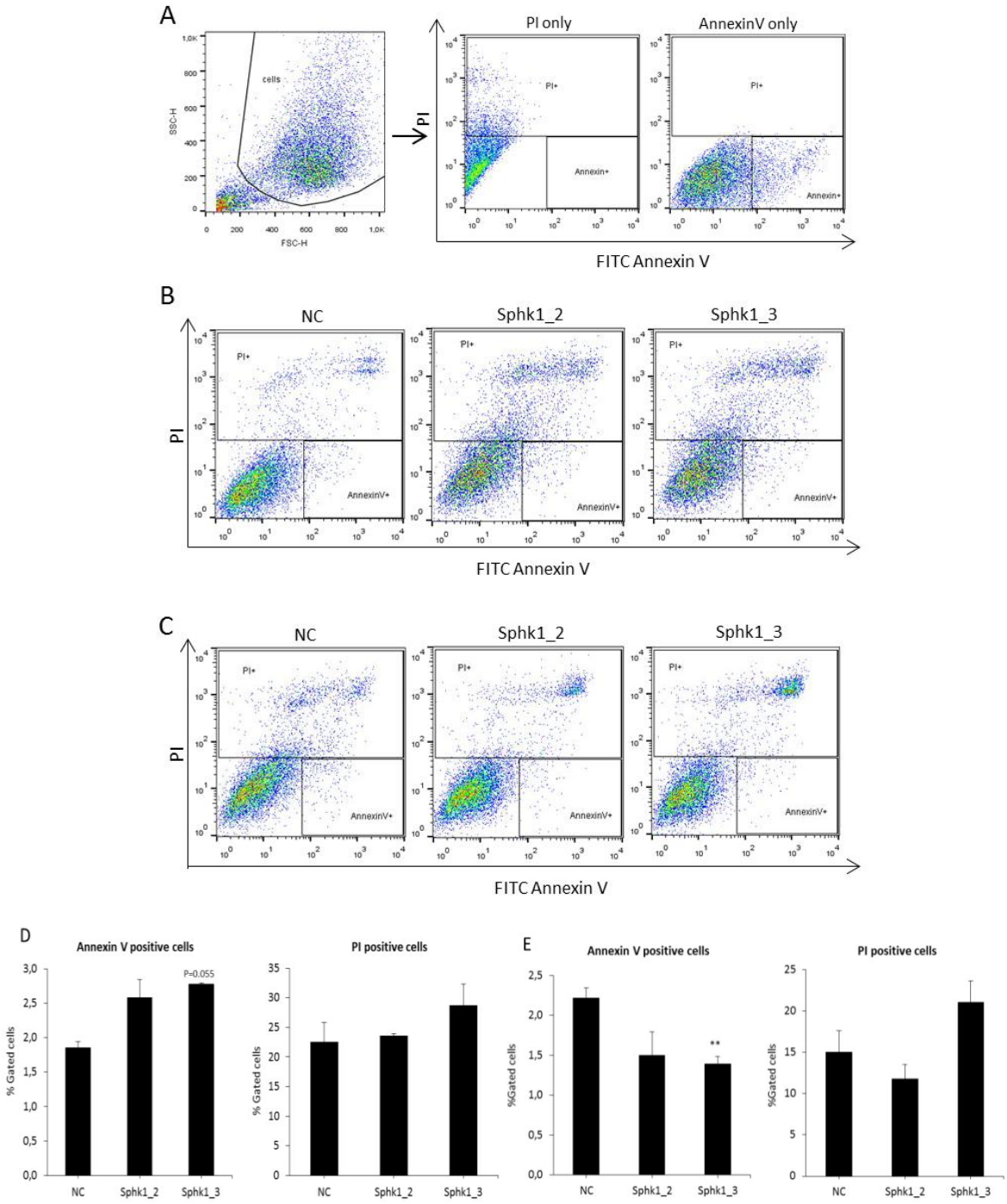

Figure 24: Flow cytometry analysis of apoptosis of MSCs 24h after Sphk1 knock down. MSCs were transfected with siRNAs Sphk1_2 and Sphk1_3 at 20nM final concentration using RNAiMax reagent, including unspecific siRNA as negative control (NC). 24h after transfection cells were detached and stained with FITC-AnnexinV and PI. Fluorescent signal was detected by flow cytometry. (A) FACS plots depict gating for size (exclusion of cell debri) and single stained populations (PI only and AnnexinV only) were used to define AnnexinV+PI- and PI+AnnexinV- gates respectively.. (B) Representative FACS plots of ingWAT MSC and (C) iBAT MSC 24h after transfection. Histograms of AnnexinV+ and PI+ ingWAT (D) and iBAT (E) cell populations. FSC-H, forward scatter-height; SSC-H, side scatter-height; PI, propidium iodide. n=3, mean ± SEM, ANOVA on ranks not significant.

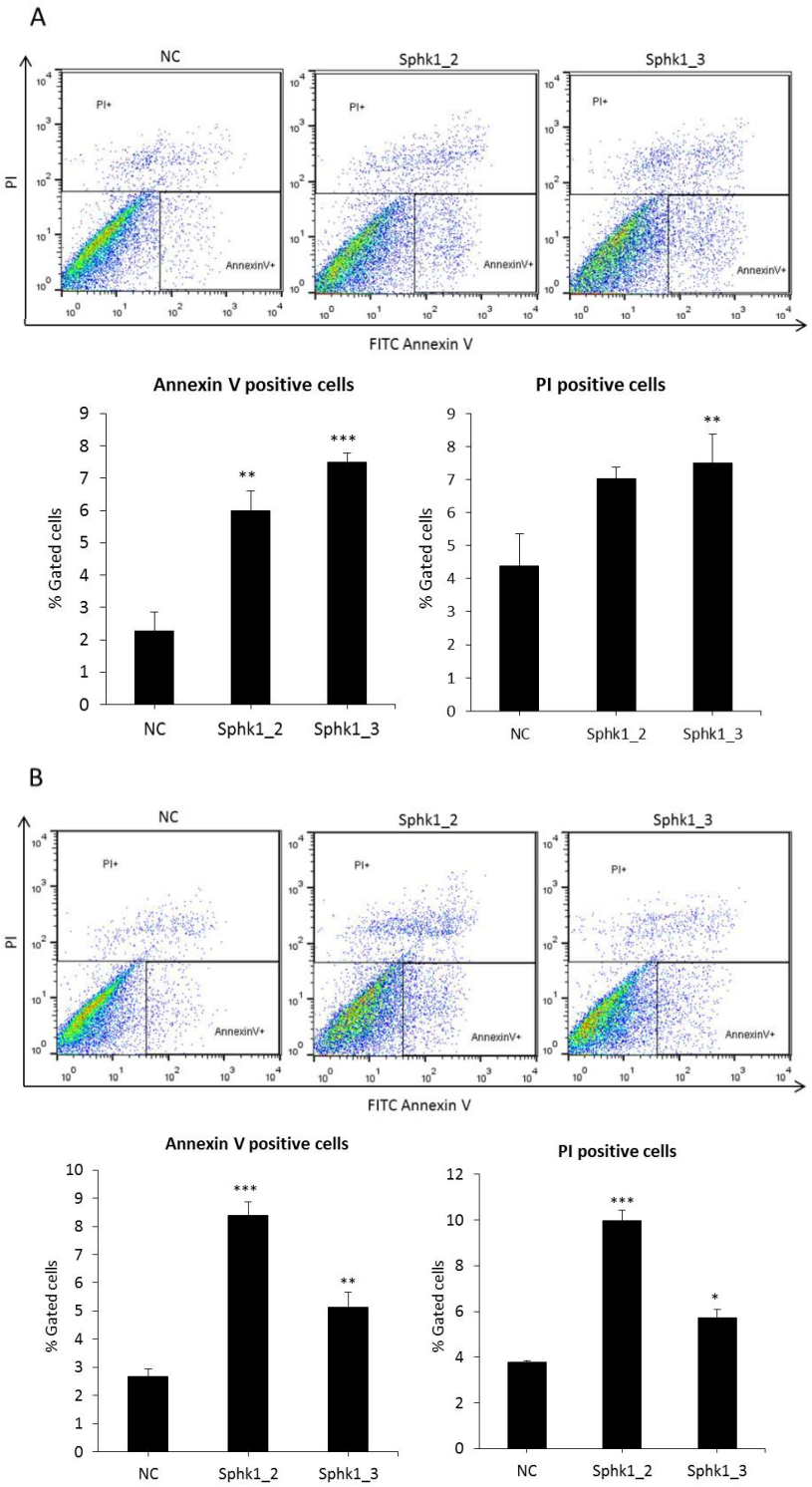

Figure 25: Flow cytometry analysis of viability of MSC with Sphk1 knock down at day 4 of differentiation. MSCs were transfected with siRNAs Sphk1_2 and Sphk1_3 at 20nM final concentration using RNAiMax reagent, including unspecific siRNA as negative control (NC). At day 4 of differentiation cells were detached and stained with FITC-AnnexinV and PI. Fluorescent signal was detected by flow cytometry. Cells were gated for size (exclusion of cell debri) and single stained populations were used to define AnnexinV+PI- and PI+AnnexinV- gates, as depicted in Figure 24. Representative FACS plots of (A) ingWAT MSC and (B) iBAT MSC, with respective histograms of AnnexinV+ and PI+ cell populations. PI, propidium iodide. One-way ANOVA and Holm-Sidak post-hoc test compared to NC *P<0.05, **P<0.01, ***P<0.001.

3.3.6. Analysis of *Sphk1* early knock down in cell cycle of adipose tissue MSCs

After induction of differentiation, MSCs undergo mitotic clonal expansion before exiting the cell cycle, and this is necessary to proceed with differentiation (Algire et al. 2013). Considering that S1P promotes cell proliferation and survival, it was hypothesized that Sphk1 knock down would have negative effects on cell cycle progression. The effect of *Sphk1* knock down was explored at 8 hours after induction of differentiation, to analyze cells before exiting the cell cycle. Analysis was performed by measuring incorporation of the nucleoside analog 5-ethynyl-2´-deoxyuridine (EdU) during DNA synthesis, which is later detected by a click reaction by covalently binding a fluorescent dye with a picolyl azide to the alkyne present in EdU (Qu et al. 2011).

Adipose tissue MSCs were transfected with siRNA Sphk1_2, Sphk1_3 and negative control, and induced to differentiate 24 hours after transfection. At 5 hours after differentiation induction, cells were incubated with 10 µM EdU for 3 hours, and at 8 hours after differentiation induction cells were harvested and underwent click reaction for EdU labeling, followed by detection by flow cytometry (Figure 26).

After gating cells for size and doublet exclusion (Figure 26 A), EdU positive (EdU^+) and EdU negative (EdU^-) populations, stages of the cell cycle were defined according to DNA content determined by PI signal. In ingWAT MSCs, *Sphk1* knock down with siRNA Sphk1_2 significantly increased EdU incorporation (8% more compared to NC), indicating that more cells were actively cycling (Figure 26 B, 27 A), and of these there was a significant increase in cells in S/G2/M (4%) and in G1 (3%). With siRNA Sphk1_3 there was a significant decrease in EdU^- cells in G1 (-13%) and a significant increase in EdU^- cells in S/G2/M (12%), indicating an accumulation of cells in S/G2/M before EdU incubation, that fail to complete cell division during the labeling time. With Sphk1_2 there was a significant decrease in EdU^- cells in G1 (-8.5%).

In iBAT MSCs (Figure 26 C, 27 B) there was an increase in EdU incorporation with *Sphk1* knock down by both siRNAs (~2.5%). Sphk1_2 caused a significant increase in EdU^+ cells in G1 (1%) and S/G2/M (1.4%), indicating that more cells were dividing. Sphk1_3 significantly increased EdU^+ cells only in G1 (2.3%), which may indicate a slower progression through the cell cycle or an accumulation in G1. In EdU^- cells, Sphk1_3 caused a significant reduction in cells in G1 (-7%) and increased cells in S/G2/M (4.4%), indicating an accumulation of cells in S/G2/M shortly after induction and before EdU incubation.

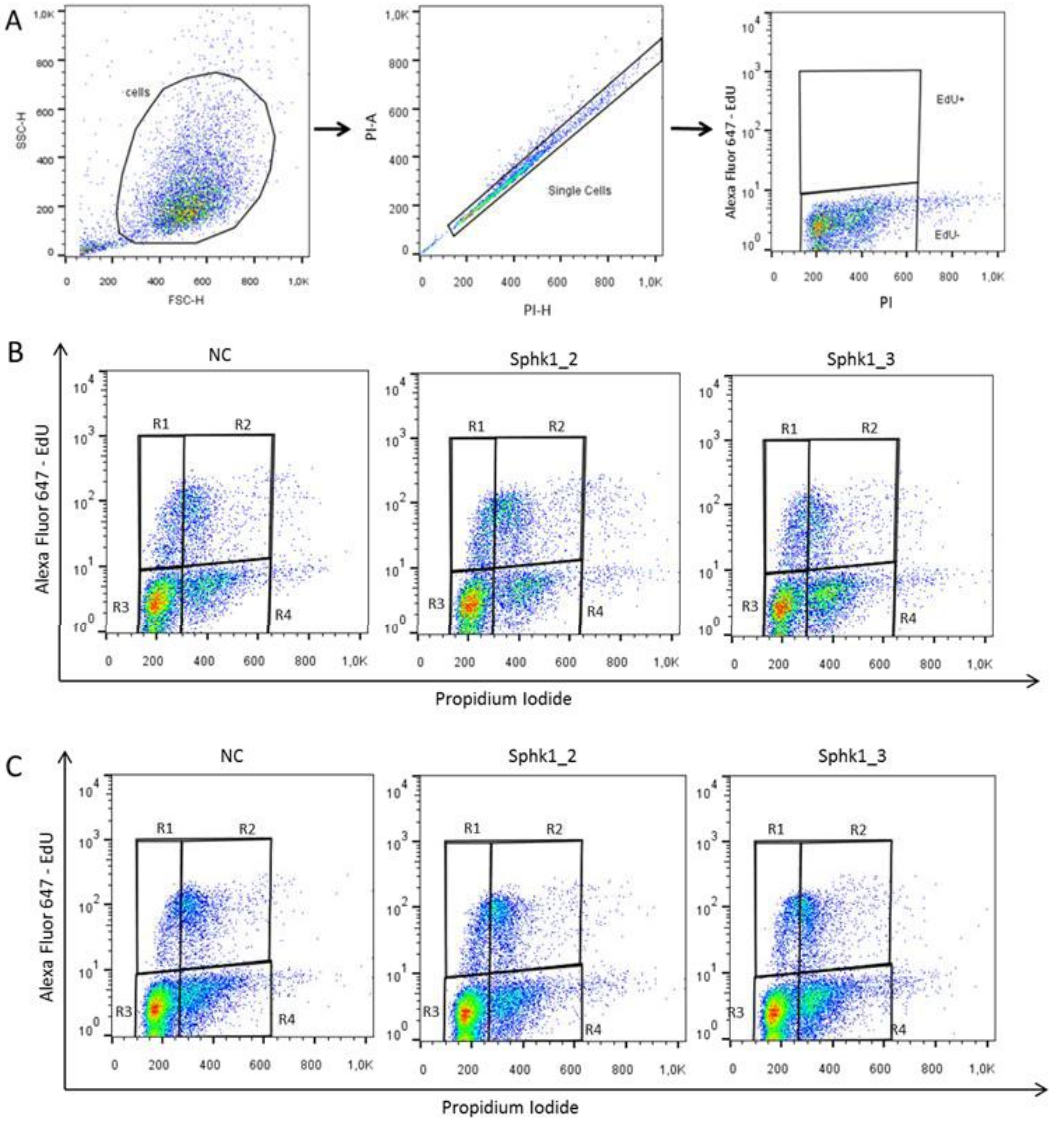

Figure 26: Flow cytometry analysis of cell cycle progression in MSCs with *Sphk1* knock down 8 hours after induction of differentiation. MSCs were transfected with siRNAs Sphk1_2 and Sphk1_3 at 20nM final concentration using RNAiMax reagent, including unspecific siRNA as negative control (NC). Cells were incubated with EdU between 5h and 8h after induction of differentiation. After EdU labeling, cells were detached, fixed in 4% PFA and click reaction with Alexa Fluor 647 was performed to allow EdU detection by flow cytometry. Cells were also stained with PI. (A) FACS plots depict gates defined for size, doublet exclusion and EdU+ gate defined with single stained PI+ cells. Representative FACS plots of (B) ingWAT MSC and (C) iBAT MSC. PI, propidium iodide; R1, G1 EdU+ cells; R2, S/G2/M EdU+ cells; R3, G1 EdU-cells; R4, S/G2/M EdU- cells.

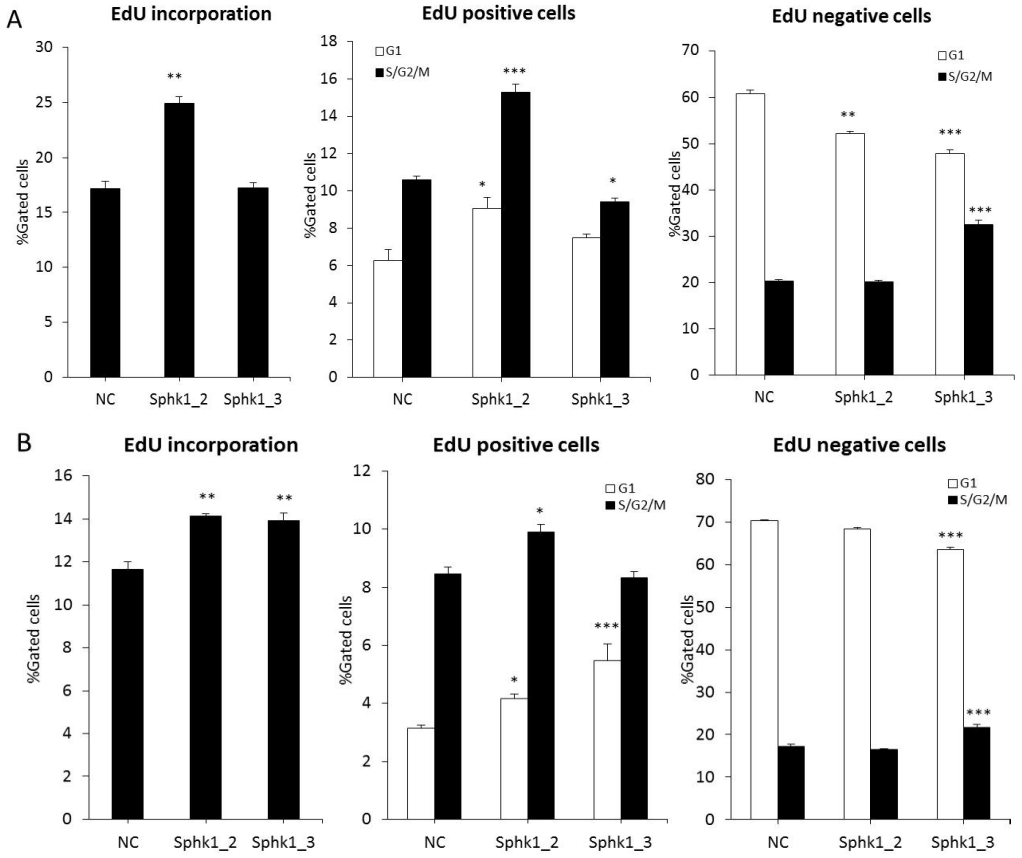

Figure 27: Flow cytometry analysis of cell cycle in MSCs with *Sphk1* knock down 8 hours after induction of differentiation. Histograms of EdU incorporation and cell cycle distribution of (A) ingWAT MSC and (B) iBAT MSC. One-way ANOVA, *P<0.05, **P<0.01, ***P<0.001.

Although Sphk1 knock down promotes DNA synthesis after differentiation induction, cells seem to accumulate in S/G2/M phase, which could be due to an arrest in this phase or a slower progression through cell division. If fewer cells are completing cell division, this would result in fewer cells entering differentiation and consequently reduced adipogenesis observed in previous experiments.

3.4. Effect of S1P in differentiation of ingWAT MSCs

The product of Sphk1, sphingosine-1-phosphate (S1P), is known to promote cellular proliferation, stimulate survival and protect against apoptosis (Alvarez et al. 2007b). *Sphk1* knock down exhibited anti-proliferative effects in adipose progenitors, so it would be expected that S1P promotes cell growth and proliferation. To prove this hypothesis and to determine if these effects are concentration dependent, ingWAT MSCs were differentiated with increasing concentrations of S1P (50 nM, 0.5 µM, 5 µM), chosen to be within relevant physiological range (Blachnio-Zabielska et al. 2012). At day 8 of differentiation cells were fixed and stained with DAPI to estimate cell density and proliferation. Bright field pictures were also taken to compare adipocyte differentiation (Figure 28 A).

There was a clear reduction in adipocyte formation with increasing concentration of S1P (Figure 28 A), indicating that high concentrations of S1P during adipogenic differentiation hinder this process. On the other hand, there was an increase in cell proliferation with increasing S1P concentration (Figure 28 B and C). Overall, these results confirm the proliferative effects attributed to S1P and also indicate that S1P reduces adipogenic differentiation. The reduced adipogenesis observed by S1P addition indicates that the observed reduction in differentiation may not be exclusively due to reduced levels of S1P, but Sphk1 signaling may be more important for normal adipogenic differentiation.

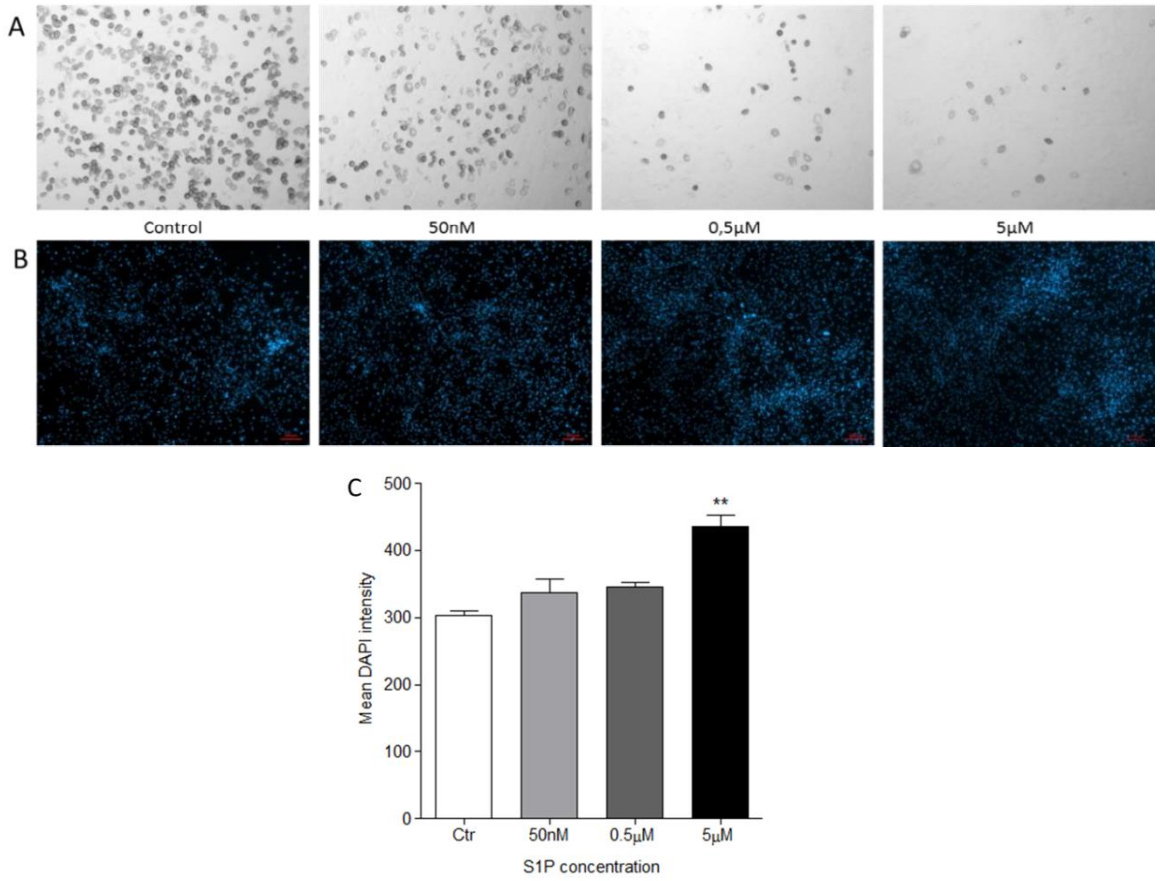

Figure 28: Effect of S1P in differentiation of ingWAT MSCs. Cells were differentiated with 50 nM, 0.5 µM and 5 µM of S1P. Cells treated only with normal differentiation medium without S1P were used as control. Bright field (A) pictures were taken to assess adipocyte number. Fluorescent pictures of DAPI staining (B) were taken to average cell density and proliferation. Magnification 100x. (C) Histogram of mean DAPI intensity from fluorescent pictures, n=3, mean ± SEM, one-way ANOVA and Holm-Sidak post-hoc test compared to NC, **P<0.01.

In conclusion, the results presented indicate that Sphk1/S1P signaling is important for normal adipogenic differentiation, especially in brown adipocytes, and also for proper function of mature adipocytes. Loss of Sphk1/S1P signaling not only affects expression of genes important for adipogenesis and mature function, but also reduces cell cycle progression at the beginning of differentiation and increases cell death at later stages of the process.

4. Discussion

Sphingolipid metabolites have been identified as important lipid modulators of numerous cell functions. These metabolites are known to function not only as intracellular second messengers, but also in the extracellular space. Sphingosine 1-phosphate has numerous functions as an important extracellular mediator that binds to cell surface S1P receptors. Previous studies have shown that Sphk1 and S1P play an important role in adipocyte differentiation and adipose tissue metabolism, both in normal and obese metabolic state (Jun et al. 2006; Hashimoto et al. 2009; Wang et al. 2014). Moreover, Vegiopoulos *et al.* verified that Sphk1 is upregulated during adipogenic differentiation of MSCs and in response to adrenergic stimulation (unpublished data), and microarray expression profiling data from published studies also indicates that Sphk1 is induced in adipose tissue in response to cold exposure (Li et al. 2005; Xue et al. 2009). Therefore, it was the aim of this study to further investigate the role of Sphk1 in MSC activation, adipocyte differentiation and mature adipocyte function.

4.1. Sphk1 is upregulated by cold exposure and adrenergic stimulation

In accordance to gene expression profiling, *Sphk1* levels were found highly upregulated in BAT in response to cold exposure, and to some extent also in abdWAT. This transient upregulation may protect cells from apoptosis related to increased ceramide levels resulting from cell activation in response to cold exposure. It could also stimulate progenitor proliferation and differentiation to promote BAT hyperplasia and increase BAT thermogenic capacity. Additionally, it might contribute to the recruitment of inflammatory cells that may be important for tissue remodeling.

In vitro differentiation of ingWAT and iBAT MSCs revealed that *Sphk1* is also upregulated by adrenergic stimulation, with a greater induction in brown compared to white adipocytes. These results point to an important role for Sphk1 in brown adipocyte function and, in order to characterize it, loss-of-function experiments were initially performed in the brown adipocyte cell line BATkl2.

4.2. Sphk1 knock down affects mature adipocyte function

The knock down of *Sphk1* in mature BATkl2 adipocytes caused changes in gene expression that indicate a significant effect in adipocyte function. The reduction in expression of *Pgc1α*, the main regulator of mitochondrial biogenesis, and *Cox7a1*, a subunit of complex IV of the electron transport chain, point to a reduction in mitochondrial biogenesis and impairment of oxidative capacity of brown adipocytes.

The physiological relevance of Sphk1 was further explored in MSCs isolated from white and brown adipose tissue. *Sphk1* knock down in differentiated iBAT MSCs resulted in a strong downregulation of brown marker genes. The effects were most consistent in *Prdm16*, *Dio2*, *Cidea* and *Cpt1b*. These genes are important for thermogenesis, promoting *Ucp1* expression and mitochondrial respiration (Gesta et al. 2007). Therefore their downregulation may indicate that knock down of Sphk1 in differentiated brow adipocytes impairs their thermogenic activity in response to adrenergic stimulation.

IngWAT MSCs were differentiated with $cPGI_2$ to induce browning and investigate the relevance of Sphk1 in this process and function of beige adipocytes (control cells were treated with vehicle EtOH). The knock down of Sphk1 in differentiated white and beige MSCs caused a significant reduction in expression of white markers *Fabp4*, *Retn* and *Cebpα*, and the effect on brown markers was not consistent except for *Cidea*, which was clearly upregulated both in white and beige adipocytes.

Considering the position of Sphk1 in sphingolipid metabolism (see Figure 7 in Introduction), knock down may result not only in reduction of its product S1P, but also in an accumulation of substrates sphingomielin and ceramide. The latter has been reported to interfere with insulin signaling by blocking activation of Akt/PKB (Chavez & Summers 2012) and consequently reducing expression of *Cebpα* (Fernández-Veledo et al. 2006), which could explain some of the observed changes in gene expression given its role in regulating the expression of adipogenic genes. Also, insulin signaling is important for induction of adipogenesis, so impaired insulin signaling caused by *Sphk1* knock down could explain the reduction in expression of adipogenic markers. Measuring insulin responsiveness would help determine if this is one mechanism behind the phenotype. In addition, reduced adipocyte survival could also explain the reduction in adipogenic marker genes.

De novo lipogenesis does not seem to be much affected by *Sphk1* late knock down, as no significant differences were observed in lipid droplet size and expression of lipogenesis genes, except *Acaca*, which was significantly downregulated in beige adipocytes. Mitochondrial genes were not affected in a similar way by *Sphk1* knock down, with $cPGI_2$ induction increasing expression of *Cox8b* but decreasing that of *Cox7a1*. NE–induced lipolysis rate in beige adipocytes was increased with Sphk1 knock down, even though expression of lipolysis genes. On the other hand, *Sphk1* knock down reduced basal lipolysis in brown and white adipocytes. NE-induced lipolysis was reduced in white adipocyte but was not altered in brown adipocytes.

In rat white adipocytes, activation of S1PR by S1P promotes cAMP signaling, resulting in stimulation of lipolysis (Jun et al. 2006). One could speculate that reduced S1P levels caused by Sphk1 knock down fail to increase cAMP levels required for activation of PKA and subsequently lipolysis. While this could be the case for basal lipolysis, given that it was reduced in white and beige adipocytes with Sphk1 knock down, NE –stimulated lipolysis may be regulated differently by Sphk1/S1P signaling, since it was increased in beige adipocytes with Sphk1 knock down. It would be relevant to measure the levels of ceramide, sphingosine and S1P in adipocytes with Sphk1 knock down to determine if these effects are mediated by accumulation of ceramide/sphingosine. Although many methods can be employed for analysis of sphingolipids, the combination of high-performance liquid chromatography (HPLC) with tandem mass spectrometry (MS/MS) provides a high level of sensitivity, structural specificity, and quantitative precision for analysis of small samples (Haynes et al. 2009), and would thus be the most suitable method. In order to determine the role of accumulating ceramide/sphingosine in the knock down phenotype, functional experiments could be performed by adding S1P to rescue the knock down and also by pharmacologically inhibiting ceramide synthesis to prevent its accumulation.

A rescue experiment with S1P and pharmacological inhibition of Sphk1 would also help clarify the inconsistencies observed with the two siRNAs, and confirm the specificity of the obtained results.

4.3. Sphk1 knock down impairs adipogenic differentiation

Knock down of *Sphk1* in undifferentiated BATkl2 cells reduced adipogenesis and caused a significant reduction in expression of brown and adipogenic marker genes, both in basal and NE–stimulated conditions. Responsiveness to adrenergic stimulation was significantly reduced, which could indicate that Sphk1 is important for adrenergic signaling. Jun et al. 2006 reported that micromolar concentrations of S1P activate AC via S1PR, inducing cAMP production and PKA activation. It could be speculated that activation of the cAMP/PKA pathway by S1P supports or reinforces PKA activation by adrenergic signaling, thus providing an explanation for the reduction in NE responsiveness observed by Sphk1 knock down. Expression of lipolysis enzymes and basal lipolysis rate were also reduced, which could indicate that reduction in adipogenesis caused by *Sphk1* knock down impaired the proper assembly and function of the lipolysis machinery.

The knock down of Sphk1 in undifferentiated iBAT MSCs did not produce significant changes in basal expression of brown and adipogenic genes, and the effects on NE responsiveness were not consistent between siRNAs, which could be explained by off-target effects. Also, the transfection itself was quite toxic for the cells, which was not observed in ingWAT MSCs. This could be due to a greater sensitivity of iBAT MSCs and may also have contributed to the inconsistency of the results.

On the other hand, Sphk1 knock down in undifferentiated ingWAT MSC had a significant effect on expression of adipogenic genes, downregulating *Fabp4*, *Retn* and *Cebpα*, but upregulating *Cebpβ.* The only significant difference between white and beige adipocytes was a strong upregulation of *Cidea* in the presence of $cPGI_2$, which may indicate that Sphk1 plays a similar role in adipogenesis of white and beige cells. Moreover, the expression of *Pgc1α* and mitochondrial genes was significantly reduced, which indicates that the presence of Sphk1 during differentiation is important for mitochondrial biogenesis and proper assembly of the oxidative machinery.

Overall, the changes observed in gene expression indicate that Sphk1 plays a relevant role in adipogenic differentiation from the beginning of the process and also in differentiated adipocytes, given that loss of function reduces expression of genes required for mature function. These results are in line with the findings of Hashimoto et al. 2009 that reported Sphk1 levels to be elevated during differentiation, both at mRNA and protein level, and that pharmacological inhibition and gene silencing markedly attenuated adipogenesis, measured by reduced lipid accumulation and reduced expression of adipocyte marker genes *PPARγ*, *aP2* (*Fabp4*) and C/*EBPα*. Moreover, considering that S1P functions in a paracrine but also autocrine manner and S1PR activation promotes CREB phosphorylation, reducing the levels of S1P could result in reduced activation of CREB, a transcription factor relevant for adipogenic differentiation, and therefore reduce the expression of adipogenic genes. However, this may not be the case, since Sphk1 knock down resulted in increased expression of *Cebpβ*, a known target gene of CREB (Impey et al. 2004), and addition of S1P reduced differentiation, which indicates that specifically Sphk1 signaling, and not S1P, is important for differentiation.

Ceramide, sphingosine and S1P are elevated in subcutaneous adipose tissue of diet-induced obese (DIO) mice (Hashimoto et al. 2009) and obese humans (Blachnio-Zabielska et al. 2012). Contrary to the normal metabolic state, elevated levels of S1P are not associated with metabolic

health of adipose tissue. Wang et al. 2014 reported that Sphk1/S1P signaling induces adipose inflammation and reduces adipogenesis in vivo, leading to adipose dysfunction and consequent insulin resistance. Sphk1 and S1P levels were found elevated in plasma and adipose tissue of DIO mice and in adipose tissue of diabetic vs. non-diabetic obese humans. Genetic disruption of Sphk1/S1P signaling using *Sphk1* knockout mice (*Sphk1*$^{-/-}$) caused a significant improvement in adipose tissue health by decreasing adipocyte pro-inflammatory and chemotactic signals, attenuating adipose tissue macrophage accumulation and inflammation, increasing adipogenesis, and contributing to improved systemic insulin sensitivity. Moreover, pharmacological inhibition of Sphk1 in DIO wild type mice shifted the adipose tissue environment from pro-inflammatory to anti-inflammatory, which resulted in upregulation of interleukin-10 and adiponectin (anti-inflammatory cytokines), with consequent improvement of insulin sensitivity and glucose homeostasis. Furthermore, *Sphk1*$^{-/-}$ mice on high-fat diet (HFD) had smaller adipocytes compared to WT and increased expression of adipogenic markers, which suggests that Sphk1/S1P signaling may regulate and limit adipogenesis during weight gain. It is important to refer that decreases in S1P were not associated with changes in plasma or adipose tissue ceramide, which suggests that the improvements in adipose function and glucose homeostasis in Sphk1$^{-/-}$ mice are due to the specific decrease in SK1/S1P signaling and not to changes in ceramide content.

Another study reported that mice fed a HFD with FTY720-phosphate (FTY720-P), a synthetic analogue of S1P, were resistant to obesity. The reduced fat accumulation was attributed to reduced adipogenesis and increased lipolysis. Treatment of 3T3-L1 cells with FTY720-P also reduced adipocyte differentiation and increased lipolysis, by reducing expression of differentiation marker genes *PPARγ*, *C/EBPα* and *adiponectin*, and upregulating the expression of the lipolysis regulators HSL, ATGL and perilipin. However, it is important to notice that FTY720 needs to be phosphorylated by Sphk2 to form the active compound FTY720-P. Sphk1 promotes cell growth and inhibits apoptosis, whereas Sphk2 has been reported to have anti-proliferative and pro-apoptotic effect (Maceyka et al. 2005). A possible explanation for the opposing effects is that the two proteins are located in, or translocated to, different compartments within the cell, and the resulting localized production of S1P will have distinct functions. While Sphk1 is mostly located in the cytosol, Sphk2 is associated mostly with internal membranes such as the endoplasmic reticulum, where S1P production leads to calcium release and apoptosis (does not signal through S1PRs). Therefore, it seems that cytosolic S1P formed by SphK1 has a different function than S1P produced at the ER and/or other membranes by SphK2 (Maceyka et al. 2005), and so the opposing effects of FTY720-P may not be comparable to endogenous S1P produced by Sphk1.

4.4. Sphk1 knock down reduces cell viability and cell cycle progression

S1P produced by Sphk1 is a pro-survival factor, promoting cell proliferation and protecting against apoptosis. Therefore it was hypothesized that Sphk1 early knock down would affect cell viability and proliferation. Although Sphk1 knock down in undifferentiated MSCs did produce a tendency for increase in apoptosis and cell death, the effects were only significant later in the differentiation process, i.e. at day 4 of differentiation. At this stage, a significant increase in apoptosis and cell death was observed both in ingWAT and iBAT adipocytes. This could explain the strong reduction in expression of adipogenic and brown marker genes observed in the early knock

down experiments, indicating that Sphk1 knock down selectively reduced viability of adipocyte precursors and maturing adipocytes. This increase in apoptosis may be due to reduction in the levels of S1P or accumulation of ceramide. While the former has anti-apoptotic properties, the latter plays a clear role in apoptosis (Cuvillier et al. 1996). Ceramide production is a common response to apoptosis-inducing agents, and it is thought to involve a direct action on mitochondria (Siskind 2005). Several enzymes involved in ceramide synthesis are localized to the mitochondria and may play a role in generating a local pool of ceramide that promotes apoptosis. Ceramide accumulation in the outer mitochondrial membrane forms channels that increase membrane permeability and allow release of pro-apoptotic proteins from the intermembrane space to the cytosol, resulting in activation of caspases (Tirodkar & Voelkel-Johnson 2012). As mentioned above, measuring the levels of ceramide and S1P would help clarify the mechanism behind increased cell death. Measuring the expression of Sphk2 would also be relevant to determine if a compensation mechanism causes increased production of S1P by Sphk2 in the mitochondrial outer membrane, which is converted back to ceramide and promotes apoptosis (Maceyka et al. 2005). On top of that, maturing adipocytes may rely on insulin for survival, so reduction in insulin signaling caused by *Sphk1* knock down could explain the increased cell death of maturing adipocytes.

Sphk1 knock down produced significant effects on cell cycle and proliferation. Although there was an increase in the number of cells incorporating EdU, *Sphk1* knock down caused an accumulation of cells in S/G2/M phase that did not incorporate EdU during the labeling time. The cells that did incorporate EdU seemed to accumulate in G1 without progressing to S/G2/M. This could be explained by a slower progression through the cell cycle or by an arrest in these phases. Zhang et al. 1991 reported that S1P stimulates DNA synthesis and cell division in Swiss 3T3 fibroblasts, and acts synergistically with a variety of growth factors, such as insulin, epidermal growth factor, fibroblast growth factor, and FCS. It was later reported that S1P modulates Ca^{2+} signaling in response to mitogenic factors (Fatatis & Miller 1999). On the other hand, increased ceramide levels induce expression of cyclin/Cdk inhibitory protein p21, resulting in a decrease in cells in the S- and G2/M phases due to induction of G1 cell cycle arrest (Ogretmen & Hannun 2004; Gusain et al. 2012). Also, accumulation of the ceramide percursor dihydroceramide is associated with cyclin D1 expression modulation and delayed G1/S transition of cell cycle (Gagliostro et al. 2012), which further supports the anti-proliferative effect of ceramide accumulation. However, *Sphk1* knock down caused an increase in DNA synthesis, which indicates that the effect is probably not due to ceramide accumulation.

Dai et al. 2014 reported that Sphk1 and Sphk2 are equally responsible for insulin induced cell cycle progression and proliferation of MCF7 breast cancer cells. They also reported that knockdown of *SphK1* and *SphK2* significantly inhibited both insulin-promoted cell cycle progression and cell growth. Also, insulin-induced phosphorylation of ERK1/2 and Akt, the two established downstream signals involved in insulin's mitogenic action, was significantly inhibited by double knockdown of Sphk1 and Sphk2. Considering the current knowledge of the mechanism responsible for Sphk1/S1P proliferative effect, the effects of Sphk1 knock down on cell cycle could be attributed not only to reduced Sphk1/S1P signaling but also to ceramide accumulation.

Addition of S1P during differentiation of ingWAT MSCs clearly reduced adipogenesis in a concentration dependent manner. The reduced adipogenesis did not result from increased cell

death but rather from increased proliferation, which was detected by increased intensity of DAPI signal. After induction of differentiation cells undergo mitotic clonal expansion before exiting the cell cycle, which is necessary to proceed with differentiation. This result is in line with previous studies that reported S1P to have proliferative effects, mostly mediated by S1PR signaling and activation of ERK1/2 (Brinkmann 2007). Moreover, recent evidence indicate that S1P may play a significant role in the regulation of many aspects of embryonic and adult stem cell biology (Pébay et al. 2007). In muscle satellite cells, conversion of sphingomyelin into S1P promotes transition from a quiescent to proliferative state and is important for muscle regeneration (Nagata et al. 2006), and increase in cellular S1P levels promotes proliferation and expression of cell surface pluripotency markers in murine embryonic stem cells (Smith et al. 2013).

4.5. Outlook

The mechanism by which Sphk1 influences adipocyte differentiation require further investigation. As mentioned above, measuring the concentration of S1P, ceramide and other sphingolipids in cells with and without *Sphk1* knock down is important to determine the alterations in sphingolipid signaling. A rescue of the *Sphk1* knock down phenotype could be performed by adding an adequate concentration of S1P to the cell culture medium. Additionally, S1P could be added to white and brown MSCs at different time points of the differentiation process to help distinguish the effects of S1P in undifferentiated progenitors and mature adipocytes.

Moreover, given the antagonistic effects of ceramide, a pharmacological inhibitor of ceramide synthase could be used to prevent a possible increase in ceramide synthesis due to accumulation of Sphk1 substrate sphingosine. On the other hand, inhibiting S1P phosphatase in cells with Sphk1 knock down would prevent S1P degradation back to sphingosine to promote ceramide synthesis, and could help determine if the phenotype results from an increase in ceramide.

Measuring the levels of S1P could also indicate if there is increased expression of Sphk2 to compensate for Sphk1 knock down. Although these enzymes originate the same product, S1P has been shown to have different effects depending on where and by which enzyme it is produced.

Apart from the mechanistic details, it would also be of interest to determine the importance of Sphk1 *in vivo*. For this purpose, *Sphk1*$^{-/-}$ mice could be used to analyze adipogenesis in white and brown adipose tissue. Also, exposure of *Sphk1*$^{-/-}$ mice to cold and adrenergic stimulus would shed light on the role of Sphk1 in activation of brown adipose tissue. If possible, a tissue specific knock out could indicate if the activation of Sphk1/S1P signaling results from autocrine or paracrine regulation of S1P levels.

5. Conclusions

In summary, this study shows that Sphk1/S1P signaling plays an important role in adipose MSC differentiation and in mature adipocyte function. *Sphk1* knock down in mature adipocytes affected expression of lipolysis and mitochondrial genes, which indicates that Sphk1 is important for assembly of the oxidative machinery and therefore its deficiency may disturb oxidative capacity of mature adipocytes. More importantly, the strong phenotype produced by *Sphk1* knock down in brown adipocytes indicates that Sphk1 is required for normal brown adipocyte differentiation. Mature function was also significantly affected; specifically the basal lipolysis rate was reduced. In addition, *Sphk1* knock down significantly reduced differentiation of white MSCs, both in normal conditions and in the presence of a browning stimulus, i.e. $cPGI_2$, measured by reduced expression of brown and adipogenic marker genes.

Sphk1 is also important for cell viability and proliferation. The knock down of *Sphk1* in white and brown MSCs significantly increased cell death by apoptosis and induced cell cycle arrest in S/G2/M phase, which also contributed to the reduced differentiation phenotype. Finally, S1P was shown to promote cell proliferation and reduce adipogenesis in a concentration dependent manner.

All in all, this study shows that Sphk1 plays an important role in adipose tissue biology, and is of particular relevance to brown adipose tissue. However, its effects are not always the same, with Sphk1/S1P signaling having different effects in normal metabolic state and in obesity.

Overall, it appears that Sphk1/S1P signaling does not simply promote adipogenesis in general, but regulates its extent in relation to the metabolic state of the organism, suggesting a complex and fine-tuned regulation of this signaling pathway, which makes it an attractive target for therapeutic modulation of obesity.

6. References

Algire, C., Medrikova, D. & Herzig, S., 2013. White and brown adipose stem cells: from signaling to clinical implications. *Biochimica et biophysica acta*, 1831(5), pp.896–904.

Alvarez, S.E., Milstien, S. & Spiegel, S., 2007a. Autocrine and paracrine roles of sphingosine-1-phosphate. *Trends in endocrinology and metabolism: TEM*, 18(8), pp.300–7.

Alvarez, S.E., Milstien, S. & Spiegel, S., 2007b. Autocrine and paracrine roles of sphingosine-1-phosphate. *Trends in Endocrinology and Metabolism*, 18(8), pp.300–7.

Argraves, K.M. & Argraves, W.S., 2007. HDL serves as a S1P signaling platform mediating a multitude of cardiovascular effects. *Journal of lipid research*, 48(11), pp.2325–33.

Bartness, T.J., Vaughan, C.H. & Song, C.K., 2010. Sympathetic and sensory innervation of brown adipose tissue. *International journal of obesity (2005)*, 34 Suppl 1(S1), pp.S36–42.

Beranger, G.E. et al., 2013. In vitro brown and "brite"/"beige" adipogenesis: human cellular models and molecular aspects. *Biochimica et Biophysica Acta*, 1831(5), pp.905–14.

Berry, R. & Rodeheffer, M.S., 2013. Characterization of the adipocyte cellular lineage in vivo. *Nature Cell Biology*, 15(3), pp.302–8.

Bikman, B.T. & Summers, S.A., 2011. Ceramides as modulators of cellular and whole-body metabolism. *The Journal of Clinical Investigation*, 121(11), pp.4222–4230.

Blachnio-Zabielska, A.U. et al., 2012. Sphingolipid content of human adipose tissue: relationship to adiponectin and insulin resistance. *Obesity*, 20(12), pp.2341–7.

Blaho, V. a & Hla, T., 2014. An update on the biology of sphingosine 1-phosphate receptors. *Journal of lipid research*.

Brinkmann, V., 2007. Sphingosine 1-phosphate receptors in health and disease: mechanistic insights from gene deletion studies and reverse pharmacology. *Pharmacology & therapeutics*, 115(1), pp.84–105.

Cannon, B. & Nedergaard, J., 2004. Brown adipose tissue: function and physiological significance. *Physiological Reviews*, 84(1), pp.277–359.

Chavez, J.A. & Summers, S.A., 2012. A ceramide-centric view of insulin resistance. *Cell Metabolism*, 15(5), pp.585–94.

Chechi, K., Carpentier, A.C. & Richard, D., 2013. Understanding the brown adipocyte as a contributor to energy homeostasis. *Trends in Endocrinology and Metabolism*, 8, pp.1–13.

Cuvillier, O. et al., 1996. Suppression of ceramide-mediated programmed cell death by sphingosine-1-phosphate. *Nature*, 381(6585), pp.800–3.

Dai, L. et al., 2014. Sphingosine kinase (SphK) 1 and SphK2 play equivalent roles in mediating insulin's mitogenic action. *Molecular endocrinology (Baltimore, Md.)*, 28(2), pp.197–207.

Fatatis, a & Miller, R.J., 1999. Cell cycle control of PDGF-induced Ca(2+) signaling through modulation of sphingolipid metabolism. *FASEB journal : official publication of the Federation of American Societies for Experimental Biology*, 13(11), pp.1291–301.

Fedorenko, A., Lishko, P. V & Kirichok, Y., 2012. Mechanism of fatty-acid-dependent UCP1 uncoupling in brown fat mitochondria. *Cell*, 151(2), pp.400–413.

Fernández-Veledo, S. et al., 2006. Ceramide mediates TNF-alpha-induced insulin resistance on GLUT4 gene expression in brown adipocytes. *Archives of physiology and biochemistry*, 112(1), pp.13–22.

Frühbeck, G. & Gómez-Ambrosi, J., 2013. Adipose tissue: Structure, Function and Metabolism. In *Encyclopedia of Human Nutrition, Volume 1*. Elsevier, pp. 1–13.

Gagliostro, V. et al., 2012. Dihydroceramide delays cell cycle G1/S transition via activation of ER stress and induction of autophagy. *The international journal of biochemistry & cell biology*, 44(12), pp.2135–43.

Galic, S., Oakhill, J.S. & Steinberg, G.R., 2010. Adipose tissue as an endocrine organ. *Molecular and cellular endocrinology*, 316(2), pp.129–39.

Gesta, S., Tseng, Y.-H. & Kahn, C.R., 2007. Developmental origin of fat: tracking obesity to its source. *Cell*, 131(2), pp.242–56.

Gusain, A. et al., 2012. Anti-proliferative effects of tricyclodecan-9-yl-xanthogenate (D609) involve ceramide and cell cycle inhibition. *Molecular neurobiology*, 45(3), pp.455–64.

Hansen, J.B. & Kristiansen, K., 2006. Regulatory circuits controlling white versus brown adipocyte differentiation. *The Biochemical Journal*, 398(2), pp.153–68.

Hashimoto, T., Igarashi, J. & Kosaka, H., 2009. Sphingosine kinase is induced in mouse 3T3-L1 cells and promotes adipogenesis. *Journal of lipid research*, 50(4), pp.602–10.

Haynes, C. a et al., 2009. Sphingolipidomics: methods for the comprehensive analysis of sphingolipids. *Journal of chromatography. B, Analytical technologies in the biomedical and life sciences*, 877(26), pp.2696–708.

Hla, T. & Dannenberg, A.J., 2012. Sphingolipid signaling in metabolic disorders. *Cell metabolism*, 16(4), pp.420–34.

Holland, W.L., Bikman, B.T., et al., 2011. Lipid-induced insulin resistance mediated by the proinflammatory receptor TLR4 requires saturated fatty acid-induced ceramide biosynthesis in mice. *The Journal of clinical investigation*, 121(5), pp.1858–70.

Holland, W.L., Miller, R. a, et al., 2011. Receptor-mediated activation of ceramidase activity initiates the pleiotropic actions of adiponectin. *Nature medicine*, 17(1), pp.55–63.

Huang, P.-I. et al., 2011. PGC-1α mediates differentiation of mesenchymal stem cells to brown adipose cells. *Journal of atherosclerosis and thrombosis*, 18(11), pp.966–80.

Hursting, S.D. et al., 2012. Obesity, energy balance, and cancer: new opportunities for prevention. *Cancer Prevention Research*, 5(11), pp.1260–72.

Impey, S. et al., 2004. Defining the CREB Regulon : A Genome-Wide Analysis of Transcription Factor Regulatory Regions. *Cell*, 119, pp.1041–1054.

Jun, D.-J. et al., 2006. Sphingosine-1-phosphate modulates both lipolysis and leptin production in differentiated rat white adipocytes. *Endocrinology*, 147(12), pp.5835–44.

Kolak, M. et al., 2012. Expression of ceramide-metabolising enzymes in subcutaneous and intra-abdominal human adipose tissue. *Lipids in health and disease*, 11, p.115.

Lafontan, M. & Berlan, M., 2003. Do regional differences in adipocyte biology provide new pathophysiological insights? *Trends in pharmacological sciences*, 24(6), pp.276–83.

Lafontan, M. & Langin, D., 2009. Lipolysis and lipid mobilization in human adipose tissue. *Progress in Lipid Research*, 48(5), pp.275–97.

Lee, Y.-H. et al., 2012. In vivo identification of bipotential adipocyte progenitors recruited by β3-adrenoceptor activation and high-fat feeding. *Cell Metabolism*, 15(4), pp.480–91.

Li, P. et al., 2005. Metabolic and cellular plasticity in white adipose tissue II: role of peroxisome proliferator-activated receptor-alpha. *American journal of physiology. Endocrinology and metabolism*, 289(4), pp.E617–26.

Lim, H. & Dey, S.K., 2002. Minireview: A Novel Pathway of Prostacyclin Signaling-Hanging Out with Nuclear Receptors. *Endocrinology*, 143(9), pp.3207–3210.

Liu, H. et al., 2000. Molecular cloning and functional characterization of a novel mammalian sphingosine kinase type 2 isoform. *The Journal of biological chemistry*, 275(26), pp.19513–20.

Lodhi, I.J., Wei, X. & Semenkovich, C.F., 2011. Lipoexpediency: de novo lipogenesis as a metabolic signal transmitter. *Trends in endocrinology and metabolism: TEM*, 22(1), pp.1–8.

Maceyka, M. et al., 2012. Sphingosine-1-phosphate signaling and its role in disease. *Trends in cell biology*, 22(1), pp.50–60.

Maceyka, M. et al., 2005. SphK1 and SphK2, sphingosine kinase isoenzymes with opposing functions in sphingolipid metabolism. *The Journal of Biological Chemistry*, 280(44), pp.37118–29.

Martin, S.J. et al., 1995. Early redistribution of plasma membrane phosphatidylserine is a general feature of apoptosis regardless of the initiating stimulus: inhibition by overexpression of Bcl-2 and Abl. *The Journal of experimental medicine*, 182(5), pp.1545–56.

Mena, R.M. de, Scanlan, T.S. & Obregon, M.-J., 2013. The T3 Receptor β1 Isoform Regulates UCP1 and D2 Deiodinase in Rat Brown Adipocytes.

Minokoshi, Y. et al., 2002. Leptin stimulates fatty-acid oxidation by activating AMP-activated protein kinase. *Nature*, 415(6869), pp.339–43.

Moreno-navarrete, J.M. & Fernández-real, J.M., 2012. Chapter 2 - Adipocyte Differentiation M. E. Symonds, ed. *Adipose Tissue Biology*, pp.17–39.

Mullur, R., Liu, Y.-Y. & Brent, G.A., 2014. Thyroid hormone regulation of metabolism. *Physiological reviews*, 94(2), pp.355–82.

Nagata, Y. et al., 2006. Entry of muscle satellite cells into the cell cycle requires sphingolipid signaling. *The Journal of cell biology*, 174(2), pp.245–53.

Nnodim, J.O. & Lever, J.D., 1988. Neural and vascular provisions of rat interscapular brown adipose tissue. *The American journal of anatomy*, 182(3), pp.283–93.

Ogretmen, B. & Hannun, Y. a, 2004. Biologically active sphingolipids in cancer pathogenesis and treatment. *Nature reviews. Cancer*, 4(8), pp.604–16.

Olivera, A. et al., 1999. Sphingosine kinase expression increases intracellular sphingosine-1-phosphate and promotes cell growth and survival. *The Journal of cell biology*, 147(3), pp.545–58.

Olivera, A., Allende, M.L. & Proia, R.L., 2013. Shaping the landscape: metabolic regulation of S1P gradients. *Biochimica et biophysica acta*, 1831(1), pp.193–202.

Park, A., Kim, W.K. & Bae, K.-H., 2014. Distinction of white, beige and brown adipocytes derived from mesenchymal stem cells. *World journal of stem cells*, 6(1), pp.33–42.

Pébay, A., Bonder, C.S. & Pitson, S.M., 2007. Stem cell regulation by lysophospholipids. *Prostaglandins & other lipid mediators*, 84(3-4), pp.83–97.

Pham, T.-C.T. et al., 2008. Molecular recognition in the sphingosine 1-phosphate receptor family. *Journal of molecular graphics & modelling*, 26(8), pp.1189–201.

Pitson, S.M., 2011. Regulation of sphingosine kinase and sphingolipid signaling. *Trends in biochemical sciences*, 36(2), pp.97–107.

Qu, D. et al., 2011. 5-Ethynyl-2'-deoxycytidine as a new agent for DNA labeling: detection of proliferating cells. *Analytical biochemistry*, 417(1), pp.112–21.

Rodeheffer, M.S., Birsoy, K. & Friedman, J.M., 2008. Identification of white adipocyte progenitor cells in vivo. *Cell*, 135(2), pp.240–9.

Rosen, E.D. & MacDougald, O. a, 2006. Adipocyte differentiation from the inside out. *Nature reviews. Molecular cell biology*, 7(12), pp.885–96.

Schulz, T.J. & Tseng, Y.-H., 2013. Brown adipose tissue: development, metabolism and beyond. *The Biochemical journal*, 453(2), pp.167–78.

Seale, P. et al., 2008. PRDM16 controls a brown fat/skeletal muscle switch. *Nature*, 454(7207), pp.961–7.

Seale, P., 2010. Transcriptional control of brown adipocyte development and thermogenesis. *International Journal of Obesity*, 34(S1), pp.S17–S22.

Siskind, L.J., 2005. Mitochondrial ceramide and the induction of apoptosis. *Journal of Bioenergetics and Biomembranes*, 37(3), pp.143–53.

Smith, G.S., Kumar, A. & Saba, J.D., 2013. Sphingosine Phosphate Lyase Regulates Murine Embryonic Stem Cell Proliferation and Pluripotency through an S1P2/STAT3 Signaling Pathway. *Biomolecules*, 3(3), pp.351–368.

Spiegel, S. & Milstien, S., 2003. Sphingosine-1-phosphate: an enigmatic signalling lipid. *Nature reviews. Molecular cell biology*, 4(5), pp.397–407.

Steppan, C.M. et al., 2001. The hormone resistin links obesity to diabetes. *Nature*, 409(6818), pp.307–12.

Strable, M.S. & Ntambi, J.M., 2010. Genetic control of de novo lipogenesis: role in diet-induced obesity. *Critical reviews in biochemistry and molecular biology*, 45(3), pp.199–214.

Summers, S.A. et al., 1998. Regulation of Insulin-Stimulated Glucose Transporter GLUT4 Translocation and Akt Kinase Activity by Ceramide. *Mol. Cell. Biol.*, 18(9), pp.5457–5464.

Tang, Q.Q. & Lane, M.D., 2012. Adipogenesis: from stem cell to adipocyte. *Annual Review of Biochemistry*, 81, pp.715–36.

Tang, W. et al., 2008. White fat progenitor cells reside in the adipose vasculature. *Science (New York, N.Y.)*, 322(5901), pp.583–6.

Tirodkar, T.S. & Voelkel-Johnson, C., 2012. Sphingolipids in apoptosis. *Experimental oncology*, 34(3), pp.231–42.

Tseng, Y.-H., Cypess, A.M. & Kahn, C.R., 2010. Cellular bioenergetics as a target for obesity therapy. *Nature reviews. Drug discovery*, 9(6), pp.465–82.

Vegiopoulos, A. et al., 2010. Cyclooxygenase-2 controls energy homeostasis in mice by de novo recruitment of brown adipocytes. *Science*, 328(5982), pp.1158–61.

Villarroya, F. & Vidal-Puig, A., 2013. Beyond the sympathetic tone: the new brown fat activators. *Cell Metabolism*, 17(5), pp.638–43.

Virtue, S. & Vidal-Puig, A., 2008. It's not how fat you are, it's what you do with it that counts. *PLoS Biology*, 6(9), p.e237.

Wang, J. et al., 2014. Sphingosine kinase 1 regulates adipose proinflammatory responses and insulin resistance. *American journal of physiology. Endocrinology and metabolism*, 306(7), pp.E756–68.

World Health Organization, 2013. *Obesity and overweight - Fact sheet N°311*,

Wu, J. et al., 2012. Beige adipocytes are a distinct type of thermogenic fat cell in mouse and human. *Cell*, 150(2), pp.366–76.

Wu, J., Cohen, P. & Spiegelman, B.M., 2013. Adaptive thermogenesis in adipocytes: is beige the new brown? *Genes & Development*, 27(3), pp.234–50.

Xue, Y. et al., 2009. Hypoxia-independent angiogenesis in adipose tissues during cold acclimation. *Cell metabolism*, 9(1), pp.99–109.

Yamauchi, T. et al., 2001. The fat-derived hormone adiponectin reverses insulin resistance associated with both lipoatrophy and obesity. *Nature medicine*, 7(8), pp.941–6.

Zechner, R. et al., 2012. FAT SIGNALS - Lipases and lipolysis in lipid metabolism and signaling. *Cell Metabolism*, 15(3), pp.279–91.

Zeve, D., Tang, W. & Graff, J., 2009. Fighting fat with fat: the expanding field of adipose stem cells. *Cell Stem Cell*, 5(5), pp.472–81.

Zhang, H. et al., 1991. Sphingosine-1-phosphate, a novel lipid, involved in cellular proliferation. *The Journal of cell biology*, 114(1), pp.155–67.

Zhang, J.-W. et al., 2004. Role of CREB in transcriptional regulation of CCAAT/enhancer-binding protein beta gene during adipogenesis. *The Journal of biological chemistry*, 279(6), pp.4471–8.

Zilberfarb, V. et al., 2001. Effect of dexamethasone on adipocyte differentiation markers and tumour necrosis factor-α expression in human PAZ6 cells. *Diabetologia*, 44(3), pp.377–386.